ATTAINABLE REGIONS

IN

CHEMICAL REACTION SYSTEMS

A Thesis submitted for the degree of

Doctor of Philosophy in the Faculty of

Engineering of the University of London

by

COLIN BERNARD SCHLESINGER

Department of Chemical Engineering and Chemical Technology

Imperial College

London S.W.7

August 1966

ABSTRACT

The attainable region is a mapping in the space of those variables which affect the economics of the process (the objective variables) and describes the totality of physically realisable systems.

Attainable regions are investigated for the important practical example of a reversible reaction with irreversible decay of product.

$$A \underset{2}{\overset{1}{\rightleftharpoons}} B \xrightarrow{3} C$$

This may be regarded as representing a general class of reaction systems and includes a number of special cases. The reactions are carried out in either an ideal tubular reactor or an ideal stirred tank.

For certain values of the activation energies the attainable region will not fill out the stoichiometrically attainable space. The border of the region is generally most important in such a case and one way to develop this is by tracing out all possible reaction paths. This will be

tedious in general however, and the Pontryagin Maximum Principle can be used to generate border points directly. Alternatively the attainable region may be propagated forwards in time by a transformation of border points.

The attainable region depends only on the initial conditions and parameter values chosen for the system. It is applicable to all cost functions plotted in the space spanned by the objective variables, in particular to cost functions arising if there is recycle of unconverted raw material.

ACKNOWLEDGEMENTS

I am especially grateful to the South African Industrial Cellulose Corporation for the award of their Scholarship, which has enabled me to proceed overseas for graduate research.

My sincere appreciation is due Professor K.G. Denbigh F.R.S., for accepting me at Imperial College and for his supervision during part of this work.

To Professor Fritz Horn, who has been friend and advisor, my thanks for his generous assistance and for many stimulating and interesting discussions. It has been a pleasure and a privilege to work for him.

I wish finally to express my appreciation to Rice University for a Research Assistantship and to the National Science Foundation for support under systems grant GU-1153, during the later period of this study.

To Sheila

TABLE OF CONTENTS

	Page
TITLE PAGE	1
ABSTRACT	2
ACKNOWLEDGEMENTS	4
LIST OF FIGURES	11
LIST OF TABLES	14
CHAPTER 1 INTRODUCTION	
1.1 IDEAL REACTOR TYPES	16
1.2 CHEMICAL REACTION SYSTEM	18
1.3 SET OF ADMISSIBLE CONTROLS	19
1.4 THE ATTAINABLE REGION	21
1.4.1 Concept of the attainable region	21
1.4.2 Classification of optimisation problems	23
1.4.3 Optimisation and the attainable region	25
1.5 THE STOICHIOMETRICALLY ATTAINABLE REGION	27
1.6 STATEMENT OF THE PROBLEM	29
1.7 SOLUTION TO THE PROBLEM	30
1.7.1 The stirred tank reactor	30
1.7.2 The tubular reactor	30

Page

CHAPTER 2 THE ISOTHERMAL ATTAINABLE REGION

2.1 INTRODUCTION 33

2.1.1 Comparison of different reactor types 33

2.1.2 The yield problem for a single reaction 34

2.2 THE IRREVERSIBLE REACTION $A \longrightarrow B$ 35

2.3 THE REVERSIBLE REACTION $A \rightleftharpoons B$ 37

2.4 THE CONSECUTIVE REACTIONS $A \longrightarrow B \longrightarrow C$ 41

2.4.1 The yield problem 41

2.4.2 The output problem 44

2.5 THE REVERSIBLE REACTION WITH IRREVERSIBLE DECAY OF PRODUCT $A \rightleftharpoons B \longrightarrow C$ 47

2.5.1 The yield problem 47

2.5.2 The output problem 55

2.6 SUMMARY 61

CHAPTER 3 THE ATTAINABLE REGION FOR PERFECT TEMPERATURE CONTROL

3.1 THE OUTPUT PROBLEM FOR $A \rightleftharpoons B$ 62

3.2 THE OUTPUT PROBLEM FOR $A \longrightarrow B \longrightarrow C$ 63

3.3 THE YIELD PROBLEM FOR $A \rightleftharpoons B \longrightarrow C$ 65

3.4 THE OUTPUT PROBLEM FOR $A \rightleftharpoons B \longrightarrow C$ 72

Page

3.4.1 Generation of the border of the attainable region 72

3.4.2 The Pontryagin Maximum Principle 75

3.4.3 Optimal Control Policy 76

3.4.4 Solution of the optimal problem 81

3.4.5 Numerical integration procedure 84

3.4.6 Upper bound on the control 86

3.4.7 Some difficulties in the forward integration 87

3.4.8 Discussion of the results 101

3.5 THREE-DIMENSIONAL MODEL OF THE ATTAINABLE REGION 109

3.6 APPLICATION TO SPECIFIC OBJECTIVE FUNCTIONS 113

CHAPTER 4 DETERMINATION OF THE ATTAINABLE REGION BY NON-ANALYTICAL PROCEDURES

4.1 THE ANALOGUE COMPUTER 122

4.1.1 Chemical reaction system 123

4.1.2 Closed solution 125

4.1.3 The computer method 125

4.1.4 The isothermal attainable region 128

4.1.5 Conclusions 130

Page

4.2 PROPAGATION OF THE ATTAINABLE REGION BORDER BY TRANSFORMATION OF BORDER POINTS 130

4.2.1 Geometric interpretation of the Pontryagin Maximum Principle 131

4.2.2 Application to a discrete system 133

4.2.3 Transformation equations 134

4.2.4 Determination of border points 137

4.2.5 Algorithm for determining the attainable region 140

4.2.6 The computer programme 142

4.2.7 Results obtained with the procedure 146

4.2.8 Discussion 153

CHAPTER 5 THE ISOTHERMAL ATTAINABLE REGION FOR THE SUCCESSIVE REVERSIBLE REACTIONS $A \rightleftharpoons B \rightleftharpoons C$ IN A YIELD PROBLEM

5.1 THE SYSTEMS EQUATIONS 155

5.2 EQUILIBRIUM 157

5.3 THE CASE $(\alpha - \beta) < 0$ 158

5.4 THE CASE $(\alpha - \beta) = 0$ 162

5.5 THE CASE $(\alpha - \beta) > 0$ 162

5.6 PHYSICAL SIGNIFICANCE OF THE RESULTS 164

5.7 DISCUSSION 167

Page

CHAPTER 6 DISCUSSION

6.1 INITIAL CONDITIONS 169

6.2 THE SOLUTION OF OPTIMAL PROBLEMS 170

6.3 PERFECT TEMPERATURE CONTROL 170

6.4 COMPARISON BETWEEN ATTAINABLE REGIONS FOR TUBULAR REACTOR AND SINGLE TANK 171

6.5 CONCLUSIONS 171

REFERENCES 173

NOMENCLATURE 176

APPENDICES 178

LIST OF FIGURES

Figure		Page
2.1	Isothermal attainable region for $A \rightleftharpoons B$ in an output problem	40
2.2	Tubular reactor system and tank reactor	45
2.3	Isothermal trajectories for tube and tank for $A \rightarrow B \rightarrow C$	45
2.4	Isothermal attainable region for $A \rightarrow B \rightarrow C$ in an output problem	40
2.5	Isothermal trajectories for $A \rightleftharpoons B \rightarrow C$ in a yield problem, with $\alpha > 0$	50
2.6	Isothermal attainable region for $A \rightleftharpoons B \rightarrow C$ in a yield problem, with $\alpha = 0$ and $\alpha > 0$	56
2.7	Effect of a on the isothermal attainable region for $\alpha = 0$	51
2.8	Isothermal attainable region for $A \rightleftharpoons B \rightarrow C$ in an output problem	59
3.1	Section of attainable region for $A \rightleftharpoons B \rightarrow C$ at $\phi = \phi_e$	73
3.2	The Hamiltonian as function of control	78
3.3	The Hamiltonian as function of control for $b = 1/3$	73
3.4	Illustration of how $\lambda(0)$ values generate optimal trajectories and hence the attainable region border	96
3.5	Adjoint mapping	102

Figure		Page
3.6	Optimal control trajectories for $K_u = 2$	103
3.7	Attainable region for $A \rightleftharpoons B \rightarrow C$ with $K_u = 2$	105
3.8	Attainable region for $A \rightleftharpoons B \rightarrow C$ with $K_u = 100$	106
3.9	Three-dimensional representation of the attainable region with $K_u = 100$	108
3.10	Comparison between attainable regions for exothermic reversible reaction with and without irreversible decay of product	110
3.11	Three-dimensional model of the attainable region	111
3.12	Solution to example 1	114
3.13	Solution to example 2	119
4.1	Analogue computer circuit for determination of attainable region	127
4.2	Attainable region for $A \rightleftharpoons B$ and $A \rightarrow B$; $A \rightarrow C$ in the output problem	129
4.3	Transformation of a border point on the attainable region from stage $(\nu - 1)$ to stage ν	138
4.4	Rotation of search directions	138
4.5	Development of the attainable region by digital computer	147
4.6	Attainable region for stage 25	148
4.7	Comparison between Pontryagin solution and non-analytical method for $\xi = 0.07$	149

Figure		Page
4.8	Comparison between Pontryagin solution and non-analytical method for ξ = 0.10, 0.75 and 0.95	151
5.1	Isothermal attainable region for A$\rightleftharpoons$B$\rightleftharpoons$C with $(\alpha - \beta) < 0$ and (b/a) = 1	160
5.2	Isothermal trajectories for α = -1, β = -0.9 and (b/a) = 1	161
5.3	Effect of (b/a) on the isothermal attainable region for $(\alpha - \beta)$ = -1	160
5.4	Isothermal attainable region for A$\rightleftharpoons$B$\rightleftharpoons$C with $(\alpha - \beta)$ = 0 and (b/a) = 1	163
5.5	Isothermal attainable region for A$\rightleftharpoons$B$\rightleftharpoons$C with α = -1 and $(\alpha - \beta) \geq 0$	163
5.6	Isothermal attainable region for A$\rightleftharpoons$B$\rightleftharpoons$C with α = 2 and $(\alpha - \beta) \geq 0$	165
A3.1	Sign of the adjoint ratio λ	192
A3.2	Behaviour of the ratio of state variables X	192

LIST OF TABLES

Table		Page
1.1	System $A \rightleftharpoons B \rightarrow C$ with pure A initially	20
2.1	$A \rightleftharpoons B \rightarrow C$ in isothermal tubular reactor: Comparison of published values for x_{Be} (max) with values obtained from the isothermal attainable region	53
3.1	Insensitivity of the forward integration solution to variation in $\lambda(0)$	90
3.2	To show that $b \rightarrow 1/3$ as $\lambda(0) \rightarrow -\infty$	92
3.3	Effect of $\lambda(0) \rightarrow \rho_1$ on the optimal control	95
4.1	Set of controls K	143
4.2	Optimal control policies	152
A.1	Isothermal results for $K_u = 2$	202
A.2	Isothermal results for $K_u = 100$	203

CHAPTER ONE

INTRODUCTION

In the optimisation of a given system, it is required to choose those operating conditions for which some predetermined objective function takes on a maximal (minimal) value. This objective function is related to the economics of the process.

In practice the objective function depends on relatively few variables. (These objective variables in turn depend on many control variables, even infinitely many, in a variational problem). The attainable region is a mapping in the space of the objective variables and has been introduced into chemical reaction technique by Horn [1].

The usefulness of the concept of the attainable region is that it can generate systems mathematically which, for given input conditions, are optimal for a variety of objective functions. This is in contrast to Dynamic Programming [2] and related methods, where systems are generated which are optimal for only one objective function and a variety of input conditions.

The present study deals with attainable regions in chemical reaction systems and represents a geometrical approach to chemical reactor optimisation. In this introduction, the reaction systems under consideration are characterised and development of their attainable regions is discussed. The significance of these attainable regions in reactor optimisation is indicated, which leads to a specific formulation of the problem and consideration of methods of solution.

1.1 IDEAL REACTOR TYPES

Consider a system of stoichiometrically independent chemical reactions. (By stoichiometrically independent we mean that no single reaction can be expressed as a linear combination of the others). This study will be concerned with two ideal reactor types in which a number of such reactions is being carried out. These reactor types are the plug flow tubular reactor and the single continuous stirred tank reactor which is perfectly mixed. We need not specify segregation or maximum mixedness [3] for the latter, since we shall only be dealing with linear kinetics.

Consider at first an ideal tubular reactor with the above reactions. The system may be described at constant pressure by the set of simultaneous ordinary differential equations

$$\frac{dx_i}{dt} = v_i(x_1, x_2, \ldots, x_n, T) \qquad i = 1,2,\ldots,n \qquad (1.1)$$

$$T = T(t)$$

with specified initial conditions

$$x_i(0) = x_{io} \qquad i = 1,2,\ldots,n \qquad (1.2)$$

Here the x_i are state variables describing the composition of the reacting mixture, e.g. x_1 may be conversion to desired product and x_2 conversion to undesired product. The variable t is related to reactor volume or catalyst mass and provides a measure of the reaction time, whilst the functions v_i are reaction rates. For linear kinetics,

$$v_i = a_{io} + \sum_{j=1}^{n} a_{ij}x_j \qquad i = 1,2,\ldots,n \qquad (1.3)$$

where the a_{io}, a_{ij} are temperature dependent. In general n is the number of stoichiometrically independent reactions.

Now consider the same reactions carried out at constant pressure in an ideal tank reactor. In this case the state equations may be written

$$x_{ie} = x_{io} + \tau v_i(x_{1e}, x_{2e}, \ldots, x_{ne}, T) \qquad i = 1,2,\ldots,n \quad (1.4)$$

where the x_{ie} describe exit composition, which is by definition identical to composition of reacting mixture in the tank. The variable τ is the mean residence time.

The condition of constant pressure specified above is not too restrictive. The pressure drop across a tubular reactor will generally be small compared to the pressure itself, and pressure changes must usually be large before any pressure effect becomes significant on the kinetics.

1.2 CHEMICAL REACTION SYSTEM

We will investigate the case of a reversible reaction followed by an irreversible reaction.

$$A \underset{2}{\overset{1}{\rightleftharpoons}} B \xrightarrow{3} C \qquad (1.5)$$

Here there are two stoichiometrically independent reactions.

We will suppose only A to be present initially and B to be the desired product, which may decay to the undesired side product C. It will be assumed that all reactions are first order and that the reaction velocity constants have Arrhenius temperature dependence[4]

$$k_i = H_i \exp(-E_i/RT) \qquad i = 1,2,3 \tag{1.6}$$

H_i is the frequency factor and E_i the activation energy of reaction i.

The above reaction system will include a number of special cases, which are shown in table (1.1). For general discussions on these reactions, the reader is referred to standard texts on kinetics and chemical reaction engineering.

1.3 SET OF ADMISSIBLE CONTROLS

In this study two admissible control sets will be considered.

(i) Perfect temperature control: This is the set of all piecewise continuous functions T(t) restricted by

$$0 \leq T \leq T_u \tag{1.7}$$

(ii) Isothermal temperature control: This is a subset of (i). It describes the set of isothermal controls T subject to the same constraints (1.7).

In what follows, the term "attainable region" will relate to (i) and "isothermal attainable region" to (ii).

TABLE 1.1

System $A \underset{k_2}{\overset{k_1}{\rightleftharpoons}} B \xrightarrow{k_3} C$ with pure A initially

$k_i (i = 1,3)$ = reaction velocity constant

(i)	$k_2 = k_3 = 0$	$A \longrightarrow B$
(ii)	$k_3 = 0$	$A \rightleftharpoons B$
(iii)	$k_2 = 0$	$A \longrightarrow B \longrightarrow C$
(iv)	All k_i non-zero	$A \rightleftharpoons B \longrightarrow C$

1.4 THE ATTAINABLE REGION

1.4.1 Concept of the attainable region

We have mentioned that the objective variables are those variables which directly affect the objective function. Let us denote the vector of state variables x_i by $\underline{x}$ and suppose $\underline{x}, t$ are the objective variables in the tubular reactor system. A given admissible temperature policy $T = T(t)$ applied to the reactor will produce an exit composition $\underline{x}_e$ from feed $\underline{x}_o$ in time t_e. This $\underline{x}_e$ is the end condition on a path or trajectory starting from $\underline{x}_o$. With the above temperature policy, all intermediate compositions along the path $\underline{x} = \underline{x}(t)$ can also be reached or attained from $\underline{x}_o$ in some time $t \leq t_e$. Hence all points on this path are attainable points from the initial condition $\underline{x}_o$. The path then becomes the attainable region for the given initial condition and temperature policy.

Now consider a set of admissible control policies $T(t)$. These will generate a set of attainable trajectories, all starting at $\underline{x}_o$. The union of all these trajectories is called the attainable region for the given initial condition $\underline{x}_o$ and the set of control policies considered. It determines

all those points in objective variable space which are attainable from $\underline{x}_o$ by means of some admissible control policy $T(t)$, in reaction time $t \leq t_e$.

The preceeding arguments may be similarly extended to the ideal tank reactor. In this case $\underline{x}_e$ and τ may be considered the objective variables. The attainable region now consists of all those points in objective variable space which are attainable from $\underline{x}_o$ by means of admissible temperature T, in ideal tank reactors with mean residence time $\leq \tau$.

Thus far the only mention of optimisation has been in introducing the objective variables. It should be noted that the attainable region can be obtained without reference to any specific optimisation problem. The attainable region is a geometric representation of the solution to the state equations, plotted in objective variable space. The analogue to this in the study of systems of differential equations is reflected in the reachable zone proposed by Roxin [5,6], whilst Halkin [7] has introduced the concept of a set of reachable events, which he extends to systems described by difference equations [8].

Choosing the objective variables is a prerequisite for obtaining the attainable region. The objective variables already used have been the state of the system $\underline{x}$ and a measure of the time (t, τ). It would be convenient if optimisation problems could in general be categorised in terms of objective variables. Such a classification will now be discussed.

1.4.2 Classification of optimisation problems

Two useful classes of chemical reactor optimisation problems have been proposed by Denbigh[9].

(i) Yield problems: Here the objective function depends explicitly on overall conversion or yield only. If the objective function be denoted M,

$$M = M(x_{1e}, x_{2e}, \ldots, x_{ne}) \qquad (1.8)$$

Such a situation might be envisaged when raw material is expensive and tends to predominate costs.

(ii) Output problems: The objective function is now dependent on reaction time as well as overall conversion. For the tube,

$$M = M(x_{1e}, x_{2e}, \ldots, x_{ne}, t_e) \qquad (1.9a)$$

whilst for the tank

$$M = M(x_{1e}, x_{2e}, \ldots, \tau) \qquad (1.9b)$$

This means that capital costs associated with the equipment must also be taken into account. Note that output problems will include yield problems as a class of subproblems.

The remaining problems are those in which reactor or control parameters are included as arguments of the objective function. A typical example would be the situation where a cost must be associated with each control policy considered. These problems always form the final stages of optimisation and the yield and output problems still provide valuable information about attainable limits of operation.

The application of attainable regions to the first two classes of optimisation problems mentioned above, will now be indicated.

1.4.3 Optimisation and the attainable region

The attainable region represents the totality of physically realisable reactors for a given system. Any optimisation problem postulated for the system must have a solution in objective variable space which corresponds to a physically realisable reactor. Hence this solution must lie on the border or inside the attainable region.

Consider (say) the output problem for a tubular reactor, where it is required to optimise a particular $M(\underline{x}_e, t_e)$. The solution to such a problem may be obtained by superimposing the contours of M on to a plot of the attainable region in the objective variable space $(\underline{x}_e, t_e)$. For instance, consider $\underline{x} = (x_1\ x_2)$ with x_1 the conversion to desired product and x_2 the conversion to undesired product. An objective function $M = M(x_{1e}, x_{2e}, t_e)$ is to be maximised for an optimal reactor. This immediately implies certain qualitative information about M, viz. M will decrease if t_e increases whilst x_{1e} and x_{2e} are held constant. M will also decrease if t_e and x_{1e} remain constant and x_{2e} is increased. On the other hand an increase in x_{1e} at constant x_{2e}, t_e will

give rise to an increase in M. Hence M cannot have an optimal value for free variation of x_{1e}, x_{2e} and t_e and an optimal operating point will lie on the border of the attainable region.

We have just considered an objective function M which depends on conversion to desired product x_{1e}, on conversion to undesired product x_{2e} and on reaction time t_e. We are therefore dealing with the three-dimensional (or 3-D) objective variable space (x_{1e}, x_{2e}, t_e). Hence we will call such a problem a 3-D output problem. If only conversion to desired product and reaction time mattered economically, but not conversion to undesired product, we would have a two-dimensional (or 2-D) output problem. On the other hand, if reaction time were economically unimportant and only conversions x_{1e} and x_{2e} affected the objective function, we would have a 2-D yield problem.

When the border of the attainable region in the 3-D output problem is projected on to the x_{1e}-t_e plane, it provides the border of the attainable region in the 2-D output problem. However, when projected on to the x_{1e}-x_{2e} plane,

it provides the border of the 2-D yield problem attainable region.

1.5 THE STOICHIOMETRICALLY ATTAINABLE REGION

The attainable region describes the kinetics of the system. We now introduce the stoichiometrically attainable region to represent the stoichiometry.

For only A initially present, the stoichiometry of the reaction system (1.5) dictates that at all times and in both reactor types

$$C_A + C_B + C_C = C_{Ao} \tag{1.10}$$

Introduce the dimensionless variables

$$x_i = C_i/C_{Ao} \qquad i = A,B,C \tag{1.11}$$

Then equation (1.10) becomes

$$x_A + x_B + x_C = 1 \tag{1.12}$$

For the 3-D output problem in the space (x_{Be}, x_{Ce}, t_e), the stoichiometrically attainable region is then bounded by the planes $x_{Be} = 0$, $x_{Ce} = 0$ and $x_{Be} + x_{Ce} = 1$. It lies

between the limits

$$0 \leq t_e \leq \infty \tag{1.13}$$

For the 2-D yield problem this reduces to the triangle $x_{Be} = 0$, $x_{Ce} = 0$, $x_{Be} + x_{Ce} = 1$, whilst for the 2-D output problem the bounds become

$$0 \leq x_{Be} \leq 1 \tag{1.14}$$

together with the limits (1.13). If we consider the temperature T to be unbounded, then for certain relations between the activation energies, the attainable region will essentially fill out the stoichiometrically attainable space. Introducing an upper limit T_u will cause the attainable region to shrink, but the problem remains basically one of design, e.g. to devise constructional materials for achieving as high an operating temperature as possible.

In some instances however, the attainable region will not fill out the stoichiometrically attainable region, even if the control be unbounded. The border of the attainable region is now important for the solution of many optimisation problems.

In this study we shall mainly be concerned with the latter situation.

1.6 STATEMENT OF THE PROBLEM

For given input conditions, the attainable region depends on the reaction system, reactor type and objective variable space. The reaction system of table (1.1) will be considered in this study, with input conditions of pure A only, carried out in each of the ideal reactors described in #1.1. Attainable regions will be investigated for the 2-D yield problem and both 2-D and 3-D output problems. For each problem, the attainable regions for tube and tank will be compared. Of particular interest will be those cases where the stoichiometrically attainable region is not essentially filled out.

Attainable regions have already been published for some of the problems; these will be referenced in the appropriate sections of the text.

1.7 SOLUTION TO THE PROBLEM

It has been the author's intention to present a comprehensive development of the attainable region for the sequence of reactions in table (1.1). Where well-known results have been included in the present work, this has been for the sake of completeness.

1.7.1 The stirred tank reactor

This will be dealt with in chapter two. A tank reactor operating in the steady state involves only one temperature T and the problem is simple. This would not be so for a cascade of tank reactors, but such a case is excluded from the present study.

1.7.2 The tubular reactor

The isothermal attainable region will be investigated in chapter two. Useful qualitative information may be obtained from such a study, especially since an isothermal attainable region which essentially fills the stoichiometrically attainable space, clearly implies that the attainable region will exhibit the same behaviour. This is

because the set of admissible controls for the latter is less restrictive. In those cases where the stoichiometrically attainable region is not filled, it is of interest to see to what extent the isothermal attainable region differs from the attainable region.

The isothermal problem is simple since each solution corresponds to only one temperature. Analytical solutions should be obtained where possible, otherwise numerical integration procedures are indicated. An analogue computer could be used to advantage, though care must be exercised when dealing with non-linearities.

The problem is variational in nature for the more general attainable region discussed in chapter three. Consider a 3-D output problem such as in #1.4.3. One way to develop the border of the attainable region in (x_{1e}, x_{2e}, t_e) space is by tracing out all possible reaction paths, but this will be tedious in general and the Pontryagin Maximum Principle[10] may be used to generate border points directly. This employs the fact that each border point will be optimal for some appropriately chosen objective function. (By appropriately chosen we mean an M such as in #1.4.3).

An alternate approach will be adopted in chapter four. The system will be approximated by a large but finite number of isothermal stages and the attainable region propagated forwards in time by a transformation of border points from one stage to the next. The method is suggested theoretically by a geometrical approach to optimal control[8] and is related to the Pontryagin Maximum Principle.

Finally in chapter five some suggestions relating to the attainable region for the system $A \rightleftharpoons B \rightleftharpoons C$ will be made, based on an analogue computer study of the isothermal yield problem.

CHAPTER TWO

THE ISOTHERMAL ATTAINABLE REGION

2.1 INTRODUCTION

We shall consider in this chapter the attainable region obtained with isothermal temperature control for a feed of pure A. Since a tank reactor operates at a fixed temperature in the steady state, it may be included in an isothermal study.

2.1.1 Comparison of different reactor types

The suitability of the attainable region for a qualitative comparison of different types of reactors, has been pointed out by Horn [1].

(i) A tubular reactor with perfect temperature control may be compared to a reactor in which not all temperature profiles are realisable (e.g. an isothermal reactor). The attainable region for the latter will certainly be contained in that for the former; however it is important to know whether the difference

between the two regions is significant. If not, there is no need to improve the less sophisticated reactor.

The isothermal approach in this chapter will indicate for which conditions the isothermal reactor is the optimal one. Then more sophisticated control will be investigated in chapter three for the remaining cases, to establish the difference between the two reactor types.

(ii) A tubular reactor and a tank reactor may be compared. In general, any relationship may exist between them; one will be superior to the other if its attainable region contains that of the other.

The attainable regions for the tank reactor and isothermal tubular reactor will be compared in this chapter.

2.1.2 The yield problem for a single reaction

For any single reaction carried out in either the tube or the tank, a one-dimensional stoichiometric attainable region will always be obtained in objective variable space.

How closely the attainable region approaches this will depend in general on the temperature limits.

2.2 THE IRREVERSIBLE REACTION A⟶B

We need only consider the output problem. The isothermal results for first order reaction are well-known for both tube and tank [11].

Tube: $$x_{Be} = 1 - \exp(-kt_e) \tag{2.1}$$

Tank: $$x_{Be} = k\tau/(1 + k\tau) \tag{2.2}$$

The x_{Be} are defined in equation (1.11).

The reaction velocity constant $k = k(T)$ is a monotone increasing function of T from equation (1.6). We may therefore regard k as the control variable for convenience, rather than T. The inequality constraints (1.7) now become

$$0 \leq k \leq k_u \tag{2.3}$$

with $k_u < H$ for finite T_u.

Levenspiel [11] has shown that to achieve a given conversion x_{Be}, a longer holding time is required in the tank than

in a tube at the same temperature, i.e. $\tau/t_e \geq 1$. This ratio will increase with reaction order for all positive reaction orders. Similar conclusions are reached by Denbigh[12]. Douglas[13] compares the plot of x_{Be} vs. kt_e for the tube with the corresponding plot (x_{Be} vs. $k\tau$) for the tank. The conversion profile for the tube is shown to lie above that for the tank. One can readily deduce this by inspection of equations (2.1) and (2.2), since it can be shown that for all y,

$$1 - \exp(-y) \geq y/(1 + y) \qquad (2.4)$$

To investigate the isothermal attainable regions for tube and tank, we are interested in the (x_{Be}, time) space. Equations (2.1) and (2.2) indicate that for each reactor type, the border of the isothermal attainable region will be the corresponding isothermal $k = k_u$. Since any isothermal for the tube always lies above the corresponding isothermal for the tank, the isothermal attainable region for the tube must contain that for the tank.

If k were unconstrained, any x_{Be} in $0 \leq x_{Be} \leq 1$ could be attained at any time and the stoichiometrically attainable

region would be filled out. This is still true for all practical purposes if a reasonably large k_u is permitted. Since the optimal temperature for both reactor types is the highest allowable operating temperature, consideration of the attainable region for control policies other than isothermal is clearly unnecessary.

2.3 THE REVERSIBLE REACTION $A \underset{2}{\overset{1}{\rightleftharpoons}} B$

This is typical of many industrially important reactions, some better known examples being the oxidation of sulphur dioxide, synthesis of ammonia, and water-gas shift reaction [12]. We again consider only the output problem.

A transformation has been used by Horn and Kuchler [14] to eliminate exponential dependence on the control variable and at the same time, reduce the number of parameters to be specified (see also reference 15). If we define $k_R = k_1(T_R) = k_2(T_R)$ and make (k_1/k_R) the control variable k, then $(k_2/k_R) = k^r$, where $r = E_2/E_1$. Since k_R is a constant, k will behave in like fashion to the k in #2.2. The number of parameters has been reduced from four (i.e. H_1, H_2, E_1, E_2) to one (r).

The isothermal result for first order reaction in a tubular reactor may be found in standard texts[4,11]. In terms of the control k,

$$x_{Be} = \frac{1 - \exp\left[-(1 + k^{r-1})\, k\phi_e\right]}{1 + k^{r-1}} \qquad (2.5)$$

where ϕ_e is the dimensionless time $k_R t_e$. The corresponding equation for the tank is

$$x_{Be} = \frac{k\phi}{1 + (1 + k^{r-1})\, k\phi} \qquad (2.6)$$

with $\phi = k_R \tau$.

Now from equation (2.4) it can be shown that

$$\frac{1 - \exp(-ay)}{a} \geq \frac{y}{1 + ay} \; ; \; a > 0 \qquad (2.7)$$

Hence an isothermal trajectory for the tube in the space (x_{Be}, ϕ) will always lie above the corresponding trajectory for the tank. Consequently the isothermal attainable region for the tubular reactor will contain that for the tank.

For the endothermic reaction ($r < 1$), one obtains maximum conversion when the temperature in the reactor is as high as possible[16]. Hence the border of the isothermal attainable region in the space (x_{Be}, ϕ) is the isothermal $k = k_u$.

In the exothermic case ($r > 1$), the border of the isothermal attainable region is the envelope of all isothermal trajectories, for both reactors. The stoichiometrically attainable region is not filled out, even for unbounded k, as shown in figure (2.1a) for $r = 2$. (Horn[17] has obtained the border for the tube directly, by setting to zero the derivative of x_{Be} with respect to k).

When $r = 1$, k_R can only be used if $H_1 = H_2$, otherwise the individual rate constants k_1, k_2 must be retained. The case $r = 1$ is shown in figure (2.1b) and the optimal reactor is isothermal. In the vicinity of $r = 1$, the attainable region is sensitive to temperature bounds[18].

As expected, the isothermal attainable region for $A \rightleftharpoons B$ will be contained by that for $A \rightarrow B$, for both tube and tank. This can be deduced from the relevant equations.

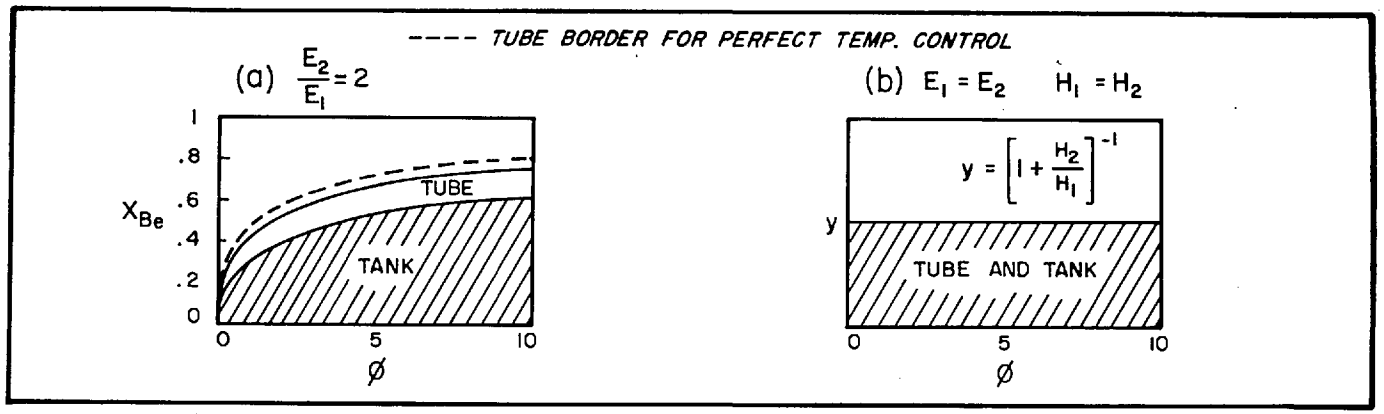


FIGURE 2.1 - ISOTHERMAL ATTAINABLE REGION FOR $A \rightleftharpoons B$ IN AN OUTPUT PROBLEM

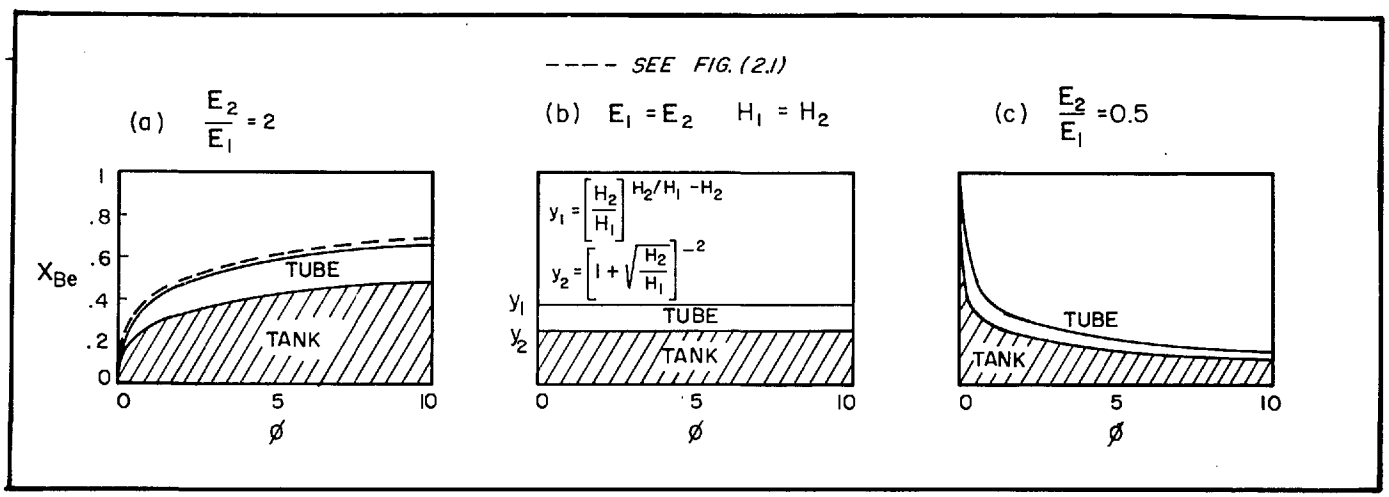


FIGURE 2.4 - ISOTHERMAL ATTAINABLE REGION FOR $A \rightarrow B \rightarrow C$ IN AN OUTPUT PROBLEM

2.4 THE CONSECUTIVE REACTIONS $A \xrightarrow{1} B \xrightarrow{2} C$

This mechanism describes many reactions of practical significance, such as the successive substitution of hydrocarbons [11] and the oxidation of methanol [12]. An excellent introduction to the theory of consecutive reactions is given by Denbigh [12].

2.4.1 The yield problem

There are now two stoichiometrically independent reactions. A satisfactory control variable is $k = k_2/k_1$; k is either a monotone increasing function of T or a monotone decreasing function of T, depending on whether $E_2 > E_1$ or $E_2 < E_1$ respectively. Since time is replaced by a variable which is temperature-dependent, such a transformation would be unsatisfactory in an output problem.

The state equations may be solved isothermally for first order kinetics [11].

Tube:

$$x_{Ae} = \exp(-\phi_e)$$

$$x_{Be} = \frac{\exp(-\phi_e) - \exp(-k\phi_e)}{k - 1} \qquad k \neq 1$$

$$= \phi_e \exp(-\phi_e) \qquad k = 1$$

$$\text{with } \phi_e = k_1 t_e \tag{2.8}$$

Tank:

$$x_{Ae} = 1/(1 + \phi)$$

$$x_{Be} = \phi/(1 + \phi)\ (1 + k\phi)$$

$$\text{and } \phi = k_1 \tau \tag{2.9}$$

Typical isothermal trajectories are presented in the literature [4,11,19]. These indicate that as $k \longrightarrow 0$, the stoichiometrically attainable region is filled out, which is to be expected from physical considerations.

Conversion to desired product B passes through a maximum on an isothermal trajectory. The position of this maximum has been compared for tube and tank by Levenspiel [11] and Denbigh [12]. For given k,

$$x_{Be}^{*}\ (\text{tube}) \geq x_{Be}^{*}\ (\text{tank})$$

$$\phi_{c}^{*}\ (\text{tube}) \leq \phi^{*}\ (\text{tank}) \qquad (2.10)$$

These results are not intuitively obvious and the interested reader may care to verify them.

From the graphical results in the literature, it would also appear that the isothermal trajectory for the tube lies above that for the tank. This can be proved analytically (see Appendix I #1). Since the border of the isothermal attainable region is a single trajectory, it follows that in a yield problem involving the consecutive first order reactions $A \rightarrow B \rightarrow C$, the isothermal attainable region for a tubular reactor will always contain that for a tank.

As a consequence, the following statement is also true (see Appendix I #2): if the consecutive first order reactions $A \rightarrow B \rightarrow C$ be carried out isothermally in a tubular reactor and in a tank reactor, with the same feed, then for equal conversion of A, the tube will produce a larger conversion to B than the tank, and in a shorter time.

Now let us denote by "tubular reactor system", a tubular reactor with bypass of raw material as in figure (2.2). Then a tank reactor with given conversion can always be represented by such a short-circuit tubular reactor system with the same conversion, for identical feed conditions. This is evident from figure (2.3). It can now be proved (see Appendix I #3) that in a yield problem involving the consecutive first order reactions $A \rightarrow B \rightarrow C$, a tank reactor can always be represented by a tubular reactor system in such a way that the holding time for the tubular reactor system is less than that for the tank.

The reaction system has also been represented on triangular coordinates for use in reactor design [20,21]. Only a single temperature is considered however and trajectories drawn for various feed conditions. In the preceeding discussion we have considered a fixed feed of pure A and a range of isothermal trajectories.

2.4.2 The output problem

The transformation $k = k_1/k_R$ may again be used as in #2.3. The solution to the state equations is now given by

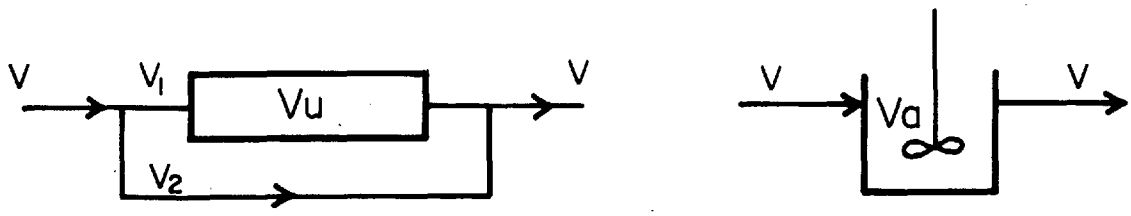


FIGURE 2.2 - TUBULAR REACTOR SYSTEM AND TANK REACTOR

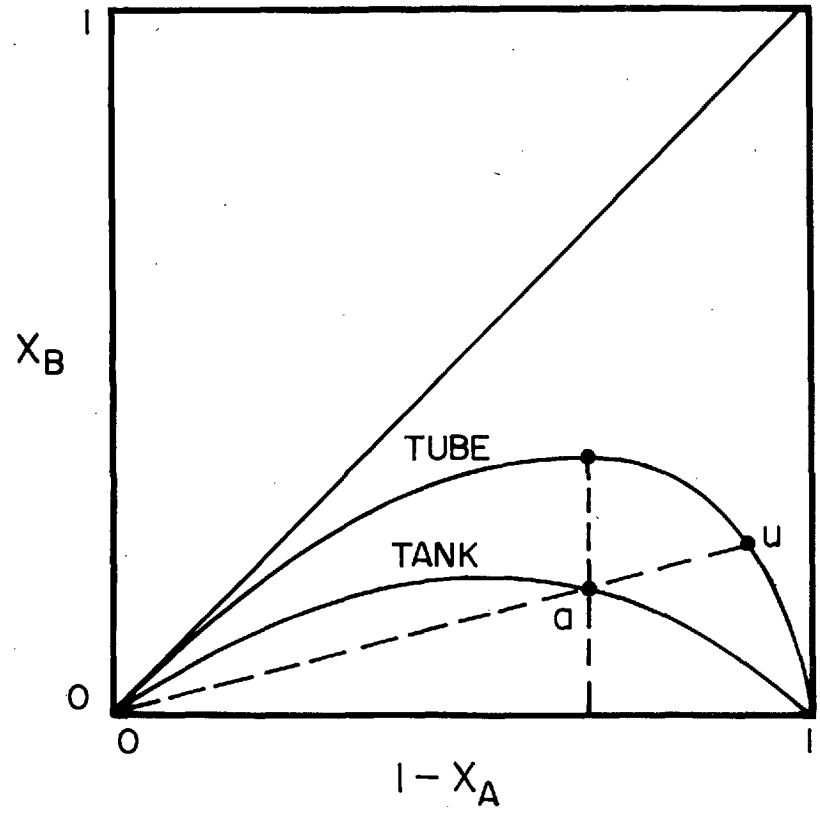


FIGURE 2.3 - ISOTHERMAL TRAJECTORIES FOR TUBE AND TANK FOR A → B → C

equations (2.8) and (2.9), with ϕ replaced by $k\phi$ and k by k^{r-1}.

Horn and Troltenier[16] state that for $r < 1$, conversion is not bounded by the kinetics. This is confirmed in figure (2.4c). The maximum x_{Be} decreases and moves to later ϕ as k decreases.

The stoichiometrically attainable region is not filled out when $r > 1$. This may be seen in figure (2.4a), where the isothermal attainable region for the tank is contained by that for the tube. Horn[17] has obtained the envelope of tubular isothermal trajectories directly by differentiation.

Use of k_R in the singular case $r = 1$ again implies $H_1 = H_2$. As shown in figure (2.4b), maximum x_{Be} is independent of k, being e^{-1} for the tube and 0.25 for the tank. These values can be predicted. It is clear from the figures that the situation alters drastically in the vicinity of $r = 1$, when the limits on the control will be important.

The isothermal attainable region for this reaction scheme is smaller than that for the reversible reaction, which would be expected from physical considerations.

2.5 THE REVERSIBLE REACTION WITH IRREVERSIBLE DECAY OF PRODUCT $A \underset{2}{\overset{1}{\rightleftharpoons}} B \xrightarrow{3} C$

This is a fairly common type of complex reaction[4]. An example with industrial potential is the catalytic dehydrogenation of ethanol into acetaldehyde, where ethyl acetate may be formed[22].

2.5.1 The yield problem

There are again two stoichiometrically independent reactions. The transformation $k = k_2/k_1$ has been used by Horn and Troltenier[16], which leads to

$$k_3/k_1 = ak^{-\alpha}, \tag{2.11}$$

where $$\alpha = \frac{E_3 - E_1}{E_1 - E_2} \quad \text{and} \quad a = \left(\frac{H_3}{H_1}\right)\left(\frac{H_2}{H_1}\right)^{\alpha} \tag{2.12}$$

The number of parameters to be specified has been reduced from six to two, and the six possible combinations for the magnitudes of the three activation energies may be grouped according to $\alpha > 0$ or $\alpha < 0$.

For linear kinetics, the systems equations for the tubular reactor are

$$\frac{dx_A}{d\phi} = - x_A + kx_B \qquad (2.13a)$$

$$\frac{dx_B}{d\phi} = x_A - (k + ak^{-\alpha})x_B \qquad (2.13b)$$

with $\phi = k_1 t$ and $x_A(0) = 1$, $x_B(0) = 0$. When integrated together with equation (1.12), these give

$$x_{Be} = \frac{\exp(-\mu_1\phi_e) - \exp(-\mu_2\phi_e)}{\mu_2 - \mu_1} \qquad (2.14)$$

$$x_{ce} = 1 + \frac{\mu_1 \exp(-\mu_2\phi_e) - \mu_2 \exp(-\mu_1\phi_e)}{\mu_2 - \mu_1}$$

where μ_1, μ_2 are the roots of

$$\mu^2 - (1 + k + ak^{-\alpha})\,\mu + ak^{-\alpha} = 0 \qquad (2.15)$$

and $\mu_1 \neq \mu_2$. The isothermal attainable region could be obtained by choosing a set (a, α) and investigating a range of k values for that set. This would be tedious and the differential equations (2.13) lend themselves readily to the use of an analogue computer.

These equations were patched on an EAI TR-10 analogue computer. The circuit was simple, requiring only two integrators, and is not shown here. Non-linear components were not incorporated, the parameters k and $ak^{-\alpha}$ being set on two separate potentiometers. An isothermal trajectory was recorded on an X-Y Variplotter for a particular (a,α), by holding k constant during integration. Successive isothermals could be generated for this (a,α) by altering the potentiometer settings for k and $ak^{-\alpha}$.

When $\alpha < 0$, the stoichiometrically attainable region is filled as $k \rightarrow 0$. The situation is interesting for $\alpha > 0$ as shown in figure (2.5). Now the stoichiometrically attainable region is not filled and the border of the isothermal attainable region is the envelope of all isothermal trajectories. It was found in practice that an upper limit $k_u = 1$ was sufficient to adequately describe this border.

Results obtained for $\alpha = 0$ (i.e. $E_1 = E_3$) are shown in figure (2.7). The effect of decreasing a is to cause the stoichiometrically attainable region to be filled as $k \rightarrow 0$. The curve $a = 1$, $k \rightarrow 0$ has been confirmed analytically.

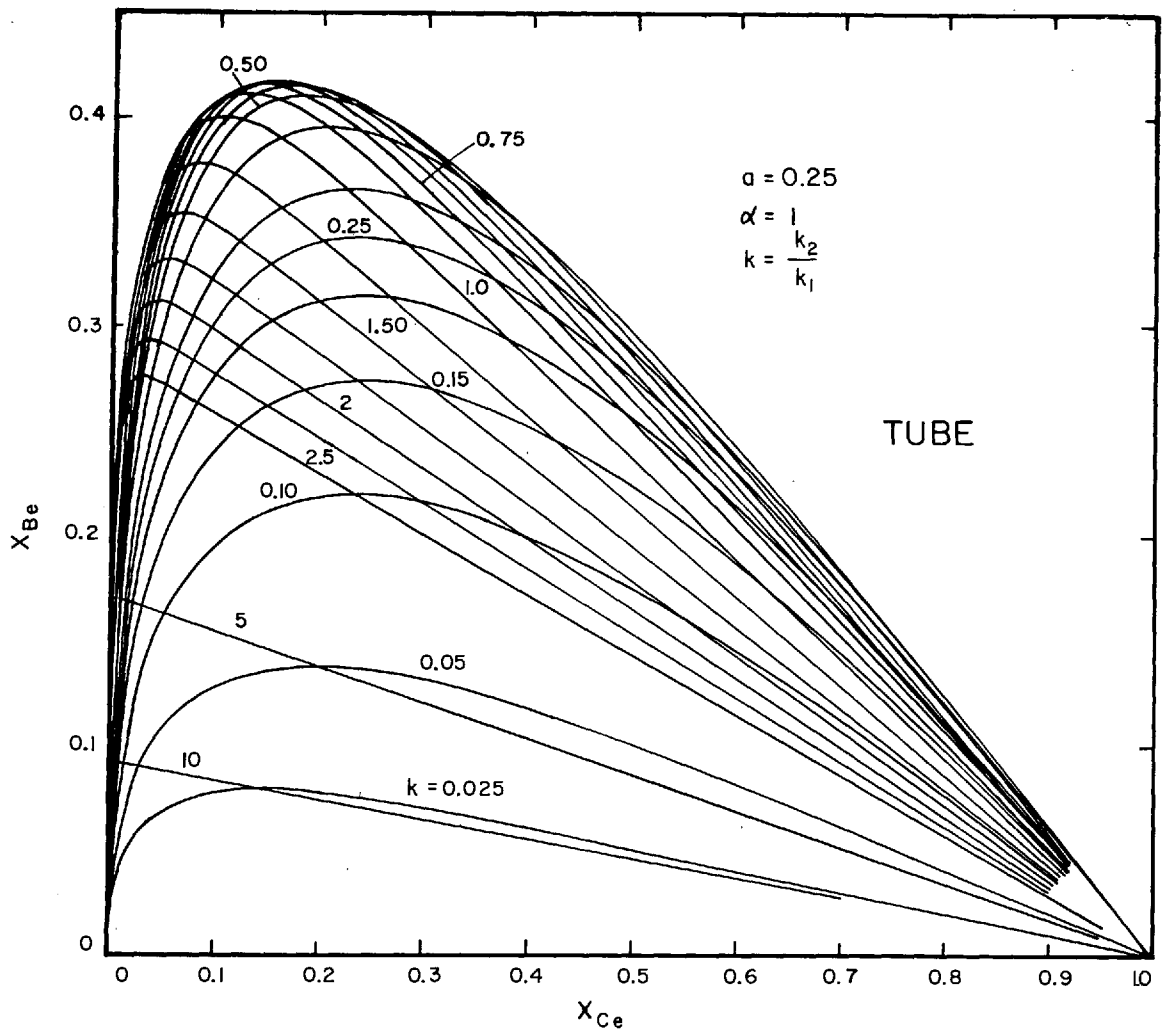


FIGURE 2.5- ISOTHERMAL TRAJECTORIES FOR $A \underset{2}{\overset{1}{\rightleftharpoons}} B \overset{3}{\rightarrow} C$ IN A YIELD PROBLEM

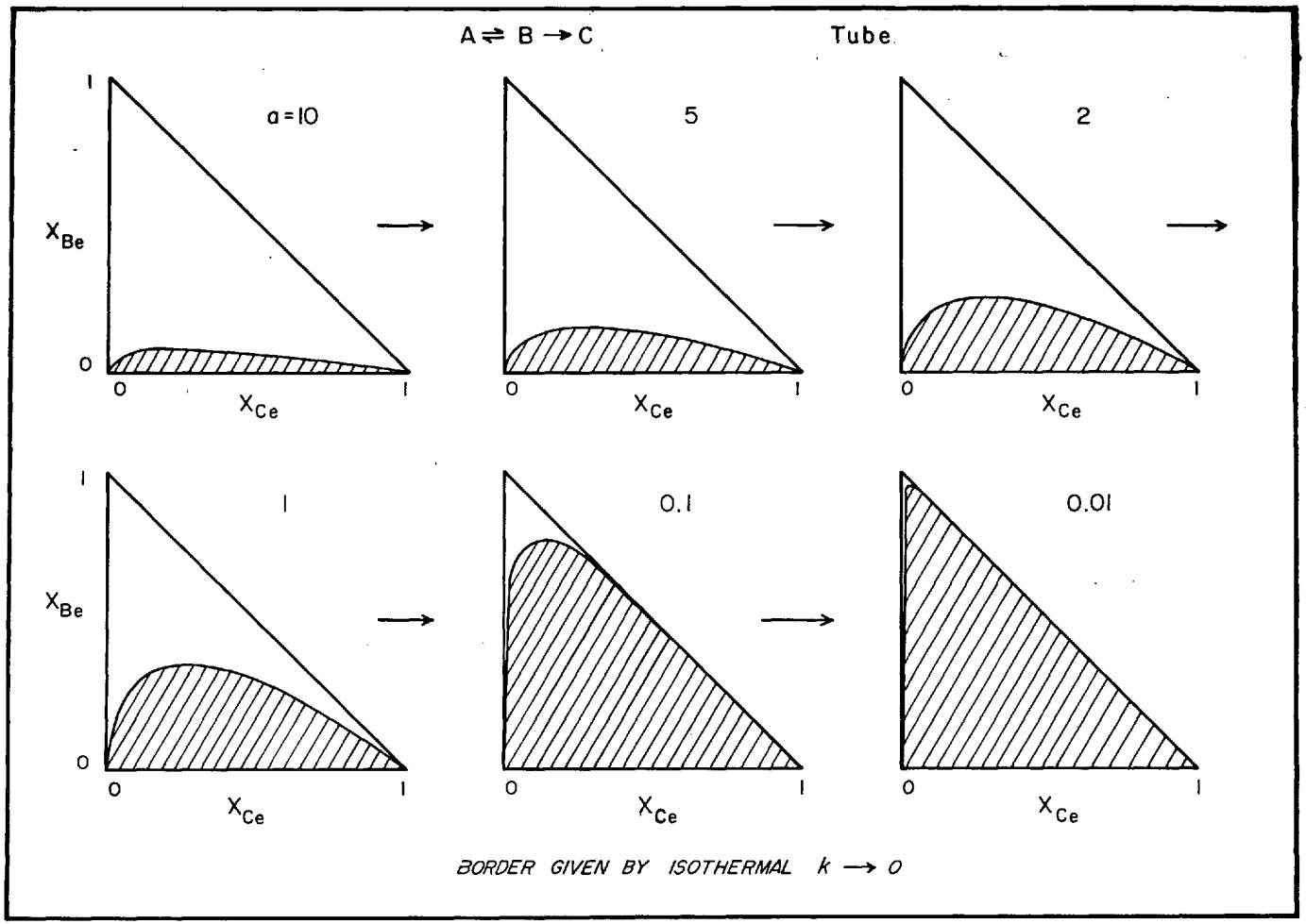


FIGURE 2.7 - EFFECT OF a ON THE ISOTHERMAL ATTAINABLE REGION FOR $\alpha = 0$

The above results agree with the observation of Horn and Troltenier[16], that when E_1 does not lie between E_2 and E_3, the system behaves qualitatively like the consecutive reactions $A \rightarrow B \rightarrow C$. They have calculated maximum conversion to B for the isothermal attainable region corresponding to $\alpha > 0$ and certain values of (a, α). For a single isothermal trajectory,

$$x_{Be}^{*}\ (\text{tube}) = \frac{1}{\mu_1}\left(\frac{\mu_2}{\mu_1}\right)^{\mu_2/\mu_1-\mu_2} \qquad \mu_1 \neq \mu_2 \qquad (2.16)$$

$$\phi_e^{*}\ (\text{tube}) = \frac{\ln \mu_1/\mu_2}{\mu_1 - \mu_2}$$

Hence maximum x_{Be} for the whole region is given by

$$x_{Be}\ (\text{max.}) = \max_{k}.\ x_{Be}^{*} \qquad (2.17)$$

We have obtained the complete border for these values of (a, α) (results not shown). Maximum x_{Be} for each region has been compared to the published values in table (2.1) and good agreement found.

Table 2.1

$A \rightleftharpoons B \rightarrow C$ in isothermal tubular reactor: Comparison of published values for x_{Be} (max.) with values obtained from the isothermal attainable region

α		0.2	1.0	4.0
a(s = 1)		0.582	0.25	0.0819
x_{Be} (max.)	Horn and Troltenier [16]	0.381	0.414	0.455
	Isothermal attainable region	0.378	0.413	0.453

$$a = \frac{\alpha^{\alpha}}{(1+\alpha)^{1+\alpha}} \quad \frac{1}{s^{1+\alpha}}$$

The systems equations for the tank are

$$x_{Be} = \frac{\phi}{(\mu_1 \phi + 1)(\mu_2 \phi + 1)}$$

$$x_{Ce} = \frac{\mu_1 \mu_2 \phi^2}{(\mu_1 \phi + 1)(\mu_2 \phi + 1)} \qquad (2.18)$$

with $\phi = k_1 \tau$ and μ_1, μ_2 the roots of (2.15). On an isothermal trajectory,

$$x_{Be}^{*}\ (\text{tank}) = (\mu_1^{\frac{1}{2}} + \mu_2^{\frac{1}{2}})^{-2}$$

$$\phi^{*}\ (\text{tank}) = (\mu_1 \mu_2)^{-\frac{1}{2}} \qquad (2.19)$$

It is of interest to note that if $\mu_1 \phi$ be replaced by ϕ and μ_2/μ_1 by k in the equations for $A \rightleftharpoons B \rightarrow C$, the resulting equations are similar to those for $A \rightarrow B \rightarrow C$. This is due to the form of the characteristic equation being the same for both reactions. Thus x_{Be} in (2.14) and (2.18) corresponds to $1/\mu_1$ of x_{Be} in (2.8) and (2.9) respectively. It can be shown that $\mu_1 > 0$ (see appendix II #2). Hence by analogy from #2.4.1, a larger x_{Be} can be attained in a shorter time for $A \rightleftharpoons B \rightarrow C$ carried out isothermally in a tubular reactor, than in a tank reactor at the same temperature.

The equations for x_{Ce} become identical for both reaction systems, for tube and tank respectively. Hence x_{Ce} will exhibit the same behaviour in both cases, if the above parameters be transposed.

Similarly x_{Be}^{*} and ϕ^{*} are $1/\mu_1$ of the corresponding values for $A \rightarrow B \rightarrow C$ (see e.g. reference 11 for the equations

to the latter system). Since $\mu_1 > 0$, we can conclude that equation (2.10) will also hold for $A \rightleftharpoons B \rightarrow C$.

Some typical results for the tank are shown in figure (2.6). These display the same qualitative behaviour as the tube for each of the three cases $\alpha < 0$ (not shown), $\alpha > 0$ and $\alpha = 0$. The isothermal attainable region for the tank is in each case smaller than the corresponding region for the tube.

An explanation for the stoichiometrically attainable region being filled when $\alpha < 0$ is as follows. As $k_2 \rightarrow 0$, the present system approaches $A \rightarrow B \rightarrow C$; we would therefore expect the stoichiometrically attainable region to be filled as (k_2/k_1) and (k_3/k_1) both tend to zero. This means k and $ak^{-\alpha}$ tend to zero, or $\alpha < 0$. For the singular case $\alpha = 0$, the stoichiometrically attainable region will be filled as $k \rightarrow 0$ and $a \rightarrow 0$.

2.5.2 <u>The output problem</u>

The transformation $k = k_1/k_R$ will again be used, when $k_2/k_R = k^r$ with $r = E_2/E_1$. It can further be shown that $k_3/k_R = ak^s$, where $s = E_3/E_1$ and a is the same as defined

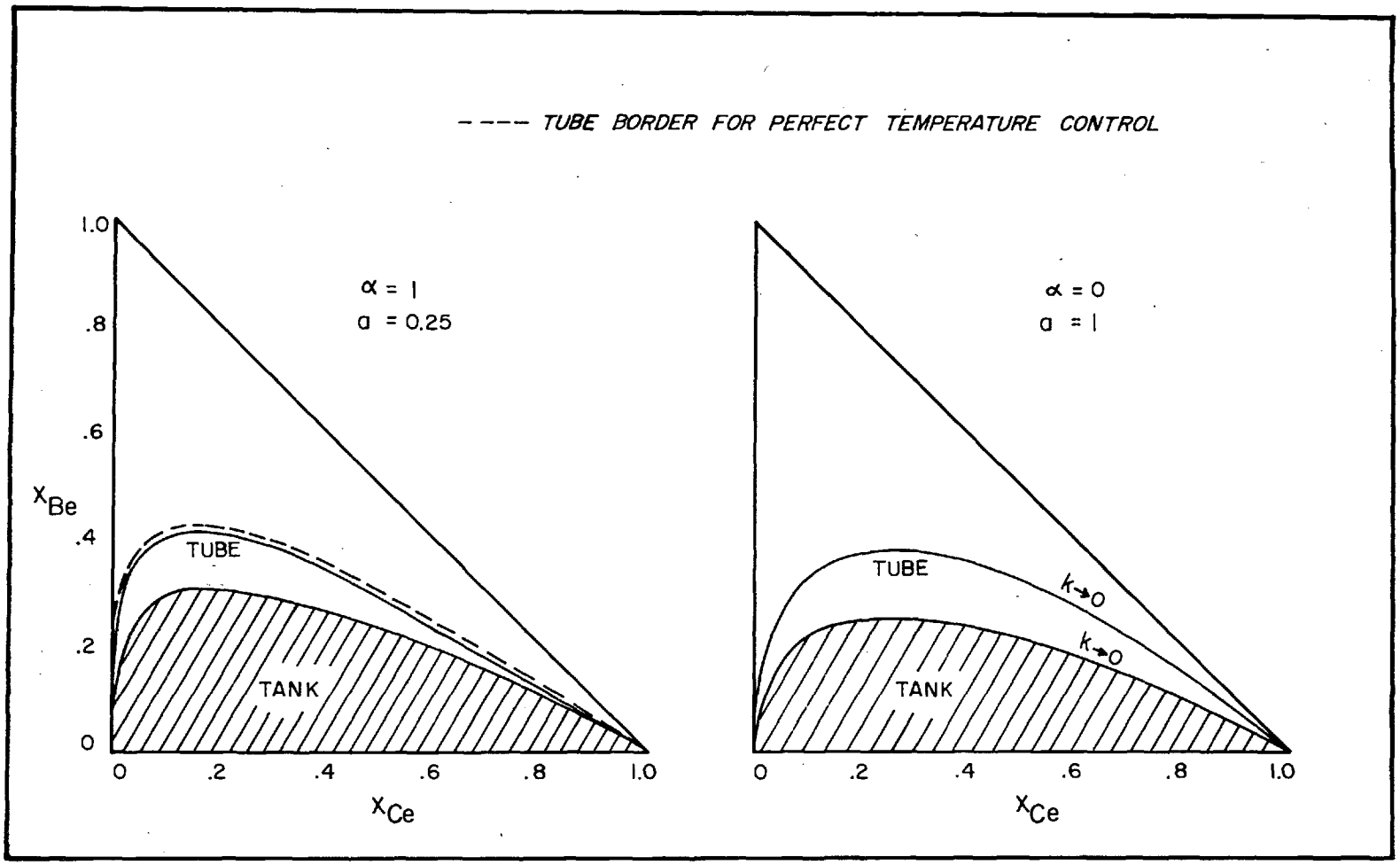


FIGURE 2.6 - ISOTHERMAL ATTAINABLE REGION FOR $A \rightleftharpoons B \rightarrow C$ IN A YIELD PROBLEM

in #2.5.1 (see Appendix II #1). There are now three parameters to be specified. Note that α in #2.5.1 is related to r and s through

$$\alpha = (s - 1)/(1 - r) \tag{2.20}$$

The differential equations governing the behaviour of the tubular reactor are now

$$\frac{dx_A}{d\phi} = - kx_A + k^r x_B; \quad x_A(0) = 1$$

$$\frac{dx_B}{d\phi} = kx_A - (k^r + ak^s)x_B; \quad x_B(0) = 0 \tag{2.21}$$

with $\phi = k_R' t$. The solution to the state equations for both tube and tank can again be obtained from the corresponding equations for the yield problem. Now ϕ in the yield problem must be replaced by $k\phi$, k by k^{r-1} and μ_i by μ_i/k (i = 1,2). The μ_i are then the roots of

$$\mu^2 - (k + k^r + ak^s)\ \mu + ak^{s+1} = 0 \tag{2.22}$$

The same conclusions will now be valid for these roots (i.e. $\mu_i > 0$ (i = 1,2) and $\mu_1 \neq \mu_2$) as for the roots of (2.15).

The isothermal attainable region has again been obtained for the three cases $\alpha < 0$, $\alpha = 0$ and $\alpha > 0$. Since α is fixed by r and s in equation (2.20), this leaves some choice in deciding which values to give r and s to achieve a given α. For purposes of comparison, the same a and α values have been used as in the yield problem.

The value $\alpha = 0$ has been achieved with s = 1, and figure (2.8b) shows this isothermal attainable region for a = 1 and r = 2. Since $k_2/k_1 = k^{r-1}$, the control k is the same as in the yield problem. The stoichiometrically attainable region is not filled for either tube or tank and the attainable region for the tube contains that for the tank.

Figure (2.8c) corresponds to a = 10, r = 2 and s = 3 (i.e. $\alpha = -2$). The control k is again the same as in the yield problem and similar qualitative behaviour is observed as for $A \rightarrow B \rightarrow C$ with $E_2 > E_1$. This is in agreement with the statement of Horn and Troltenier[16], that for $E_2 > E_1$ and $E_3 > E_1$ only the output problem is of interest.

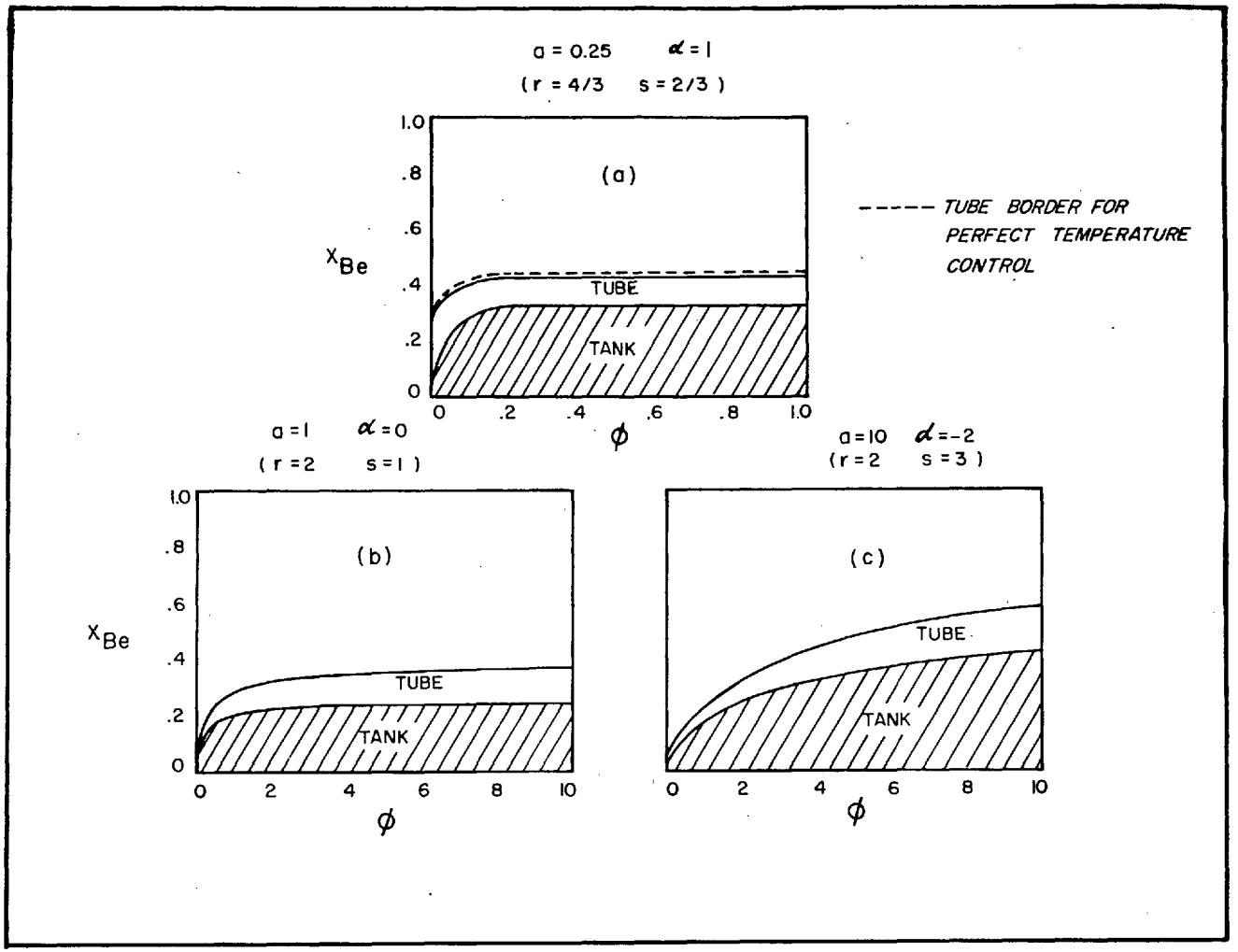


FIGURE 2.8 ISOTHERMAL ATTAINABLE REGION FOR $A \rightleftharpoons B \rightarrow C$ IN AN OUTPUT PROBLEM

To obtain $\alpha = 1$ (with $a = \frac{1}{4}$) we choose $r = 4/3$, $s = 2/3$. This makes the reversible reaction exothermic. Terms containing $k^{4/3}$ and $k^{2/3}$ will now be introduced into (2.22). Let us redefine control as

$$K = k^{1/3}, \tag{2.23}$$

then K is a monotone increasing function of the temperature T and $K \geq 0$. Also $K = k_2/k_1$, so it is the same as k in the yield problem. Equation (2.22) now becomes

$$\mu^2 - K^2(K + \tfrac{1}{2})^2\mu + \tfrac{1}{4}K^5 = 0 \tag{2.24}$$

A programme has been written for the IBM 7090 to obtain values for x_{Be} and x_{Ce} with time in the tubular reactor, for a number of K values. The differential equations (2.21) have also been patched on an EAI TR-10 analogue computer. To avoid inaccuracy, no non-linear components were included and separate potentiometers were used to set the values of K^4, K^3 and $\frac{1}{4}K^2$. Figure (2.8a) indicates the results schematically; these results check with the digital computer solutions within the accuracy of the analogue equipment. The stoichiometrically attainable region is not filled in the space (x_{Be}, ϕ).

A similar result is obtained for the tank in figure (2.8a), by calculating isothermal trajectories from the state equations. The isothermal attainable region is smaller than that for the tube.

2.6 SUMMARY

In the yield problem, the stoichiometrically attainable region is essentially filled for all the reaction systems studied, except $A \underset{2}{\overset{1}{\rightleftharpoons}} B \xrightarrow{3} C$ with E_1 between E_2 and E_3. In the output problem, the exceptions are $E_2 > E_1$ for both $A \underset{2}{\overset{1}{\rightleftharpoons}} B$ and $A \xrightarrow{1} B \xrightarrow{2} C$; also $A \underset{2}{\overset{1}{\rightleftharpoons}} B \xrightarrow{3} C$, when E_1 is between E_2 and E_3, when $E_1 < E_2$, $E_1 < E_3$ and when $E_1 = E_3$, $E_1 > E_2$.

For all the cases studied, the isothermal attainable region for the tube contained that for the tank.

In the following chapter, we will investigate more sophisticated control policies for the tubular reactor, for special cases where the stoichiometrically attainable region is not filled. This will lead to an enlarged attainable region.

CHAPTER THREE

THE ATTAINABLE REGION FOR PERFECT TEMPERATURE CONTROL

The attainable region for the tubular reactor will now be developed, with perfect temperature control as an admissible control policy. Results will be compared to the isothermal attainable region of the preceeding chapter.

3.1 THE OUTPUT PROBLEM FOR $A \underset{2}{\overset{1}{\rightleftharpoons}} B$

We will consider the exothermic reaction, i.e. $E_2 > E_1$. It has been recognised for some time that in an output problem, an optimal temperature profile may be found when this reaction is carried out in a tubular reactor. As a result the reaction has received much attention in optimisation studies, some of which are listed by Denbigh [12].

The optimal trajectory generates the border of the attainable region [17]. Optimal policy is to maximise the rate with respect to temperature at every point along the reactor. The control which makes the rate stationary is

$$k^* = (1 - x_B/rx_B)^{1/r-1} \qquad r > 1 \qquad (3.1)$$

where symbols have the meaning in #2.3. Since x_B increases along the reactor, k^* and hence temperature will decrease from inlet to outlet.

The optimal control may be substituted into the state equations and the latter integrated to yield the attainable region border. For r = 2, this gives [17]

$$\phi_e = \frac{4x_{Be}}{1 - x_{Be}} + 4 \ln (1 - x_{Be}) \qquad (3.2)$$

The border has been inserted in figure (2.1a). Attainable region and isothermal attainable region do not differ by much. This difference will increase as $E_2/E_1 \longrightarrow 1$ [14].

The border of the attainable region can also be found using the tables presented by Horn and Troltenier [16].

3.2 THE OUTPUT PROBLEM FOR $A \xrightarrow{1} B \xrightarrow{2} C$

We again consider $E_2 > E_1$. An optimal control policy will maximise conversion to desired product B in a given reaction time ϕ_e. The set of optimal temperature profiles will generate a succession of optimal trajectories, whose

envelope in the (x_{Be}, ϕ_e) space will constitute the border of the attainable region.

Bilous and Amundson[23] obtained an expression for optimal control policy, though they expressed misgivings on physical grounds over the apparent independence of their solution on the relative magnitudes of E_1, E_2. Aris[24] indicated subsequently that their results were only valid for $E_2 \succ E_1$, a problem later resolved by Coward and Jackson (see below). The problem has been solved in parametric representation by Horn[18] with a method which is essentially the Pontryagin Maximum Principle[10]. Digital solutions are presented in tabular form by Horn and Troltenier[16].

These tables have been used to obtain the border of the attainable region in figure (2.4a), for r = 2 and various end temperatures T_e (corresponding to different ϕ_e). The data has been supplemented from tables given in the appendix to Horn's dissertation[17]. There is little difference between the optimal reactor and an isothermal reactor with the same conversion. The larger the conversion, the smaller is this difference[18].

Coward and Jackson[25] use the consecutive reaction scheme to show that care must be taken in applying the Pontryagin Maximum Principle[10] in an optimisation problem. Since this provides necessary but not sufficient conditions for optimality, it is possible to obtain temperature profiles which satisfy the principle but which are not optimal temperature profiles. However for $E_2 > E_1$ and feed of pure A, their conclusions are in agreement with the controls used to generate our results.

3.3 THE YIELD PROBLEM FOR $A \underset{2}{\overset{1}{\rightleftharpoons}} B \xrightarrow{3} C$

We have shown that when E_1 lies between E_2 and E_3, the stoichiometrically attainable region is not filled. For the yield problem this does not necessarily imply that the reversible reaction be exothermic.

The concept of "instantaneous yield" has been introduced by Denbigh[26]. For a yield problem involving two stoichiometrically independent reactions, Horn shows that the optimal policy is to maximise instantaneous yield at every point along the reactor[18]. This may be regarded as analogous to maximising the rate in the reversible reaction of #3.1.

Consider once again the systems equations (2.13) for the tubular reactor. The control k is now $k(\phi)$. For instantaneous yield to be stationary with respect to k,

$$\frac{\partial}{\partial k}\left(\frac{v_2}{v_1}\right) = 0 \tag{3.3}$$

where v_1 and v_2 are the RHS of (2.13a) and (2.13b) respectively. This leads to a relationship for the optimal control

$$k^* = \frac{\alpha}{1+\alpha}\frac{1}{X} \tag{3.4}$$

where $X = x_B/x_A$ and is given by

$$\frac{dX}{d\phi} = 1 + X(1 - k - ak^{-\alpha}) - kX^2$$

$$X(0) = 0 \tag{3.5}$$

Equation (3.5) has been obtained by combining (2.13a) and (2.13b).

We will follow a procedure similar to that adopted by Horn[18] in the output problem for $A \rightarrow B \rightarrow C$. Substituting for k^* in (3.5) gives

$$\frac{dX}{d\phi} = \frac{1}{1+\alpha}\left[1 + X - \frac{aX^{1+\alpha}(1+\alpha)^{1+\alpha}}{\alpha^{\alpha}}\right] \qquad (3.6)$$

This may be integrated to yield

$$\phi_e = \int_0^{X_e} \frac{(1+\alpha)\,dX}{1 + X - aX^{1+\alpha}(1+\alpha)^{1+\alpha}\alpha^{-\alpha}} \qquad (3.7)$$

Substituting for k^* in (2.13a) and rewriting gives

$$\frac{d \ln x_A}{d\phi} = \frac{-1}{1+\alpha} \qquad (3.8)$$

Divide (3.8) by (3.6):

$$\frac{d \ln x_A}{dX} = \frac{-1}{1 + X - aX^{1+\alpha}(1+\alpha)^{1+\alpha}\alpha^{-\alpha}} \qquad (3.9)$$

Hence

$$\ln x_{Ae} = -\int_0^{X_e} \frac{dX}{1 + X - aX^{1+\alpha}(1+\alpha)^{1+\alpha}\alpha^{-\alpha}} \qquad (3.10)$$

Now

$$x_{Be} = x_{Ae} X_e \tag{3.11}$$

$$= X_e \exp\left[-\int_o^{X_e} \frac{dX}{1 + X - aX^{1+\alpha} (1 + \alpha)^{1+\alpha} \alpha^{-\alpha}}\right] \tag{3.12}$$

Put $X/X_e = \Psi$. Then from (3.7), (3.12):

$$x_{Be} = X_e \exp\left[-X_e I_1 (X_e, a, \alpha)\right]$$

$$\phi_e = (1 + \alpha) X_e I_1 (X_e, a, \alpha) \tag{3.13}$$

with

$$I_1 (X_e, a, \alpha) = \int_o^1 \frac{d\Psi}{1 + X_e \Psi - a\left[X_e \Psi (1 + \alpha)\right]^{1+\alpha} \alpha^{-\alpha}} \tag{3.14}$$

Equations (3.13) give the border of the attainable region in parametric form. For $\alpha = 1$, $a = \frac{1}{4}$ (corresponding to the isothermal case #2.5.2), equation (3.12) becomes

$$x_{Be} = X_e \exp\left[-\int_0^{X_e} \frac{dX}{1 + X - X^2}\right] \qquad (3.15)$$

This may be integrated to give

$$x_{Be} = X_e\left[B(0)/B(X_e)\right]^{1/\sqrt{5}} \qquad (3.16)$$

where

$$B(X_e) = \frac{\frac{2}{\sqrt{5}}(X_e - \tfrac{1}{2}) + 1}{\frac{2}{\sqrt{5}}(X_e - \tfrac{1}{2}) - 1} \qquad (3.17)$$

By choosing a series of X_e values, x_{Be} can be found from (3.16) and hence x_{Ae} from (3.11). Then x_{Ce} is obtained using (1.12) and the border of the attainable region may be plotted as in figure (2.6). Again attainable region and isothermal attainable region differ by very little. The border of the attainable region corresponds to a single optimal trajectory.

The solution has also been found by analogue computer. For the optimal control given by (3.4), the systems equations (2.13) reduce to

$$\frac{dx_A}{d\phi} = \frac{-x_A}{1 + \alpha} ; \qquad x_A(0) = 1$$

$$\frac{dx_B}{d\phi} = \frac{x_A}{1 + \alpha} - a\left(\frac{1 + \alpha}{\alpha x_A}\right)^{\alpha} x_B^{1+\alpha}; \qquad x_B(0) = 0 \tag{3.18}$$

These equations have been patched on the EAI TR-10 for $a = \frac{1}{4}$ and $\alpha = 1$. A quarter square multiplier and servo-multiplier were used to generate x_B^2 and x_B^2/x_A respectively. The trajectory mapped out on the Variplotter was identical to the attainable region border derived analytically.

Now x_{Be} goes through a maximum on this border. The maximum is given by

$$\frac{dx_B}{d\phi} = 0 \qquad \phi = \phi_e \tag{3.19}$$

i.e. from (2.13b) and (3.4) we get

$$a\, x_e^{1+\alpha} = \alpha^{\alpha} (1 + \alpha)^{-(1+\alpha)} \tag{3.20}$$

Substitute (3.20) into (3.14), when (3.13) transforms to

$$x_{Be}^{*} = X_e \exp\left[-X_e\, I_2(1 + \alpha,\, X_e)\right] \qquad (3.21)$$

where

$$I_2(1 + \alpha,\, X_e) = \int_0^1 \frac{d\Psi}{1 - \Psi^{1+\alpha} + X_e \Psi} \qquad (3.22)$$

These relationships for maximum x_{Be} are presented by Horn and Troltenier[16]. They obtain x_{Be}^{*} for various combinations $(1 + \alpha,\, X_e)$, including the cases in table (2.1), where $X_e \equiv s$. This enables a comparison to be drawn between x_{Be}^{*} on the attainable region border and $x_{Be}(\text{max.})$ on the border of the isothermal attainable region. Little difference is found between isothermal and optimal values, though X_e changes by a factor of 10^4 and α by a factor of 20.

We can compare the coordinates of the maximum turning point $(x_{Be}^{*},\, x_{Ce}^{*})$ in figure (2.6) with values published by the above authors. For $\alpha = 1$, $a = \frac{1}{4}$ (corresponding in (3.20) to $X_e = 1$) they report $x_{Be}^{*} = 0.423$. Then

$$x_{Ce}^{*} = 1 - x_{Ae}^{*} - x_{Be}^{*}$$

$$= 1 - (X_e + 1)\exp(-X_e I_2)$$

$$= 0.154 \text{ for } X_e = 1, \ \alpha = 1. \qquad (3.23)$$

These values are in agreement with our graphical results.

3.4 THE OUTPUT PROBLEM FOR $A \underset{2}{\overset{1}{\rightleftharpoons}} B \xrightarrow{3} C$

We now investigate the output problem for the parameter values used in the preceeding section. The only published attainable region for a 3-D output problem is due to Horn [1,28], who considered the system of parallel reactions

$$A \begin{cases} \xrightarrow{1} B \\ \xrightarrow{2} C \end{cases} \qquad (3.24)$$

with $E_2 > E_1$. In his case however, the stoichiometrically attainable region in the 2-D yield problem is filled out.

3.4.1 Generation of the border of the attainable region

Suppose that at a given time ϕ_e, the section of the output problem attainable region is a closed set in (x_{Be}, x_{Ce}) space as in figure (3.1). Such a shape is reasonable from physical considerations and the yield problem solution #3.3.

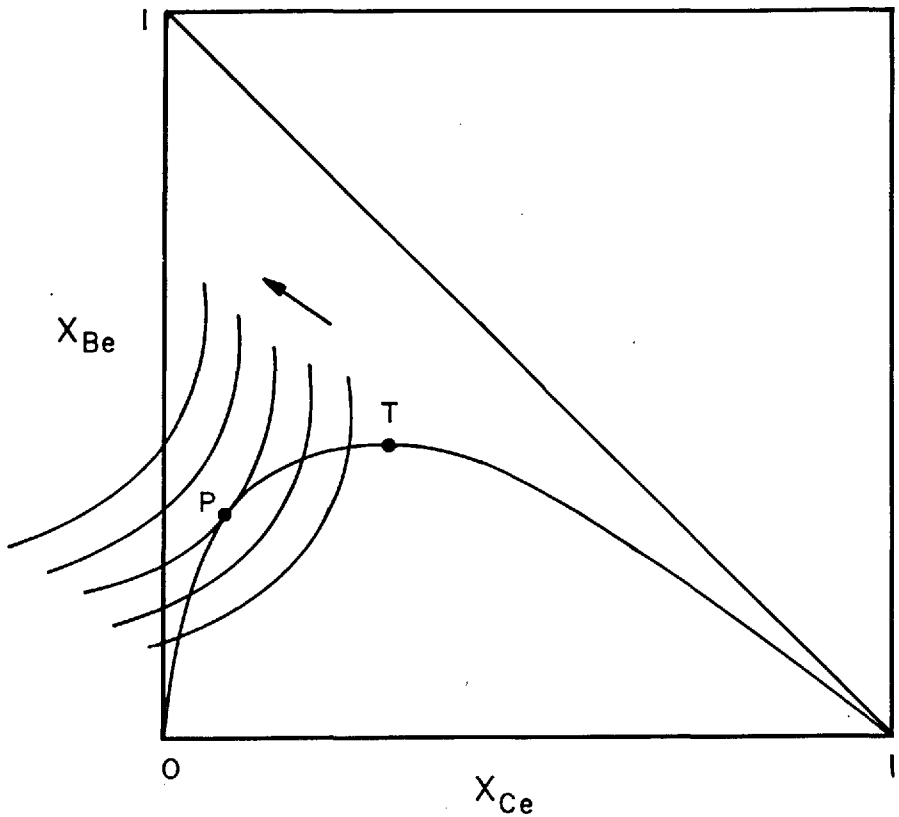
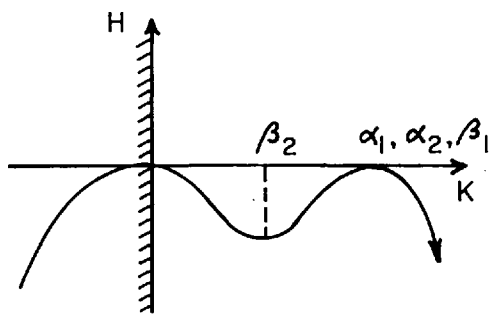


FIGURE 3.1 - SECTION OF ATTAINABLE REGION FOR $A \rightleftharpoons B \rightarrow C$ AT $\phi = \phi_e$



$\lambda_1 > 0$ (all λ)

FIGURE 3.3 - THE HAMILTONIAN AS A FUNCTION OF CONTROL FOR $b = 1/3$

Horn has suggested[1] that border points may be found by maximising linear combinations of the output variables. He also considers non-linear objective function contours when dealing with the reversible exothermic reaction[29]. Such non-linear contours have been drawn in figure (3.1), for

$$\frac{\partial M}{\partial x_{Be}} > 0 \text{ and } \frac{\partial M}{\partial x_{Ce}} < 0 \qquad (3.25a)$$

The arrow indicates the direction of increasing objective function M. All border points P between the origin and T will be generated by maximising M. Border points to the right of T will also be generated by maximising M, when

$$\frac{\partial M}{\partial x_{Be}} > 0 \text{ and } \frac{\partial M}{\partial x_{Ce}} > 0 \qquad (3.25b)$$

Although we have shown a convex set in figure (3.1), the above arguments will hold for any closed set in (x_{Be}, x_{Ce}). We now require a method for maximising M subject to the state equations (1.1) as constraints. Such a method is the Pontryagin Maximum Principle.

3.4.2 The Pontryagin Maximum Principle

Consider a physical system described by the state equations (1.1). The problem is to choose that control policy $T(t)$, bounded by (1.7) and in $0 \leq t \leq t_e$, such that an objective function

$$M = M(x_{1e}, x_{2e}, \ldots, x_{ne}) \tag{3.26}$$

is maximised.

In the solution of this problem by the Pontryagin formulation [10,27], adjoint variables λ_i are introduced, which satisfy

$$\frac{d\lambda_i}{dt} = -\frac{\partial H}{\partial x_i}, \qquad i = 1,2,\ldots,n \tag{3.27}$$

where H is the Hamiltonian, defined by

$$H = \sum_{j=1}^{n} \lambda_j v_j \tag{3.28}$$

The state equations expressed in terms of the Hamiltonian are then

$$\frac{dx_i}{dt} = \frac{\partial H}{\partial \lambda_i} \qquad i = 1,2,\ldots,n \tag{3.29}$$

with initial conditions $x_i(0) = x_{io}$. The end conditions on the λ_i are

$$\lambda_{ie} = \frac{\partial M}{\partial x_{ie}} \qquad i = 1,2,\ldots,n \tag{3.30}$$

Now the Pontryagin Maximum Principle states that to maximise M, it is necessary to choose T(t) such that H is maximised at every point along the trajectory.

3.4.3 Optimal control policy

The state equations (3.29) may be obtained for the present system from (2.21) and (1.12).

$$v_1 = \frac{dx_B}{d\phi} = k(1 - x_B - x_C) - (k^r + ak^s)\, x_B$$

$$v_2 = \frac{dx_C}{d\phi} \equiv ak^s\, x_B \tag{3.31}$$

with

$$x_B(0) = x_C(0) = 0 \tag{3.32}$$

Now to create border points, M must be maximised when $\lambda_{1e} > 0$, from (3.25) and (3.30). This is independent of the sign of λ_{2e}. For $\lambda_{2e} < 0$, points to the left of the maximum turning point on the border will be generated; the remaining border points will be found when $\lambda_{2e} > 0$.

The Hamiltonian in (3.28) now becomes

$$H = \lambda_1 \left[k(1 - x_B - x_C) - (k^r + ak^s)\, x_B\right] + \lambda_2 ak^s x_B \quad (3.33)$$

By Pontryagin, it is necessary for H to be maximised at every point when $\lambda_{1e} > 0$ to generate border points. Let us examine the Hamiltonian. In our case $a = \frac{1}{4}$, $r = 4/3$ and $s = 2/3$. We have redefined control in equation (2.23) as $K = k^{1/3}$. Hence (3.33) becomes

$$H = \lambda_1 \left[K^3(1 - x_B - x_C) - (K^4 + \tfrac{1}{4}K^2)\, x_B\right] + \lambda_2 K^2 x_B/4 \quad (3.34)$$

The Hamiltonian has been plotted as a function of control K in figure (3.2). The figure refers to a time ϕ and $\lambda_{1e} > 0$; calculations on which it is based may be found in Appendix III #1. Let us denote the ratio λ_2/λ_1 by λ. Then for all three cases $\lambda < 1$, $\lambda = 1$ and $\lambda > 1$, the Hamiltonian will be maximised for $\lambda_1 > 0$ with the control

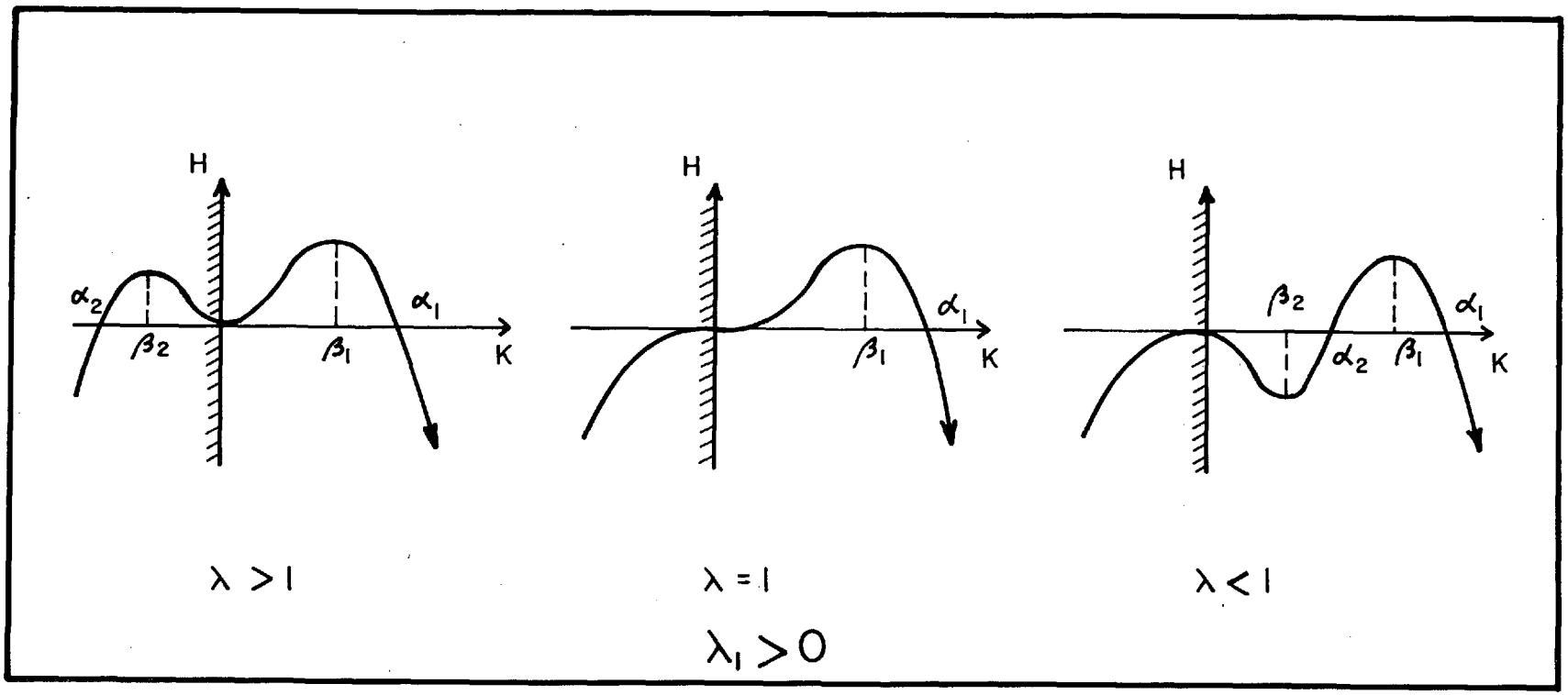


FIGURE 3.2 - THE HAMILTONIAN AS FUNCTION OF CONTROL

$$K^* = \beta_1 \qquad 0 \leq \beta_1 \leq K_u$$

$$K^* = K_u \qquad \beta_1 \geq K_u \tag{3.35}$$

Here β_1 is given from Appendix III #1 by

$$\beta_1 = \frac{3}{8X}(1 + b) \tag{3.36}$$

with

$$X = x_B/(1 - x_B - x_C) \tag{3.37}$$

as in (3.11), and

$$b = \left[1 + \frac{8}{9}(\lambda - 1)X^2\right]^{\frac{1}{2}} \tag{3.38}$$

We must now examine the sign of λ_1. The adjoint equations (3.27) become

$$\frac{d\lambda_1}{d\phi} = K^2(K + \tfrac{1}{2})^2 \lambda_1 - K^2 \lambda_2/4 \tag{3.39a}$$

$$\frac{d\lambda_2}{d\phi} = K^3 \lambda_1 \tag{3.39b}$$

These equations can be used to show that λ_1 will not change sign along any trajectory, optimal or otherwise, as long as

$\lambda(0) = \lambda_2(0)/\lambda_1(0)$ is chosen $< \rho_1$, where

$$\rho_1 = \Theta\left[1 + (1 - 4K/\Theta^2)^{\frac{1}{2}}\right]$$

and $$\Theta = (2K + 1)^2/2 \qquad (3.40)$$

The proof may be found in Appendix III #2. We will show later that it is unnecessary to choose $\lambda(0) > \rho_1$.

Now if $\lambda_1(0) > 0$, this means that $\lambda_{1e} > 0$ since $\lambda_1(\phi)$ does not change sign along a trajectory. Thus we must maximise M to create border points at any ϕ_e. Hence by Pontryagin we must maximise H for all ϕ and the optimal control policy is given by (3.35). If on the other hand $\lambda_1(0) < 0$, then $\lambda_{1e} < 0$ and we must minimise M and hence H. Again (3.35) will give the optimal control. As long as $\lambda(0) < \rho_1$, border points will be generated by the control policy (3.35).

Finally let us remark that the control transformation (2.23) has not altered the problem. Although algebraically more involved, the Hamiltonian could still be discussed in terms of control k and similar conclusions reached to those above.

3.4.4 Solution of the optimal problem

We must solve simultaneously the systems equations

$$\frac{dx_B}{d\phi} = K^2 \left[K(1 - x_C) - (K + \tfrac{1}{2})^2 x_B \right] \; ; \quad x_B(0) = 0$$

$$\frac{dx_C}{d\phi} = \frac{K^2}{4} \; x_B \; ; \qquad x_C(0) = 0 \tag{3.41}$$

together with their adjoint equations (3.39). The end conditions on the adjoint variables are given by (3.30) and optimal control K* by (3.35). We are dealing with a two-point boundary value problem since initial conditions on $\underline{x}$ and final conditions on $\underline{\lambda}$ are given.

Since the adjoint equations are linear in the adjoint variables λ_1, λ_2, we are only interested in their ratio λ and not their individual values. This is since a $\underline{\lambda}$ satisfying (3.39) may be multiplied by any constant and it will still be a solution of (3.39). Combining (3.39a) and (3.39b) gives

$$\frac{d\lambda}{d\phi} = \frac{K^2}{4} \left[\lambda^2 - (2K + 1)^2 \lambda + 4K \right] \tag{3.42}$$

The forward calculation method[1,29] may be used to solve (3.41) and (3.42) simultaneously, together with the optimal condition (3.35). Initial conditions on the state variables are given in (3.41). Each $\lambda(0)$ chosen will cause one reaction path to be traced out, and since all points on this reaction path will be optimal for some appropriately chosen M, the reaction path will lie on the border of the attainable region. Such a path will be called an optimal trajectory. By calculating a set of these trajectories for different $\lambda(0)$, the whole border can be found. Each optimal trajectory will commence at the origin (i.e. $x_B(0) = x_C(0) = 0$) and end at $x_C = 1$.

An alternate procedure may also be adopted, which makes use of the fact that the Hamiltonian is stationary along an optimal trajectory[27].

$$\sum_{i=1}^{n} \lambda_i v_i = C_1 \quad \text{(constant)} \tag{3.43}$$

For linear kinetics it can further be shown[18] that along any trajectory, not necessarily one that is optimal,

$$\sum_{i=1}^{n} \lambda_i x_i = C_2 \quad \text{(constant)} \tag{3.44}$$

If the Hamiltonian be maximised with a control which is not at its upper or lower bound,

$$\frac{\partial H}{\partial K} = \sum_{i=1}^{n} \lambda_i \frac{\partial v_i}{\partial K} = 0 \tag{3.45}$$

Horn has shown[18] that when n = 2, equations (3.43) - (3.45) may be used to eliminate the adjoint variables λ_i. A condition is then obtained for the output problem which is similar to the maximisation of instantaneous yield in the yield problem.

$$\frac{\partial}{\partial K}\left(\frac{v_2}{v_1}\right) = \frac{C}{v_1^2}\left[x_1 \frac{\partial v_2}{\partial K} - x_2 \frac{\partial v_1}{\partial K}\right] \tag{3.46}$$

where C is given by

$$C = \frac{\frac{\partial M}{\partial x_{1e}} v_{1e} + \frac{\partial M}{\partial x_{2e}} v_{2e}}{\frac{\partial M}{\partial x_{1e}} x_{1e} + \frac{\partial M}{\partial x_{2e}} x_{2e}} \tag{3.47}$$

This enables optimal control to be found as a function of the state variables $\underline{x}$ and end condition $\frac{\partial M}{\partial \underline{x}_e}$. The systems equations can then be integrated for various end conditions.

This method employs only the stationarity of the Hamiltonian and is not as strong as that in which H is maximised. No specific end conditions are given in our problem, so an iteration procedure would not be necessary for a forward calculation. There is thus no advantage in eliminating the adjoint variables.

3.4.5 Numerical integration procedure

An integration routine known as MIDAS[30] (Modified Integration Digital Analogue Simulation) was used on the IBM 7090. This requires an analogue block diagram to be first drawn from the relevant equations. Programming using MIDAS consists of interconnecting the elements of the block diagram. The source of inputs to each element must be specified according to certain rules, e.g. inputs may have to be given in a definite order. (This is clearly unnecessary for a summing element; however, for a dividing block, a distinction must be drawn between divisor and dividend in the inputs).

The routine was tested with the yield problem #3.3 and gave solutions consistent with those previously obtained. There were certain disadvantages to the method, the major difficulty relating to the step-changing procedure. The routine possessed an error estimation which enabled step length to be halved during integration for any step with results outside a predetermined accuracy. Step length could not be increased for a highly successful step however, and in the current work, gradients were so large initially that a step length of order 10^{-8} in the independent variable had to be used at the start. Consequently integration proceeded extremely slowly. Output from the routine was given to five significant figures only.

MIDAS proved eminently satisfactory for solving the isothermal problem #2.5.2 and was used initially to investigate the behaviour of the variational solution. A programme was then written which utilises a fourth order variable step length Kutta-Merson procedure [31,32] to integrate the equations on an IBM 7090. An error routine enables the step length to be doubled, halved or remain unchanged, depending on how well a previously decided error criterion is

satisfied, if at all. The error criterion is compared to a calculated estimate of the truncation error ϵ. If $\epsilon >$ preassigned accuracy, the integration interval is halved and the step repeated. If $\epsilon <$ 1/32 of the preassigned accuracy, the step length is doubled. Merson claims this method to be 20% faster than the standard fixed interval procedure.

3.4.6 Upper bound on the control

Consider the variable X in (3.37). The initial conditions on x_B, x_C are such that

$$X(0) = 0 \tag{3.48}$$

When substituted into (3.36) this gives

$$\beta_1(0) = \infty \text{ for } \lambda(0) \neq -\infty \tag{3.49}$$

Hence from (3.35), $K^*(0) = K_u$ for all $\lambda(0)$ in $-\infty < \lambda(0) < \rho_1$. Each optimal control policy will commence on the isothermal $K = K_u$.

Now $K = k_2/k_1$ and $K_u \longrightarrow H_2/H_1$ as $T \longrightarrow \infty$. For equilibrium between A and B to be sufficiently adjustable inside

the permissible temperature region, (i.e. for a fairly large K interval), $H_2/H_1 >> 1$. A reasonable figure for H_2/H_1 could be as large[4] as 10^{10}, which makes K^4 terms in (3.41) and (3.42) beyond the capacity of the computer. The effect of varying K_u from 10^2 to 10^6 was investigated for $\lambda(0) = 0$ using MIDAS. No difference was found for $K_u = 10^2$, 10^3 or 10^6 and it was decided to retain 10^2. From the isothermal study #2.5.2, $K_u = 100$ appears to restrict the attainable region by very little. Since the attainable region would be expected to shrink if K_u be lowered sufficiently, the value $K_u = 2$ was also investigated for comparison.

3.4.7 Some difficulties in the forward integration

The MIDAS programme was first used. Since $0 \leq \phi \leq \infty$, a dimensionless variable ξ has been introduced such that

$$\xi = \frac{\phi}{1 + \phi} \tag{3.50}$$

Hence $\xi = 0$ when $\phi = 0$ and $\xi = 1$ corresponds to infinite time.

The state equations (3.41) were combined to give

$$\frac{dX}{d\xi} = \frac{-K^2}{4(1-\xi)^2}\left[4K^2X^2 + (2K-1)^2X - 4K\right] \qquad (3.51)$$

with $X(0) = 0$. Now $K = K(X, \lambda)$ from (3.35), so only two differential equations, (3.51) for X and (3.42) (with the appropriate transformation to ξ) for λ, need to be solved simultaneously. However we must also obtain individual values for x_B, x_C. Hence a third equation was included with the above, by using (1.12) and (3.41) to yield

$$\frac{d \ln x_A}{d\xi} = \frac{K^3(KX-1)}{(1-\xi)^2} \qquad (3.52)$$

with $x_A(0) = 1$. This could be integrated forwards together with the equations for X and λ. The MIDAS programme may be found in Appendix IV #1.

This MIDAS programme was used with $x_A(0) = 1$, $X(0) = 0$ and various $\lambda(0)$. For $K_u = 2$, $\lambda(0)$ in the range $-10^{15} \leq \lambda(0) \leq 24.675$ was investigated, whilst for $K_u = 100$, the corresponding range was $-10^{16} \leq \lambda(0) \leq 40,399$. Typical computing time on the IBM 7090 for a single trajectory over $0 \leq \xi \leq 0.99$ was 1 minute for $K_u = 100$ and 0.5 minutes

when $K_u = 2$. Output was obtained at intervals of 0.01 in ξ and values for K and b were included in the printout, along with state and adjoint variables. A maxima/minima table, which is a feature of MIDAS, was also printed out for each run. In this table, the maximum and minimum values attained by each variable during the run are recorded.

The solution in state space was found to be insensitive to changes in $\lambda(0)$ and typical results obtained in a MIDAS computation are shown in table (3.1). The insensitivity was due to extremely large $\frac{d\lambda}{d\xi}$ initially for all $\lambda(0)$ except values in the vicinity of the roots ρ_1, ρ_2 (see Appendix III #2). Hence values of $\lambda(0)$ over a wide range had little effect on the state variables, since $\lambda(\xi)$ altered so rapidly from $\lambda(0)$ as ξ increased.

The difficulty was resolved by considering the behaviour of $\frac{d\lambda}{d\xi}$ as $\lambda(0)$ approaches either of its bounds, i.e. $-\infty \leq \lambda(0) \leq \rho_1$. These limits will be discussed separately.

(a) $\underline{\lambda(0) \rightarrow -\infty}$ We have noted that all optimal controls commence on the isothermal $K = K_u$. As $\lambda(0) \rightarrow -\infty$, $\left.\frac{d\lambda}{d\phi}\right|_o$

TABLE 3.1

Insensitivity of the forward integration solution to variation in $\lambda(0)$

$K_u = 100$ $\quad \phi_e = 0.25$ $\quad x_B(0) = x_C(0) = 0$

$\lambda(0)$	λ_e	x_{Be}	x_{Ce}
10^4	0.37461	0.35356	0.050398
10^3	0.37255	0.35357	0.050359
10^2	0.37234	0.35357	0.050356
10	0.37232	0.35357	0.050355
1	0.37232	0.35357	0.050355
0	0.37232	0.35357	0.050355
-1	0.37232	0.35357	0.050355
-10_2	0.37232	0.35357	0.050355
-10^2	0.37230	0.35357	0.050355
-10^3	0.37209	0.35357	0.050351
-10^4	0.37004	0.35359	0.050313
-10^5	0.34977	0.35372	0.049955
-10^6	0.16908	0.35441	0.047341
-10^7	-0.75398	0.35226	0.038809
-10^8	-2.0892	0.34118	0.030786
-10^9	-2.5128	0.33644	0.028723
-10^{10}	-2.5716	0.33574	0.028449
-10^{16}	-2.5784	0.33566	0.028418

gets larger and larger, causing $\lambda(0)$ to increase more and more rapidly. The time for which optimal control remains on K_u decreases, and in the limiting case this control will drop instantaneously from the isothermal. The limiting value for a in Appendix III #1 is 0, and this occurs when $A = (\lambda - 1)X^2 \longrightarrow -1$, corresponding to $\lambda \longrightarrow -\infty$. Hence b in equation (3.38) approaches 1/3 as $\lambda(0) \longrightarrow -\infty$ and this can be seen in table (3.2).

When a = 0, the roots α_1, α_2 of the Hamiltonian coincide at K = 1/2X (see Appendix III #1). The maximum turning point β_1 is also at K = 1/2X and the Hamiltonian has the shape in figure (3.3) for $\lambda_1 > 0$.

The maximum value of the Hamiltonian is now H = 0. There are two possible controls satisfying the Pontryagin Maximum Principle, one at $K^* = \beta_1$ and the other at $K^* = 0$. The latter corresponds to zero temperature, so no reaction occurs at $K^* = 0$ and we refer to this as a quench.

The following possibilities now arise:

(1) $K^* = 1/2X$ for all ξ in $0 \leq \xi \leq 1$. Then an optimal trajectory will be generated corresponding to this control.

TABLE 3.2

To show that $b \rightarrow 1/3$ as $\lambda(0) \rightarrow -\infty$

$K_u = 100$

$\lambda(0)$	b	ξ corresponding to b
-10^6	0.41983	< 0.01 *
-10^7	0.34380	< 0.01
-10^8	0.33442	< 0.01
-10^9	0.33345	< 0.01
-10^{10}	0.33335	< 0.01
-10^{16}	0.33334	< 0.01

*The first printout is at $\xi = 0.01$. The above values for b were obtained from a table of maxima and minima, which appears at the end of each set of computed results as part of the MIDAS routine.

(2) $K^* = 0$ for all ξ. No reaction occurs and the state variables remain at the origin.

(3) $K^* = 1/2X$ for varying lengths of time and $K^* = 0$ for the remaining time. This would correspond to intermittent quenching.

All three cases will correspond to $H = 0$. Now the control policy $K^* = 1/2X$ is identical to the optimal control obtained in the yield problem, since $k^* = K^* = k_2/k_1$ (see equation (3.4) with $\alpha = 1$). Hence the optimal trajectory corresponding to $H = 0$ in the 3-D output problem will generate the border of the attainable region in the 2-D yield problem.

If quenching is an admissible control, successive sections of the attainable region in time must be at least as large as preceeding sections. Hence the attainable region will either remain stationary or grow with time.

(b) $\underline{\lambda(0) \longrightarrow \rho_1}$ Once again all optimal controls will commence on the isothermal $K = K_u$. Taking $\lambda(0)$ closer to ρ_1 makes $\left.\frac{d\lambda}{d\phi}\right|_o$ diminish rapidly. The direct effect of this is to cause the control to remain on the upper bound

for longer times. This can be seen in table (3.3) for $K_u = 2$ and also in figure (3.4). This figure illustrates clearly how different $\lambda(0)$ values generate different optimal trajectories. The same occurs for $K_u = 100$, but at ξ values << the first printout time, so the effect will not be noticed.

In the limit when $\lambda(0) = \rho_1$, the optimal trajectory is the isothermal K_u. This can be seen as follows. When $\beta_1 > K_u$, $K^* = K_u$ and values of X, λ are given by the isothermal solutions of (3.51), (3.42) respectively, for $K = K_u$, $X(0) = 0$ and $\lambda(0) = \lambda_o$. The isothermal K_u ceases to be a valid optimal control when β_1 just < K_u, i.e. in the limit

$$\beta_1 = \frac{3}{8X}(1 + b) = K_u \qquad (3.53)$$

or substituting for b,

$$X(8K_u^2 - \lambda + 1) = 6K_u \qquad (3.54)$$

For $\lambda(0) = \rho_1$, $\lambda(\phi)$ remains at ρ_1 as ϕ increases, until $X(\phi)$ reaches a value which satisfies (3.54).

TABLE 3.3

Effect of $\lambda(0) \longrightarrow \rho_1$ on the optimal control

$K_u = 2$ $\rho_1 = 24.675796$ (to 8 significant figures)

$\lambda(0)$	ξ at which K* leaves K_u	$\frac{d\lambda}{d\phi}$
-10^{10}_2	0.03	
$-10^{}$	0.04	
1	0.06	
20	0.10	-92
24	0.15	-16
24.6	0.21	-1.84
24.65	0.23	-0.6275
24.67	0.27	-0.1411
24.675	0.31	-0.019375
24.6755 *	0.33	-0.007200
24.675795 *	0.39	-0.000016

*Obtained by Kutta-Merson

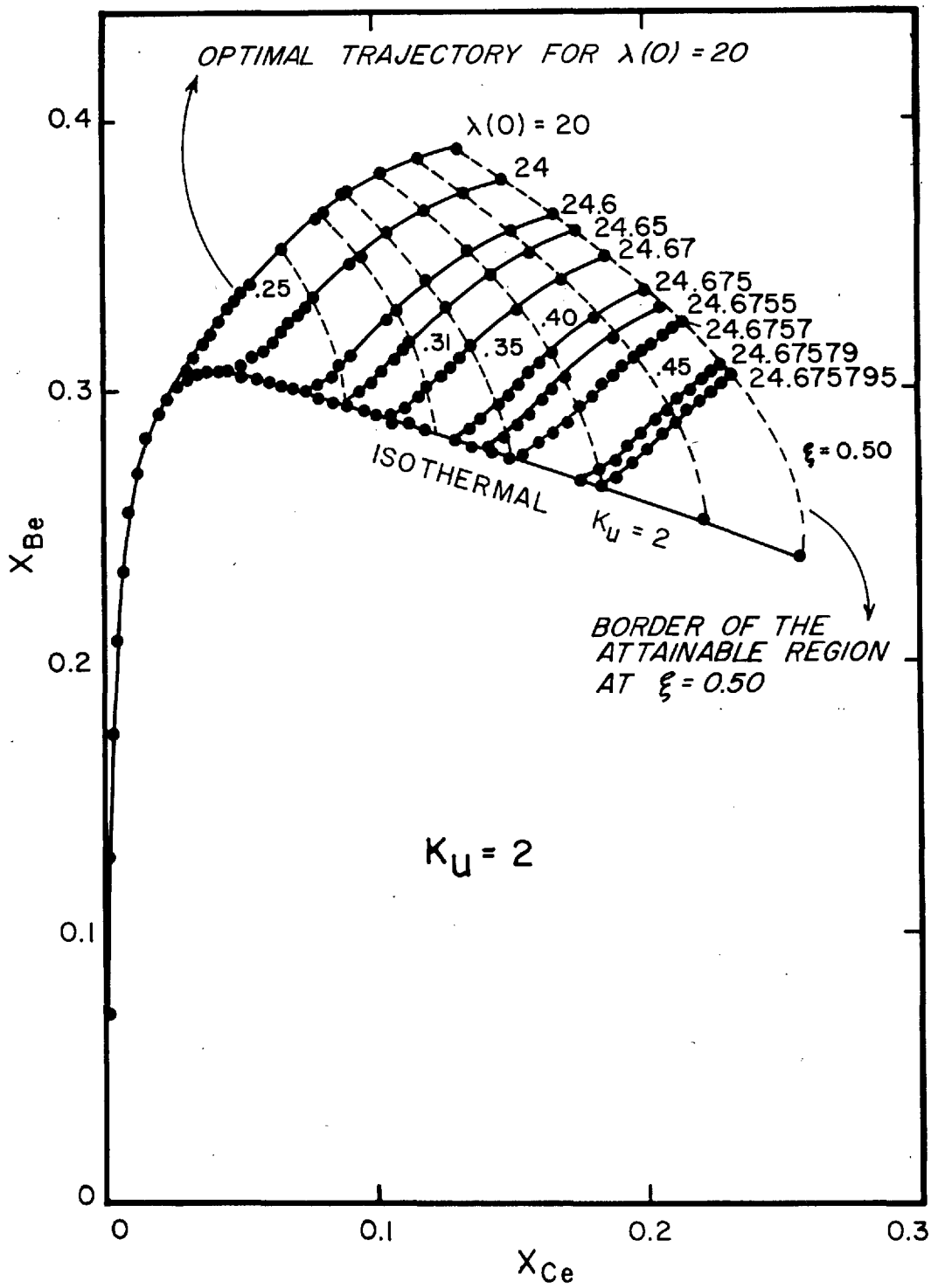


FIGURE 3.4 - ILLUSTRATION OF HOW λ(0) VALUES GENERATE OPTIMAL TRAJECTORIES AND HENCE THE ATTAINABLE REGION BORDER

i.e. $$X = 6K_u/(8K_u^2 - \rho_1 + 1)$$

$$= 0.01513 \text{ for } K_u = 100$$

But from Appendix III #3, the maximum value $X(\phi)$ can attain on the isothermal K_u is its steady state value, and for $K_u = 100$, $X(\text{steady state}) \doteq 0.01$. Hence (3.54) can never be satisfied and the optimal control is the isothermal K_u for all time. The same qualitative results can be shown for $K_u = 2$.

Now from the isothermal study #2.5.2, x_c attains its maximum value on the isothermal K_u. Hence this isothermal will bound the attainable region in the direction of the x_c axis.

Theoretically we should be able to generate the attainable region by choosing $\lambda(0)$ closer and closer to ρ_1. In practice however, we are limited by the number of significant figures the computer programme can handle. (This is five in the case of MIDAS). We know that $\lambda(0) \rightarrow \rho_1$ keeps $K^* = K_u$ for longer times; we could therefore achieve the desired result by commencing integration with values obtained

from the isothermal K_u at different times. i.e. instead of starting at $\xi = 0$ with $\lambda(0)$ very close to ρ_1, we assume that such a $\lambda(0)$ has given rise to a $\lambda(\xi_1)$ which causes control to <u>just</u> leave K_u at $\xi = \xi_1$. We can calculate $X(\xi_1)$ from the isothermal solution of (3.51) and hence find $\lambda(\xi_1)$ from (3.54). These are then the initial conditions for a forward integration with $K^* = \beta_1$. The forward integration will commence at $\xi = \xi_1$ and integrate to $1 - \xi_1$.

Now $K_u = 100$ gives $x_C(\xi) = 0.9999$ when $\xi = 0.269$. Hence we can only choose isothermal operation for $0 \leq \xi \leq 0.269$ to get useful results. Optimal control policies will consist of

$$\xi \leq \xi_1 \qquad K^* = K_u$$

$$\xi > \xi_1 \qquad K^* = \beta_1$$

$$0 \leq \xi_1 \leq 0.269$$

It can be shown that $X(\xi)$ reaches very close to its steady state value after an exceedingly short time. We will therefore use the equations for x_B and x_C. Since MIDAS can only accept initial conditions at $\xi = 0$, it will be unsuitable for solving the non-autonomous equations.

The Kutta-Merson procedure was therefore used for this part of the calculations. Equations (3.41) and (3.42) were programmed with the optimal control K* given in (3.35). The Fortran IV programme may be found in Appendix IV #2. Symbols used are self-explanatory.

Stages in the calculation are as follows:

(1) Choose ξ in $0 \leq \xi \leq \xi_u$ (For $K_u = 100$, $\xi_u = 0.269$; for $K_u = 2$, $\xi_u = 0.99$).

(2) Obtain $x_B(\xi)$ and $x_C(\xi)$ from the isothermal solutions at $K = K_u$. A complete list of the values used for both $K_u = 100$ and $K_u = 2$ may be found in tables (A.1) and (A.2).

(3) Hence obtain $X(\xi)$ from (3.37) and calculate $\lambda(\xi)$ from (3.54). (See tables (A.1) and (A.2) again).

(4) Supply initial conditions $x_B(\xi)$, $x_C(\xi)$ and $\lambda(\xi)$ to the computer programme, together with the value ξ. Integrate to $0.99 - \xi$.

For $K_u = 100$, each optimal calculation required about 0.7 minutes of IBM 7090 time. Results were printed out from ξ to $0.99 - \xi$ in intervals $\Delta\xi = 0.01$. Each line of output contained the current values of ξ, ϕ, K, b and the

state and adjoint variables. The current step length and number of steps were also included. Initial interval was 10^{-8} in independent variable ξ. A larger value made integration unstable, due to the high gradient of λ initially. It then required about 60 integration steps before the first printout, with a corresponding increase in integration interval to 0.00131. Thereafter the maximum interval 0.005 was soon reached, resulting finally in about 280 steps. (A maximum integration interval of 0.001 was also tried, with little difference in the results). A relative error criterion of 1% on x_B, x_C and λ was employed, since this gave no significant difference from a value of 0.1%.

For $K_u = 2$, the programme was tested with $\lambda(0) = 24.675$, $x_B(0) = x_C(0) = 0$, and was found to give results consistent with those obtained in MIDAS, though to 8 significant figures rather than 5. An absolute error of 10^{-5} in x_B, x_C and 10^{-4} in λ was tolerated. Results were also obtained with $\lambda(0)$ even closer to ρ_1 than was possible with MIDAS (see table (3.3)). Average computing time per trajectory was 0.5 minutes.

The programme was also used to obtain optimal trajectories for $K_u = 2$, using the part-isothermal technique previously described. A complete integration of 220 steps was achieved in about 0.5 minutes computing time.

3.4.8 Discussion of the results

A mapping of the adjoint ratio λ from initial to final values is shown in figure (3.5) for $K_u = 2$. A range of $\lambda(0)$ from -10^{15} to 24.675795 is presented, as well as trajectories obtained with isothermal operation for varying periods of time. Of interest is the fact that all trajectories converge to $\lambda_e = 0.625$, as dimensionless time $\xi \longrightarrow 1$. The trajectories for $K_u = 100$ exhibit similar behaviour.

Figure (3.6) shows the corresponding optimal control policies for $K_u = 2$. These all commence on the upper bound and drop away at later and later times. Since the reversible reaction is exothermic, a decreasing control K implies decreasing temperature profiles. The optimal temperature profiles thus behave in like fashion to the reversible exothermic reaction without product decay. In the latter case

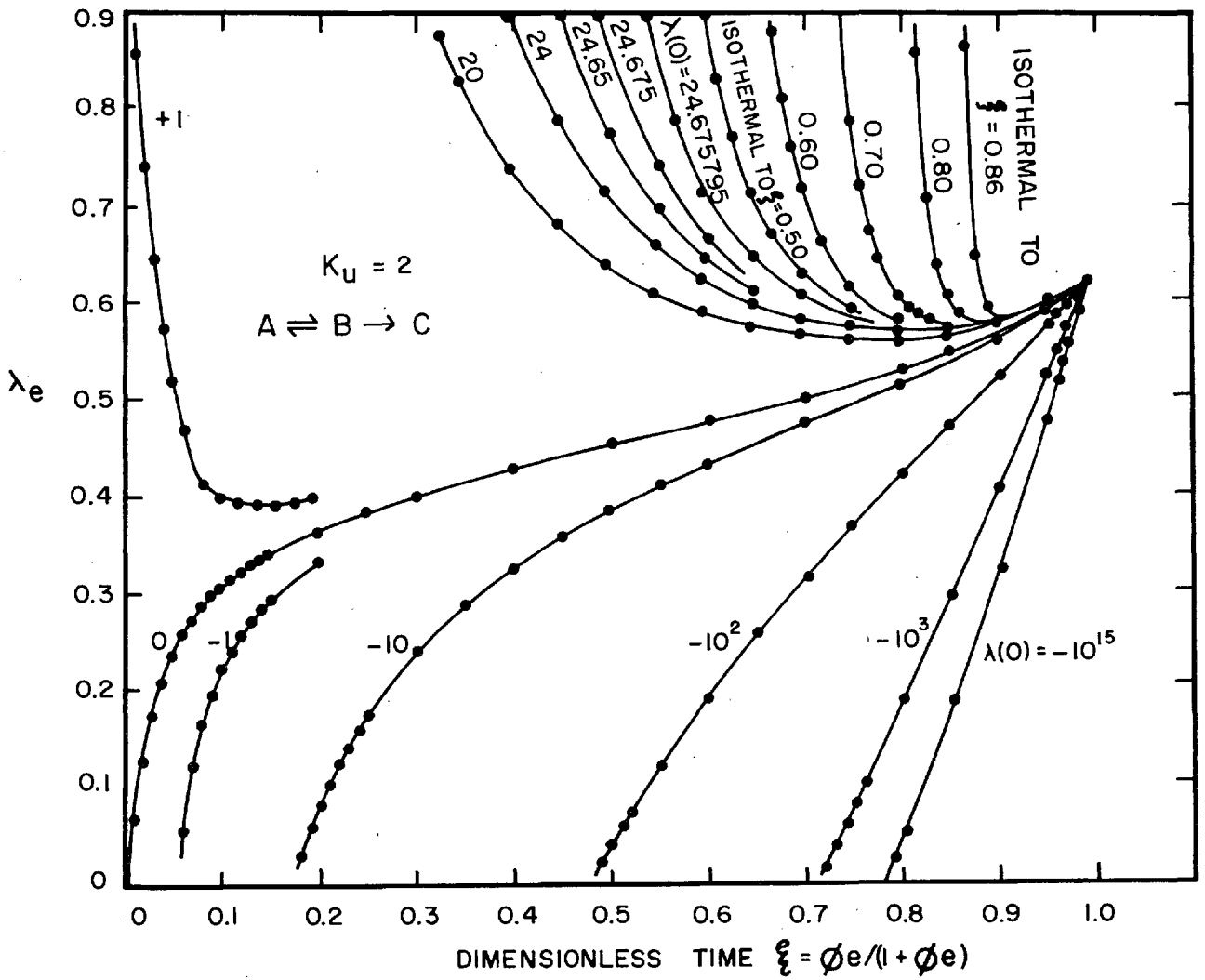


FIGURE 3.5 - ADJOINT MAPPING

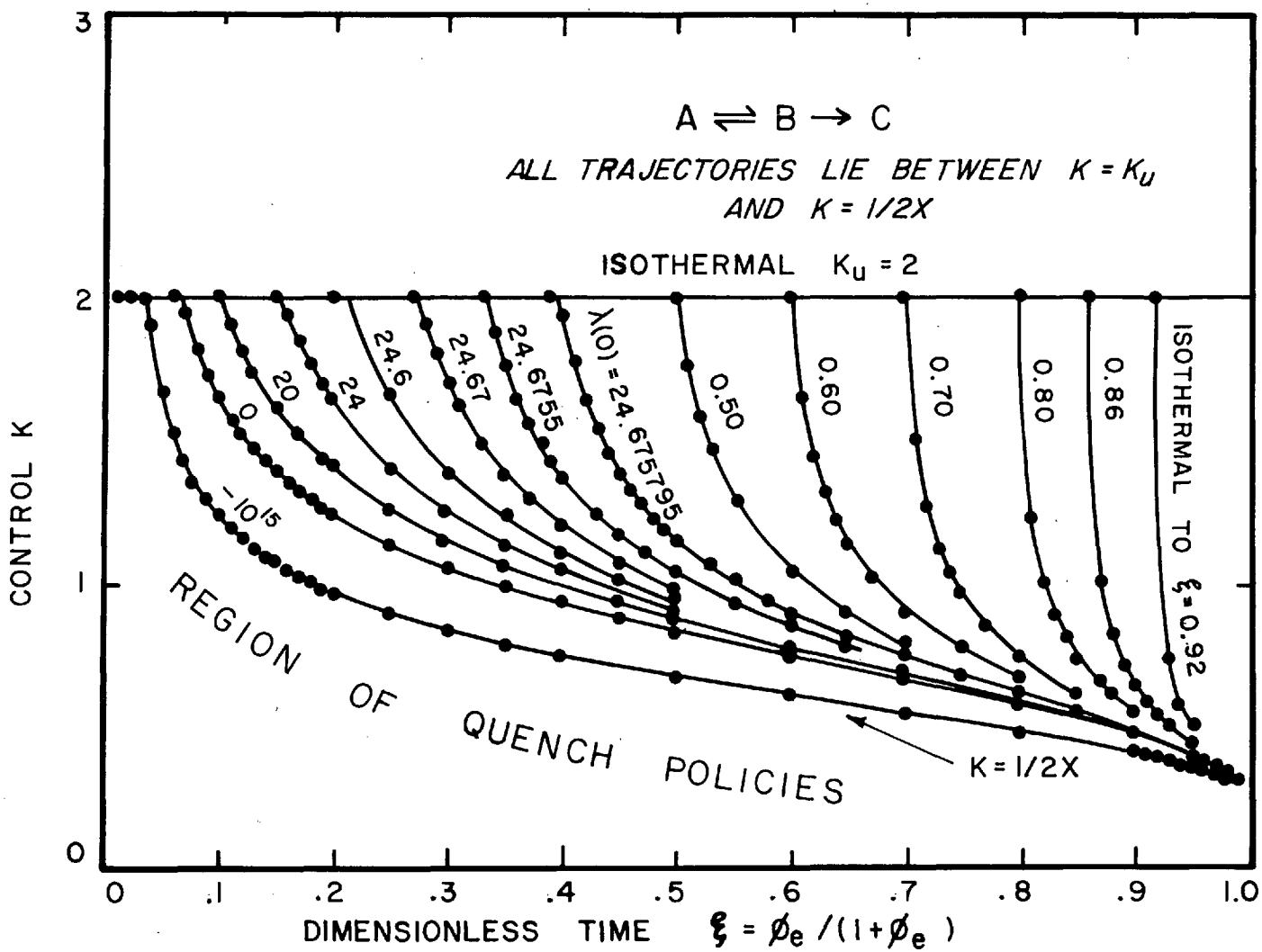


FIGURE 3.6 - OPTIMAL CONTROL TRAJECTORIES FOR $K_u = 2$

there is only one optimal temperature policy. Note too that all optimal controls (other than quench) lie between K_u and $K = 1/2X$ and approach the limit $K = 0.306$ as $\xi \longrightarrow 1$.

These limits for both K and λ as $\xi \longrightarrow 1$ may be explained as follows. Limiting values for K, λ and X are given by

$$K = \beta_1; \quad \lambda = \rho_2; \quad X = \delta_1 \tag{3.55}$$

The first describes optimal control and the second and third are the steady state solutions for λ and X respectively. The simultaneous solution of these equations will be independent of K_u, since K_u does not appear. A solution is $\lambda = 5/8$, $X = 2.6^{\frac{1}{2}}/3$, $K = 6^{\frac{1}{2}}/8$. These agree not only with the λ, K above but also with the limiting value obtained for X in the computations. The solution is the same for both $K_u = 2$ and $K_u = 100$ and this is reflected in the numerical results. Note too that $\lambda = 5/8$, $X = 2.6^{\frac{1}{2}}/3$ gives $b = 1/3$ in (3.38). We know this to be the correct limiting value for b.

The attainable region is shown in isometric form in figures (3.7) and (3.8), for $K_u = 2$, 100 respectively. The section $\xi = 1$ corresponds to the border of the 2-D yield

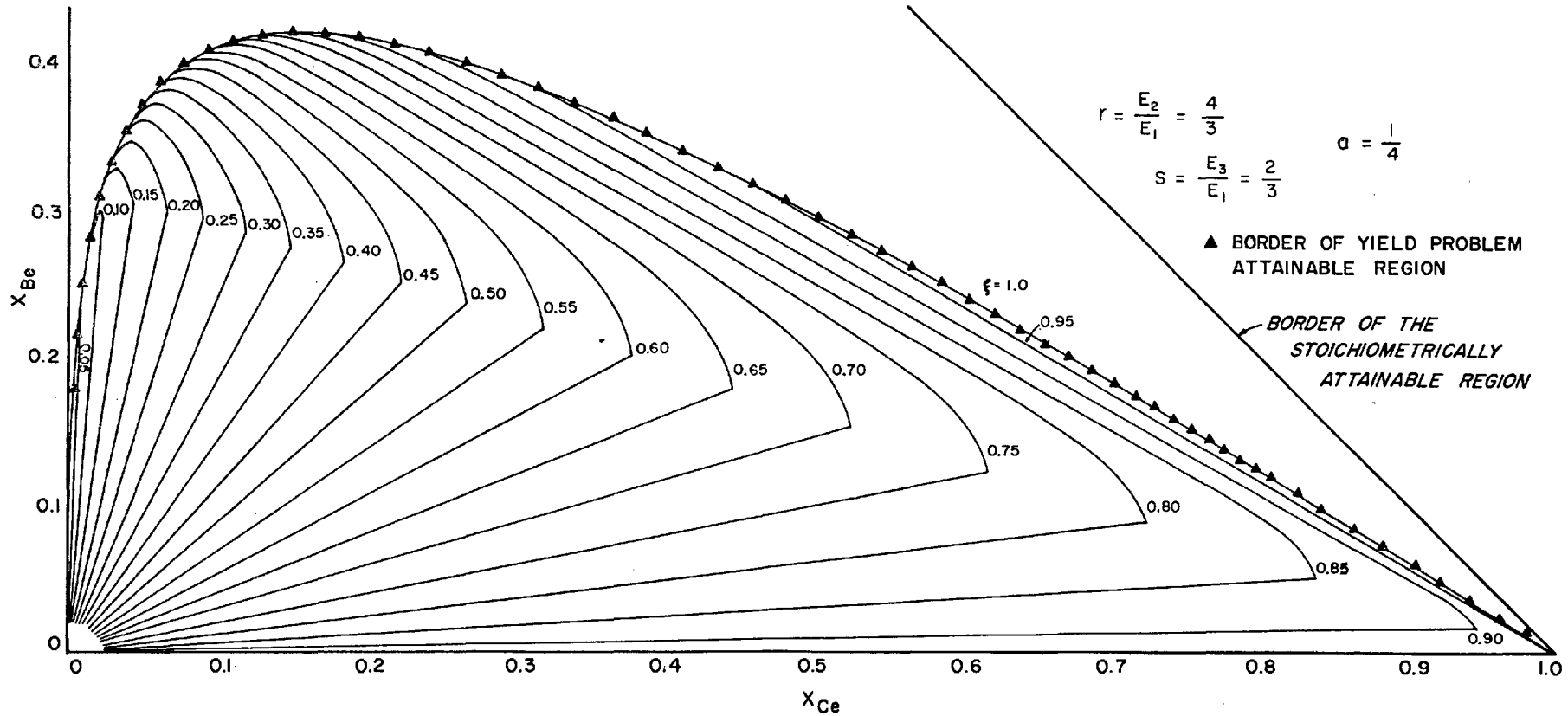


FIGURE 3.7-ATTAINABLE REGION FOR $A \rightleftharpoons B \rightarrow C$ WITH $K_u = 2$. CONSTANT END TIME SLICES

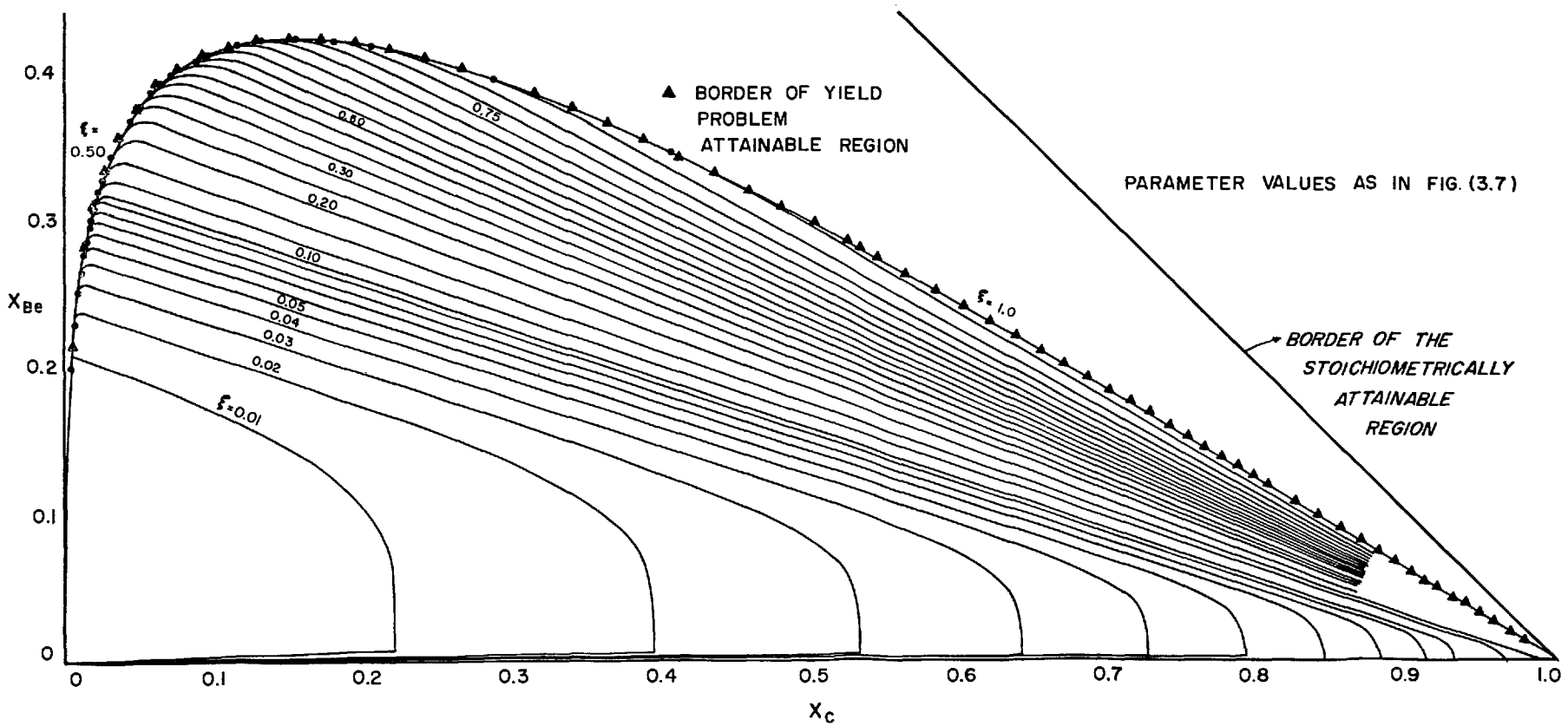


FIGURE 3.8 - ATTAINABLE REGION FOR $A \rightleftharpoons B \rightarrow C$ WITH $K_u = 100$. CONSTANT END TIME SLICES

problem attainable region #3.3. The slope of this border is $(-\lambda_e)$; as $x_{Ce} \longrightarrow 1$ this approaches 0.625 on the graph (cf. above value). It is now clear why $\lambda(0) > \rho_1$ is unnecessary, for this would cause $\lambda(\phi)$ to increase with ϕ and a λ_e of 0.625 could not be approached.

The effect of reducing K_u from 100 to 2 is to reduce the attainable region. This reduction is considerable, as can be seen from the relevant figures. There is no appreciable reduction caused by $K_u = 100$ instead of a larger value, and the effect is most pronounced at low ξ. Figure (3.9) shows a three-dimensional representation of the attainable region for $K_u = 100$.

It is of interest to compare attainable regions in the 2-D output problem for the exothermic reversible reaction with and without decay of product. The former can be obtained from figure (3.8), by selecting maximum x_{Be} on each time slice ξ. The latter may be found for $E_2/E_1 = 4/3$ in an analogous fashion to the case $E_2/E_1 = 2$ in #3.1. This means the optimal control (3.1) must be substituted into the state equations, which must then be integrated with $r = 4/3$. The resulting border of the attainable region is given by

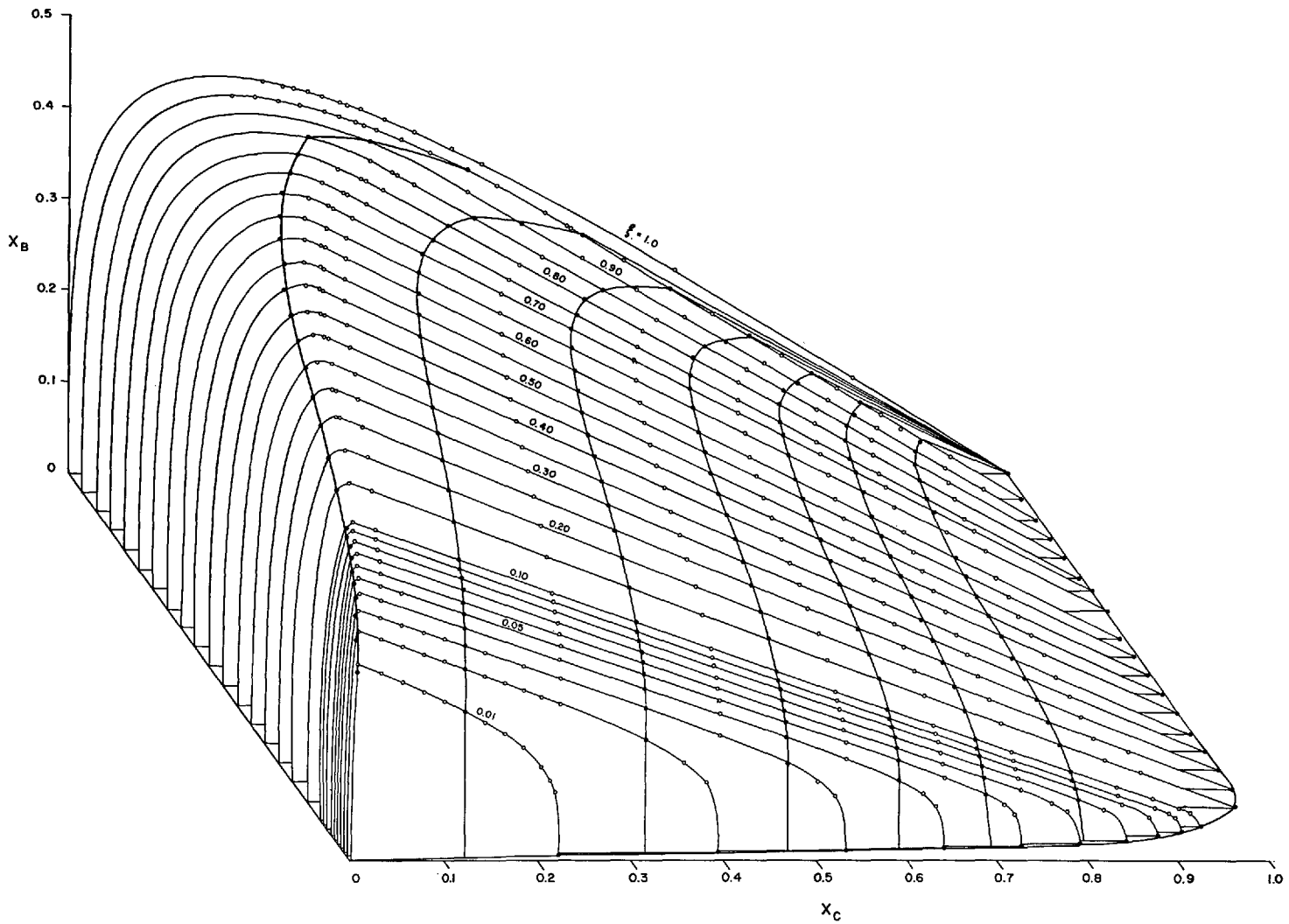


FIGURE 3.9- THREE-DIMENSIONAL REPRESENTATION OF THE ATTAINABLE REGION WITH $K_u = 100$

$$\phi = \frac{4^4}{3^3}\left[\ln(1-x_B) + \frac{x_B}{1-x_B} - \frac{1}{2}\left(\frac{x_B}{1-x_B}\right)^2 + \frac{1}{3}\left(\frac{x_B}{1-x_B}\right)^3\right] \quad (3.56)$$

Figure (3.10) shows the results. The attainable region for the reversible exothermic reaction alone is larger than that corresponding to decay of product. This is to be expected.

3.5 THREE-DIMENSIONAL MODEL OF THE ATTAINABLE REGION

A three-dimensional model has been constructed from figure (3.8) and photographs of this model are presented in figure (3.11). The base plane of the model has coordinates x_C and ξ, whilst the vertical scale is x_B.

The family of trajectories depicted is the family of optimal trajectories, which all run along the surface. The extreme left hand trajectory shown gives the border of the 2-D yield problem solution when projected on to the $x_B - x_C$ plane. Hence the maximum turning point of this trajectory gives the absolute maximum of x_B with respect to choice of control policy and reaction time. We will denote this curve the yield problem trajectory.

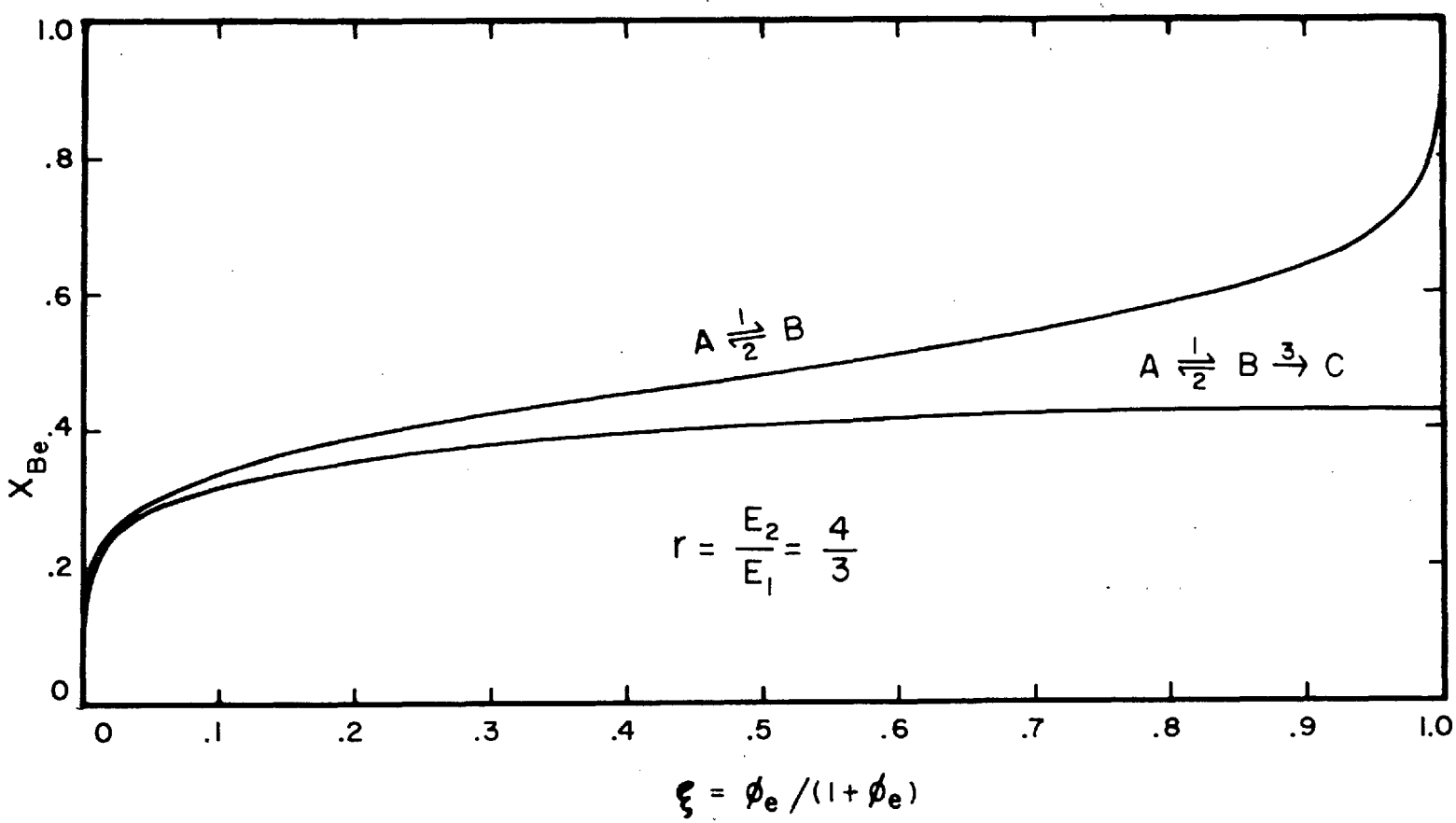


FIGURE 3.10 - COMPARISON BETWEEN ATTAINABLE REGIONS FOR REVERSIBLE EXOTHERMIC REACTION WITH AND WITHOUT IRREVERSIBLE DECAY OF PRODUCT

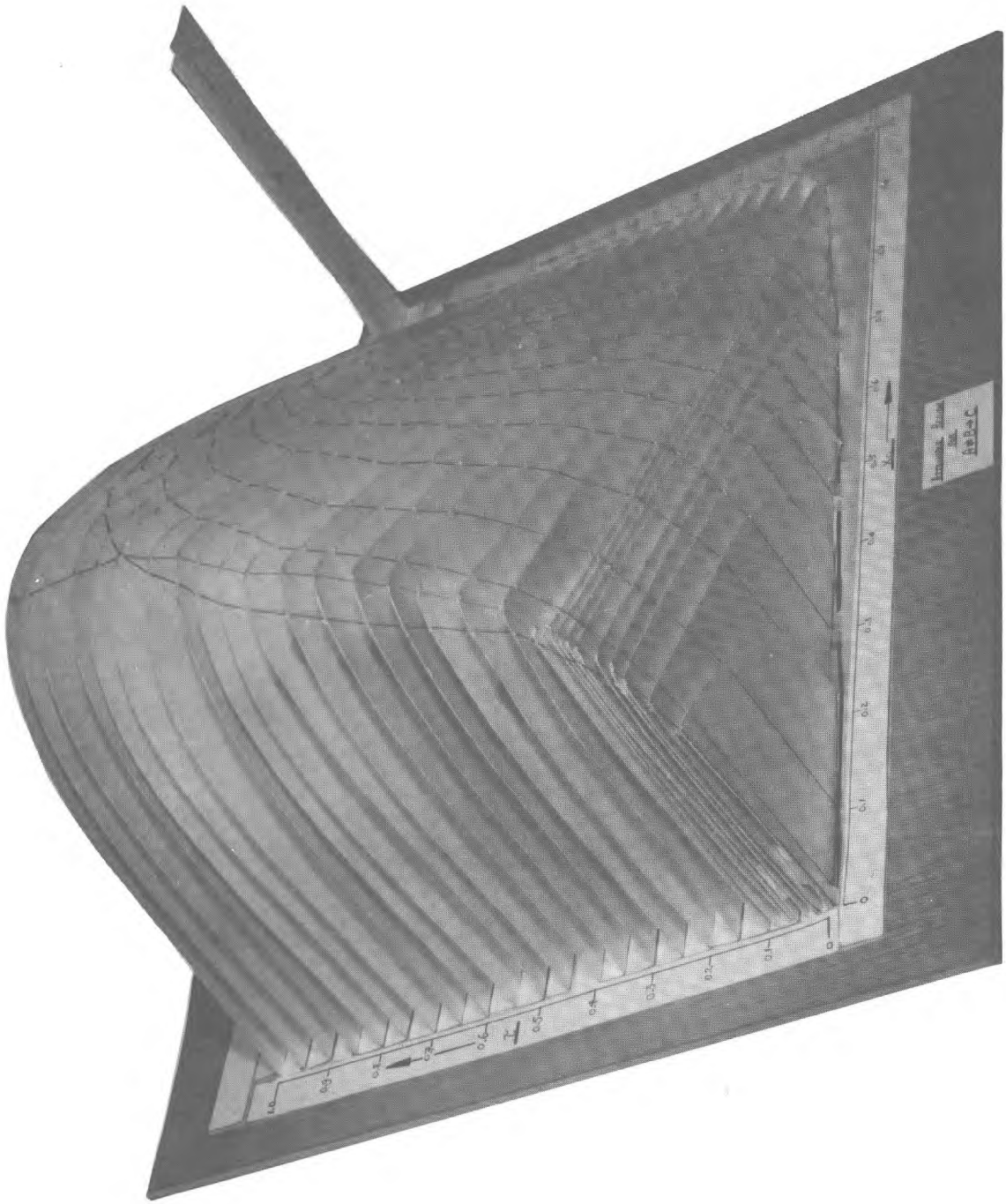


FIGURE 3.11

THREE-DIMENSIONAL MODEL OF THE ATTAINABLE REGION

The border of the 2-D output problem solution does not correspond to any one optimal trajectory, unlike the above yield problem border. The output problem border results from the projection on to the $x_B - \xi$ plane, of the curve joining the maximum x_B values for each time slice. Note that this curve flattens out at the point where it intersects the yield problem trajectory, which is to be expected.

The extreme right hand trajectory shown is the reaction path obtained by isothermal operation at the upper temperature limit. Each optimal control trajectory starts at this upper limit. No attainable region lies to the right of the isothermal reaction path K_u; however region does exist to the left of the yield problem trajectory, due to the possibility of switching to very low temperature so that no further reaction occurs. By means of this quench, the state of the system is held fixed for all subsequent time. Hence surface to the left of the yield problem trajectory can be generated by incorporating a switching policy from some finite control to quench at any point along this trajectory. In practice the reactor would of course merely be made shorter.

3.6 APPLICATION TO SPECIFIC OBJECTIVE FUNCTIONS

The attainable region we have obtained depends only on the initial conditions for the given system, once the various parameter values have been fixed. We have indicated that the region may be used in conjunction with any objective function plotted in the space. We will now illustrate this by means of two practical examples. In each case cost function contours will be obtained and superimposed on the attainable region to get the optimal operating point directly.

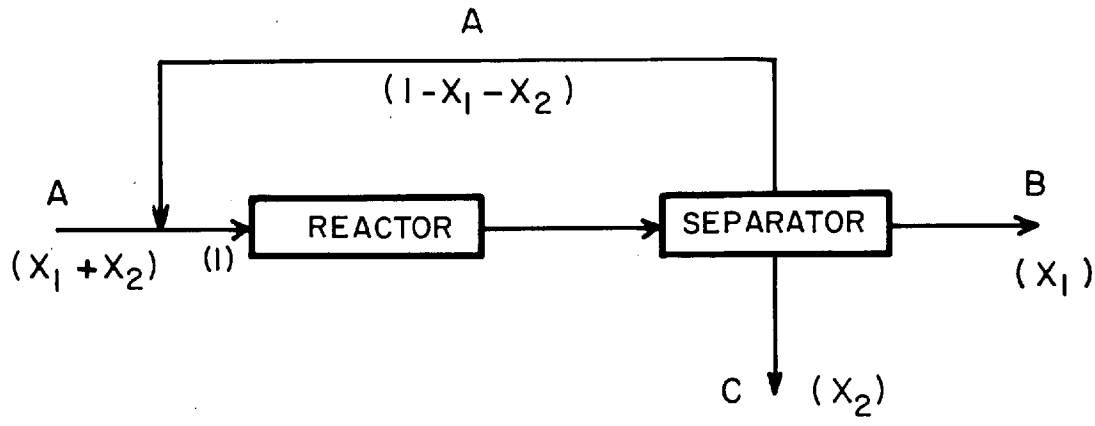
Example 1: Consider the recycle system shown in figure (3.12a). A fixed amount of pure A enters the tubular reactor and product B is desired. Separation may be considered complete, so that only A is present in the recycle.

Let x_1, x_2 be conversion to B, C respectively; then a mass balance over the system will yield the flows shown, assuming unit flow of A into the reactor.

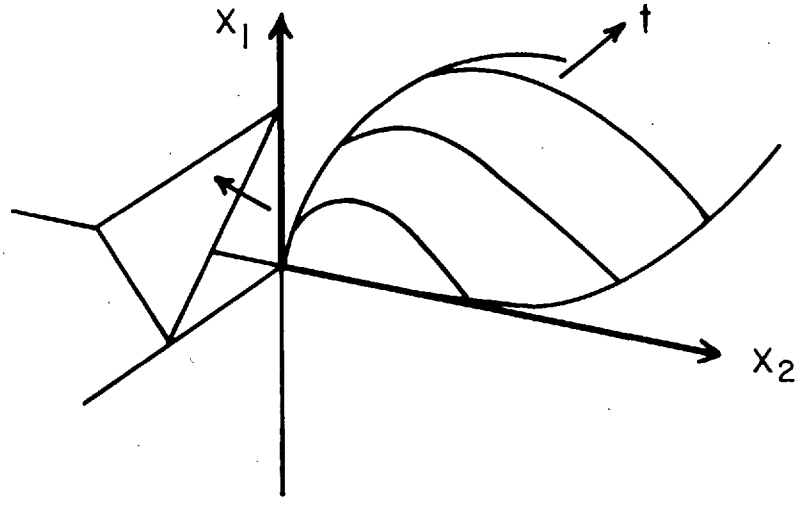
Now

$$P = \text{profit/mol. of A entering the reactor}$$

$$= x_1 C_b - (x_1 + x_2) C_a - (1 - x_1 - x_2) C_r - m C_c$$

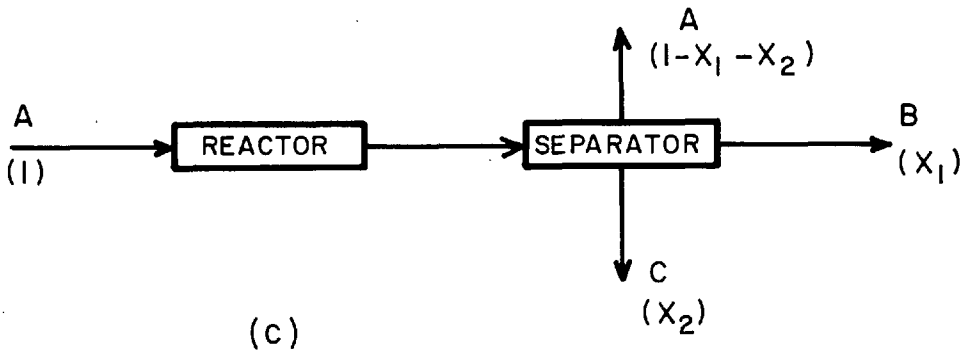


(a)

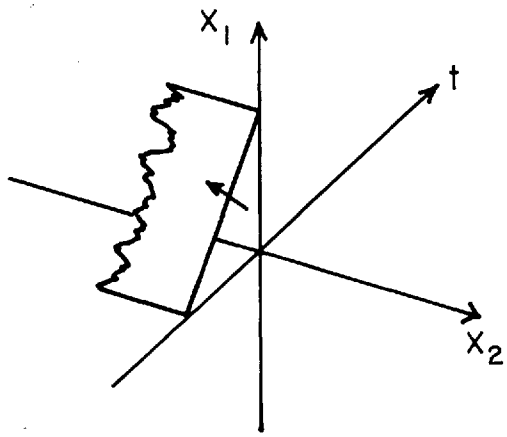


(b)

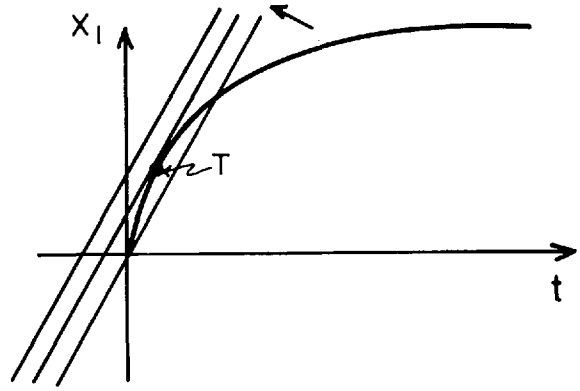
FIGURE 3.12- SOLUTION TO EXAMPLE 1



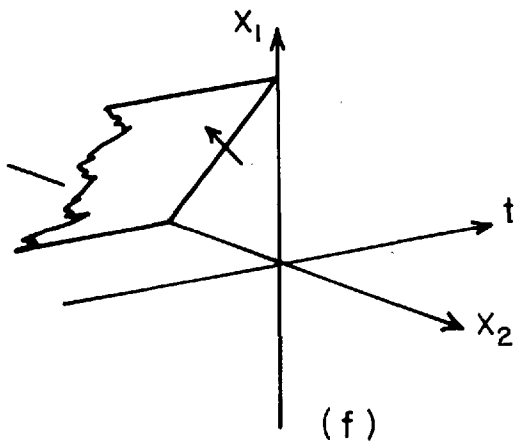
(c)



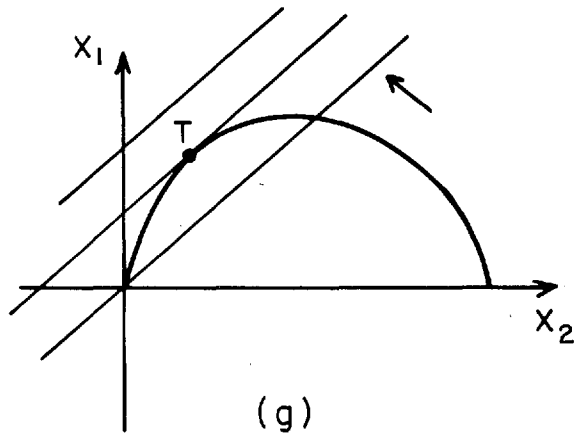
(d)



(e)



(f)



(g)

FIGURE 3.12 (CONT'D)

where

C_a = cost of raw material/mol. feed;

C_r = cost of recycling/mol. recycle;

C_c = cost of reactor/unit mass catalyst;

C_b = value of product/mol. B formed;

and

m = catalyst mass/mol. of A entering = t.

i.e.

$$(C_a - C_r - C_b)x_1 + (C_a - C_r)x_2 + C_c t + (C_r + P) = 0 \quad (3.57)$$

This equation represents a plane in the (x_1, x_2, t) space. Note that $C_a > C_r$ for recycle to be economical and $C_b > C_a$ for system to be profitable. The coefficients of x_2 and t are thus positive and that of x_1 is negative, whilst $(C_r + P)$ is positive for all P. Planes of constant P are thus parallel planes and a typical such plane is represented in figure (3.12b). The attainable region must now be considered together with these planes to solve the 3-D output problem. Since P increases in the direction indicated by the arrow, profit will be maximum on that plane which

just touches the surface of the attainable region. The point of tangency will then provide the solution.

Once the optimum point has been found by such constructions, one has to "look" for that trajectory and control policy which produced this point. This is now the optimal policy for the particular objective function under consideration.

In cases where $C_a \leq C_r$, it no longer becomes economical to recycle unconverted A and the system reduces to a reactor and separator in series as shown in figure (3.12c).

Now
$$P = x_1 C_b - C_a - tC_c, \tag{3.58}$$

or
$$(-C_b)x_1 + C_c t + (C_a + P) = 0$$

The planes of constant P are again a family of parallel planes, one member of which now contains the x_2 axis. (This plane corresponds to P = 0, with raw material supplied free). A typical plane is illustrated in figure (3.12d) with P again increasing in the direction of the arrow. The problem reduces to a 2-D output problem,

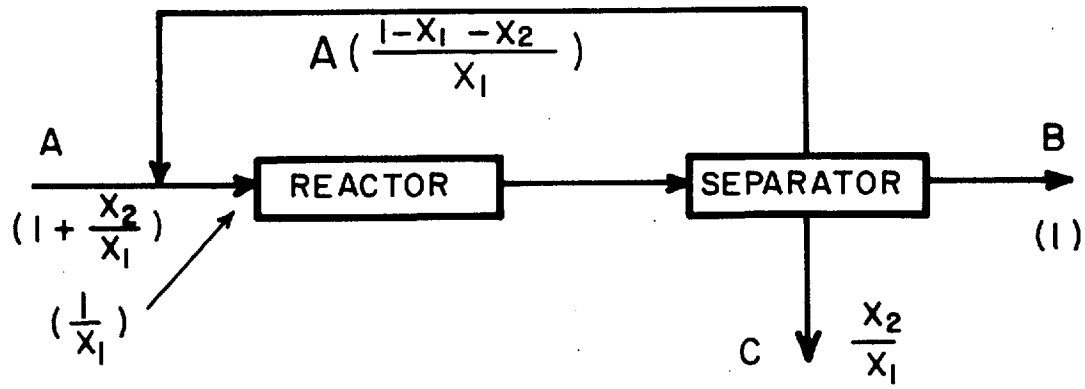
since it is obvious that only the projection of the attainable region on to the plane $x_2 = 0$ is important. This projection is shown in figure (3.12e) together with projections of the planes of constant P. The profit will be maximised at the point of tangency T.

Finally we may consider cases where costs associated with the reactor may be neglected. Putting $C_c = 0$ in (3.57) gives

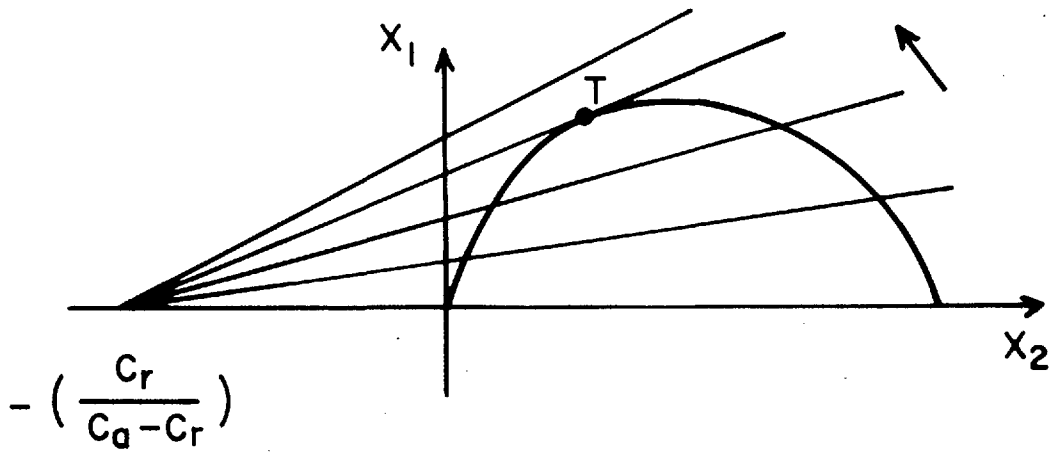
$$(C_a - C_r - C_b)x_1 + (C_a - C_r)x_2 + (C_r + P) = 0 \quad (3.59)$$

The family of parallel planes now has a member which contains the t axis. A typical member of this family is shown in figure (3.12f) where clearly only the projection of the attainable region on to the plane $t = 0$ is needed. The yield problem projections are illustrated in figure (3.12g) with P being maximised at point T.

Example 2: We will now consider the same reaction system as in the previous example, but with fixed production of B required. Based on unit production of B, a mass balance will give the flows shown in figure (3.13a).



(a)



(b)

FIGURE 3.13 - SOLUTION TO EXAMPLE 2

Again we assume costs associated with the reactor may be neglected.

Now

$$P = \text{profit/mol. of B produced}$$

$$= C_b - \left(1 + \frac{x_2}{x_1}\right) C_a - \left(\frac{1 - x_1 - x_2}{x_1}\right) C_r$$

Rearranging gives

$$(C_a - C_r - C_b + P)x_1 + (C_a - C_r)x_2 + C_r = 0 \qquad (3.60)$$

We thus have a yield problem and the solution is indicated in figure (3.13b).

The intercept on the x_2 axis is $-\left(\frac{C_r}{C_a - C_r}\right)$. Decreasing $\left(\frac{C_r}{C_a}\right)$ causes this intercept to move closer to the origin, which makes the point of tangency T on the border of the attainable region also move closer to the origin. This indicates that if recycle costs are small compared to raw material costs, it is better to obtain a low conversion in a short time and recycle a large amount.

Increasing $\left(\frac{c_r}{c_a}\right)$ makes the intercept move further away from the origin, which results in the point of tangency approaching the maximum turning point. This means we are approaching the operating point corresponding to zero recycle, which is the situation when $c_r \geq c_a$. (As $c_r \longrightarrow c_a$, so the intercept on the x_2 axis tends to $-\infty$ and the slope of the lines tends to 0).

In both this and the preceeding example, the objective function contours were chosen as planes for simplicity. In more complex situations involving the same reaction system, surfaces might be expected to result. However this will not affect the basic discussion in any way, and the same procedures may be used to maximise the profit P.

CHAPTER FOUR

DETERMINATION OF THE ATTAINABLE REGION BY NON-ANALYTICAL PROCEDURES

Thus far we have considered the Pontryagin Maximum Principle for developing the border of the attainable region. It was necessary to differentiate with respect to the state variables in order to obtain neighbouring optimal trajectories.

We shall mean by a non-analytical procedure, one in which such differentiation is avoided. As a result, the procedure will be less accurate than an analytical method. This may not be too severe a disadvantage, since models for chemical reactions are often not extremely accurate anyway.

4.1 THE ANALOGUE COMPUTER

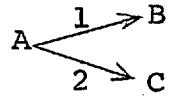
The analogue computer is well suited to dealing with sets of simultaneous ordinary differential equations, and has been used for this purpose by a number of investigators in chemical reaction studies [33,34]. We mention specifically

the work of Lee[35] on the Pontryagin Maximum Principle, and that of Bilous and Amundson[23] previously discussed. The analogue produces a continuous output and should be eminently satisfactory for generating the attainable region; indeed Horn[29] has obtained by this means an attainable region of unusual shape for the sulphonation of naphthalene.

The analogue computer has already been used in the present study, with the linear differential equations in #2.5. A succession of isothermal trajectories was traced out on the X-Y Variplotter, enabling the border of the attainable region to be found. The computer was operated in real time and successive trajectories generated by manually altering potentiometer settings. Now it should be possible to integrate at high speed and reset parameters automatically after each integration, causing the attainable region to be mapped out in an exceedingly short time. Such a method will now be discussed.

4.1.1 Chemical reaction system

The reaction system chosen was the parallel reaction scheme



(4.1)

with B the desired product. In the yield problem the stoichiometrically attainable region is essentially filled when operating at either the upper ($E_1 \geq E_2$) or lower ($E_1 \leq E_2$) temperature limits[16]. We shall therefore consider the output problem.

Horn[28] has shown that for the output problem in the space (x_{Be}, ϕ), the stoichiometrically attainable region is not filled when $E_2 > E_1$. Then an optimal policy exists and this may be deduced from the reversible exothermic reaction by the "mirror principle"[28]. The border of the attainable region does not correspond to a single reaction path, but is the envelope of all optimal trajectories.

For first order kinetics, the differential equations describing the above system are

$$\frac{dx_B}{d\phi} = k(1 - x_B - x_C); \qquad x_B(0) = 0$$

$$\frac{dx_C}{d\phi} = k^r(1 - x_B - x_C); \qquad x_C(0) = 0 \tag{4.2}$$

with $\phi = k_R t$, $k = k_1/k_R$ and $r(= E_2/E_1) > 1$.

4.1.2 Closed solution

As a check for the subsequent computer results, a closed solution was obtained for (4.2) in the isothermal case. By the mirror principle, this solution will be given by equation (2.5) for the reversible exothermic reaction. It is represented graphically in figure (2.1a) for r = 2.

4.1.3 The computer method

An EAI TR-48 analogue computer could be operated in high speed repetitive mode, corresponding at the fastest speed to a cycle every 20 miliseconds. One set of integrators could be arranged to operate in this mode; these integrators had inputs $-\frac{dx_B}{d\phi}$ and $-\frac{dx_C}{d\phi}$ from equation (4.2). Another set of integrators operated in real time, generating k. During one cycle, the differential equations were integrated for a particular control policy and a single trajectory mapped out. The short duration of the cycle ensured that parameters supplied by the real time integrators were essentially constant. However, these parameters

varied from one cycle to the next, so different parameter values would be supplied automatically for successive cycles.

Depending on the period, up to 500 curves could be generated in 10 seconds and displayed successively on the screen of a Cathode Ray Oscilloscope, where they could be photographed.

The computer circuit is elementary and may be seen in figure (4.1) for r = 2 and k essentially constant over a cycle. Two quarter square multipliers have been incorporated in the circuit to generate the necessary non-linear terms. (A servomultiplier could of course not be used). This may be compared to the situation in #2.5, where all non-linearities could be eliminated.

A time base was generated by means of an integrator in the repetitive-operation (REP-OP) mode. Flyback (after each cycle) was eliminated on the oscilloscope screen, using a square wave signal from the computer.

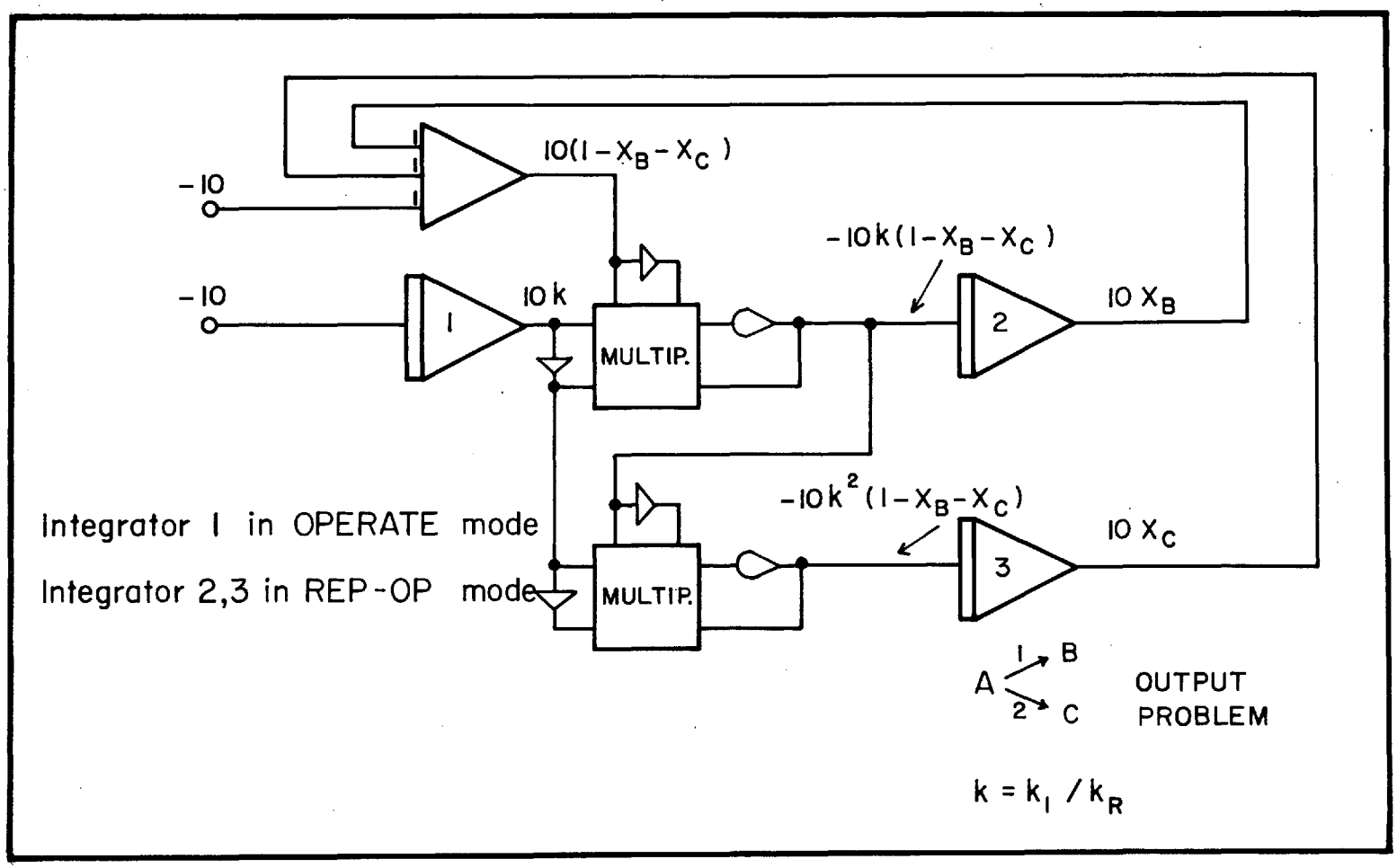


FIGURE 4.1 - ANALOGUE COMPUTER CIRCUIT FOR DETERMINATION OF ATTAINABLE REGION

4.1.4 The isothermal attainable region

The computer was first operated in REP-OP with a fixed value of k, so that a single isothermal trajectory was generated repeatedly. The value of k was then supplied by an integrator operating in real time and the isothermal attainable region generated by a series of isothermal trajectories. With a cycle time of 80 miliseconds, this gave approximately 150 curves in a run of 12 seconds duration. A medium intensity beam was maintained on the oscilloscope screen and the camera aperture set at f1.9. The resulting photograph is shown in figure (4.2).

When this is compared to figure (2.1a), the shape of the isothermal attainable region appears to be correct. However, the isothermal trajectories are not smooth curves, but show marked discontinuities in slope at a number of points. These may be traced to the non-linear components in the circuit. A quarter square multiplier has piecewise linear output and this is reflected in the above curves. As a result, there are several

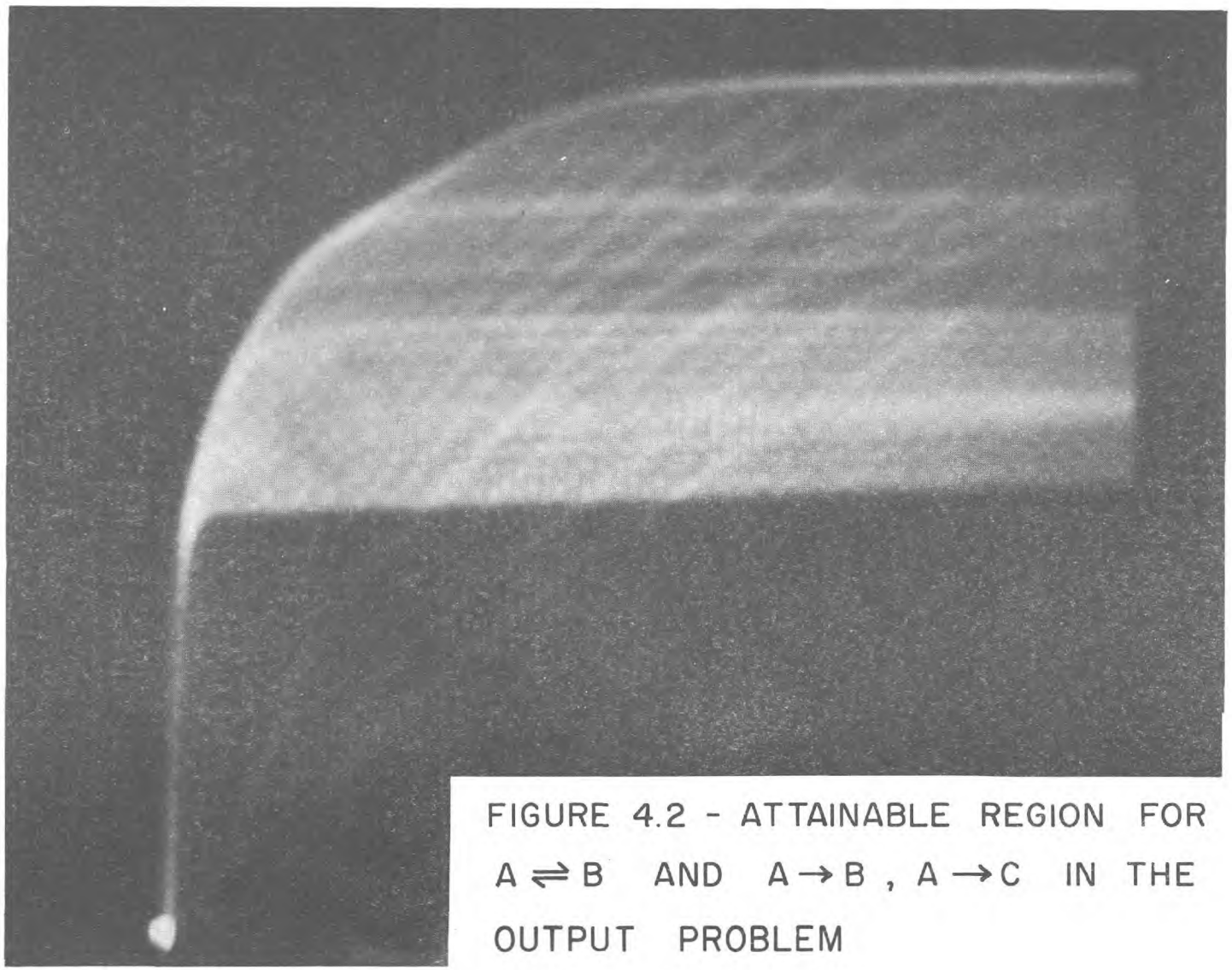


FIGURE 4.2 - ATTAINABLE REGION FOR $A \rightleftharpoons B$ AND $A \rightarrow B$, $A \rightarrow C$ IN THE OUTPUT PROBLEM

irregularities in the border of the isothermal attainable region.

The effect of these irregularities was found to be even more marked for $k = a + b\phi$. It had been hoped to obtain a gradation in light intensity on the photographs, to indicate the density of isothermal trajectories, but this was not possible.

4.1.5 Conclusions

Higher accuracy non-linear components are necessary and a hybrid computer could be used to advantage, with the digital equipment giving more sophisticated switching of parameter values than in our example. Perhaps the most promising application at this stage is as a rapid qualitative technique for obtaining the attainable region.

4.2 PROPAGATION OF THE ATTAINABLE REGION BORDER BY TRANSFORMATION OF BORDER POINTS

This is a technique for developing the attainable region by transforming border points at any time to border

points at a subsequent time. We need first to consider some geometric implications of the Pontryagin Maximum Principle [10].

4.2.1 Geometric interpretation of the Pontryagin Maximum Principle

We dealt in chapter three with an optimisation problem for a continuous system. This system was described by the set of differential equations (1.1), and to generate border points, the Hamiltonian had to be maximised (minimised) everywhere in time. The Hamiltonian is given by equation (3.28) as the scalar product of two vectors, $\underline{\lambda}$ and $\underline{v}$.

$$H(k) = \underline{\lambda} \cdot \underline{v}\,(k) \qquad (4.3)$$

From the transversality condition (3.30),

$$\underline{\lambda} = \text{grad } M \qquad (4.4)$$

i.e. at the point in question, $\underline{\lambda}$ is orthogonal to the surface M = constant. Also from (1.1) $\underline{v}$ is the velocity of propagation of the trajectory in state space. Hence the control k must be chosen such that the projection of

$\underline{v}$ (k) on to $\underline{\lambda}$ in state space is maximised (minimised). This will cause the border of the attainable region to enlarge at maximum rate.

As a consequence of this, note that H = 0 along a trajectory implies $\underline{\lambda}$ and $\underline{v}$ normal to one another. Hence the attainable region border will not enlarge with time in the direction grad M. This conforms with the quenching policies we have found to be optimal.

Halkin[7] calls the set of points which can be reached from $\underline{x}(t)$ after time dt with an admissible control, the "wavelet" associated with $\underline{x}(t)$. Then the attainable region at (t + dt) will be the union of the wavelets associated with the points $\underline{x}(t)$ of the attainable region at t. The border of the attainable region at (t + dt) is then the envelope or "wavefront" of these wavelets. According to the principle of optimal evolution proposed by Halkin, the control must always be chosen in order to maximise the velocity of the wavefront.

We wish to propagate the attainable region in a finite number of steps. Let us therefore now consider a discrete system.

4.2.2 Application to a discrete system

It has been shown by Horn and Jackson[36] that the discrete analogue of the Pontryagin Maximum Principle proposed by Katz[37] and others[38] is incorrect. Halkin[8] has pointed out that only when the set of reachable events is convex will a Discrete Maximum Principle hold. Then every point on an optimal trajectory belongs to the boundary of the set of possible events.

The transformation of the attainable region from one stage to the next in a sequence of stages has been discussed by Horn[1]. He designates the attainable region for the νth stage by $\Gamma(\nu)$, and indicates that to each point in $\Gamma(\nu - 1)$ there belongs a sub-attainable region in $\Gamma(\nu)$ corresponding to the set of admissible controls for stage ν. In cases of continuous one-to-one transformations (such as for linear transformation equations), a border point of $\Gamma(\nu)$ can only be created by a border point of $\Gamma(\nu - 1)$[1]. The attainable region for the complete sequence of stages can then be obtained by successively determining the border points of $\Gamma(0)$ (corresponding to

initial conditions), $\Gamma(1)$, $\Gamma(2)$, ... The convenience of such a construction scheme is also pointed out by Halkin[8].

We shall now apply this technique to the reaction system $A \underset{2}{\overset{1}{\rightleftharpoons}} B \xrightarrow{3} C$ carried out in a tubular reactor. We consider once again the 3-D output problem; for $E_2/E_1 = 4/3$, $E_3/E_1 = 2/3$ we can compare the results with those obtained in chapter three using the Maximum Principle.

4.2.3 Transformation equations

We consider the tubular reactor as a finite number of stages, each of which is operated isothermally. The temperature T must satisfy the constraints (1.7). We will construct successively the attainable region for each stage by using a finite number of admissible temperatures T together with the transformation equations.

From equations (3.41) and (1.12) we obtain the following simultaneous linear homogeneous equations for a stage,

$$\frac{dx_A}{d\phi} = - K^3 x_A + K^4 x_B$$

$$\frac{dx_B}{d\phi} = K^3 x_A - (K^4 + \tfrac{1}{4}K^2) x_B \qquad (4.5)$$

For a general stage ν, these may be solved to give two homogeneous linear equations

$$\underline{x}(\nu) = \underline{A}(K, \Delta\phi) \cdot \underline{x}(\nu - 1) \qquad (4.6)$$

The vector $\underline{x}$ has components (x_A, x_B) and $\underline{A}$ is a matrix of control dependent coefficients. This matrix also depends on the residence time for each stage $\Delta\phi$ and may be represented

$$A = \begin{bmatrix} F & G \\ H & W \end{bmatrix}, \qquad (4.7)$$

where

$$F = \frac{(\mu_1 - K^3) \exp(-\mu_2 \Delta\phi) - (\mu_2 - K^3) \exp(-\mu_1 \Delta\phi)}{\mu_1 - \mu_2}$$

$$G = \frac{K^4 \left[\exp(-\mu_2 \Delta\phi) - \exp(-\mu_1 \Delta\phi)\right]}{\mu_1 - \mu_2}$$

$$H = G/K$$

and

$$W = \frac{(\mu_1 - K^3)\exp(-\mu_1\Delta\phi) - (\mu_2 - K^3)\exp(-\mu_2\Delta\phi)}{\mu_1 - \mu_2} \tag{4.8}$$

Here μ_1, μ_2 are the roots of (2.24).

Note that since equations (4.5) are homogeneous, $\underline{A}$ depends on $\Delta\phi$ and not the absolute value of ϕ at any stage. However, to compare our results with those in chapter three, we must incorporate the transformation (3.50). This leads to

$$\Delta\phi = \frac{\Delta\xi}{\left[1 - \xi(\nu - 1)\right]\left[1 - \xi(\nu)\right]}, \tag{4.9}$$

where $\xi(\nu)$ is the value of ξ at the outlet to stage ν, assuming $\xi = 0$ at the input to the cascade. Now $\underline{A}$ becomes a function of $\xi(\nu)$ and must be determined for each stage.

4.2.4 Determination of border points

Assume that $\Gamma(\nu - 1)$ is known. Then we have indicated that a border point of $\Gamma(\nu - 1)$ will transform to a sub-attainable region in $\Gamma(\nu)$ with the set of admissible controls for stage ν, as in figure (4.3)[1,8]. To prevent an increase in the dimensionality of the problem, we must devise a scheme for determining the border points of stage ν. Then only these points need be considered in the subsequent transformation from stage ν to stage $(\nu + 1)$.

The objective variable space (x_B, x_C) for stage ν was divided into 100 vertical columns and 100 horizontal rows. This gave 10,000 equal squares. From the coordinates of an attainable point, the square containing it could be determined. As each point was generated, it could then be decided whether this point was the highest in its column, or furthest to the right or left in its row, of all the points thus far computed for that stage.

Additional search directions were also employed by rotating the coordinate axes through 45°, as shown in

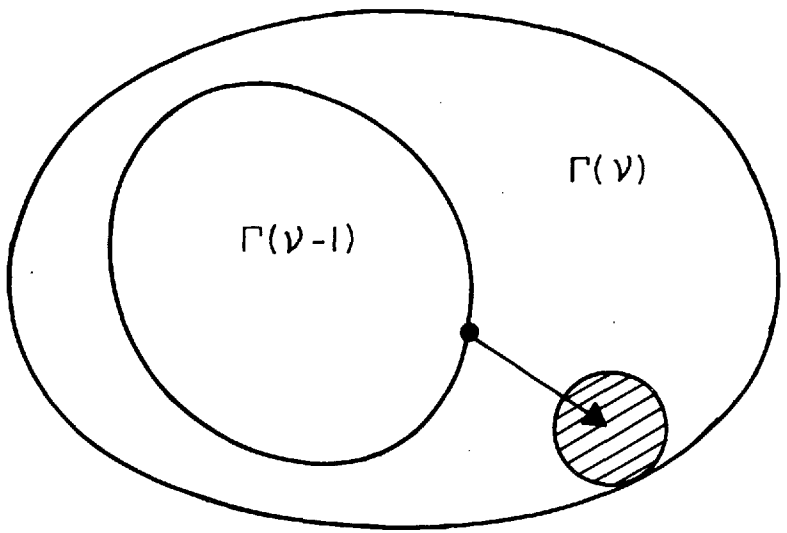
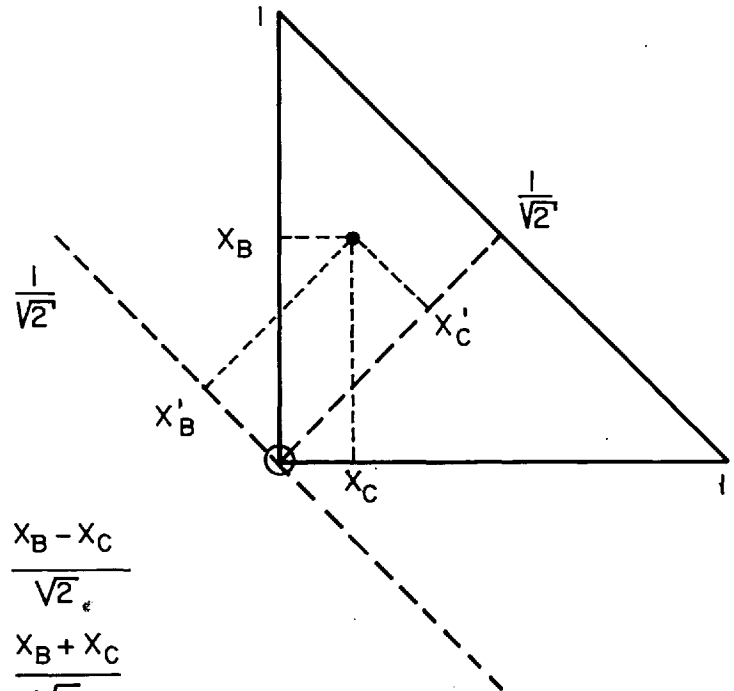


FIGURE 4.3- TRANSFORMATION OF A BORDER POINT ON THE ATTAINABLE REGION FROM STAGE $(\nu-1)$ TO STAGE ν



$$x'_B = \frac{x_B - x_C}{\sqrt{2}}$$

$$x'_C = \frac{x_B + x_C}{\sqrt{2}}$$

FIGURE 4.4- ROTATION OF SEARCH DIRECTIONS

figure (4.4). There are now columns and rows with respect to the transformed axes and a test could again be conducted for each attainable point as described above. If the original coordinates of such a point are (x_B, x_C), the transformed coordinates will be

$$\left(\frac{x_B - x_C}{\sqrt{2}} , \frac{x_B + x_C}{\sqrt{2}} \right) \qquad (4.10)$$

Obviously limitations to the dimensionality of the search are imposed by the stoichiometrically attainable region.

It is not sufficient to search only in the directions provided by the original coordinate system. If the gradient of the attainable region border is large, it is possible to select a point in a particular column (say) which is the highest in that column, and yet is further from the true border than a lower point. Using the higher point for subsequent transformations will lead to propagation of the error. (Such a search was tried initially, but rejected for this reason).

A border square can be identified as such by not being completely surrounded by attainable squares. However interior squares may possess the same property due to the finite number of control values. It was found highly inaccurate to transform border squares (as characterised by their centres, for example) rather than border points.

4.2.5 Algorithm for determining the attainable region

(i) Specify $x_A(0)$, $x_B(0)$ and hence fix input $\Gamma(0)$.

(ii) Select a satisfactory number of control values N.

(iii) For given $\Delta\xi$, compute the matrix $\underline{A}$ for each of the above control values.

(iv) Generate $\Gamma(1)$ by means of the transformation (4.6). This region will be defined by N points.

(v) Using each of these N points as input to stage 2, generate $\Gamma(2)$ with the transformation (4.6), for recomputed $\underline{A}$. Altogether N^2 points will be generated, some of which are internal and some of which are on

the border of $\Gamma(2)$. As a point is computed, check in each of the six search directions to see whether the point is a border point. If it is, store the point and relevant direction; if not, reject the point.

(vi) A current point may overwrite a previously accepted point in some direction. This previous point should then be examined to establish whether it is still optimal with respect to one of the remaining directions. If not, it may be discarded.

(vii) When all N^2 points have been generated, P of these will have been selected as border points, where $P \leq$ total number of rows and columns for all search directions. (A single point may be a border point in more than one direction). Each of the P points will have a control value associated with it, as well as having the point in $\Gamma(1)$ from which it was generated.

(viii) The P points may now be used as input to stage 3. Then $\Gamma(3)$ will be defined by P x N points

and the above procedure repeated to select its border points.

(ix) Continue in this fashion for the complete cascade.

4.2.6 The computer programme

A programme has been written in FORTRAN IV and may be found in Appendix IV #3.

Main programme: This contains the transformation equations (4.6) and directs computation from one stage to the next.

Subroutine 1: Evaluates the matrix A at each stage for the set of control values. We have used the fifty values of K shown in table (4.1); these are suggested from the isothermal study in #2.5.2 and are the only input to the programme.

Now $x_A(0) = 1$, $x_B(0) = 0$, so the transformation for the first stage yields

TABLE 4.1

Set of controls K

0	1	30
0.025	1.25	35
0.05	1.5	40
0.10	1.75	45
0.15	2	50
0.20	2.25	55
0.25	3	60
0.30	4	65
0.40	5	70
0.50	6	75
0.55	7	80
0.60	8	85
0.65	9	90
0.70	10	95
0.75	15	100
0.80	20	
0.90	25	

$$x_A(1) = F(1)$$

$$x_B(1) = H(1) \qquad (4.11)$$

This is the isothermal result of #2.5.2 and enables F(1), H(1) to be checked with the corresponding MIDAS solutions. Also for $x_A(0) = 0$, $x_B(0) = 1$, (4.12)

$$x_A(1) = G(1)$$

$$x_B(1) = W(1) \qquad (4.13)$$

The MIDAS solution for initial conditions (4.12) was also obtained and found to agree with G(1), W(1).

Subroutine 2: Maps attainable point into the columns and rows containing it. By printing out the coordinates of the point and the corresponding numbers for the columns, this subroutine could easily be checked. Note that for convenience, the rotated coordinate x_B' has been replaced by $x_B' + 1$.

Subroutine 3: The point is now tested in each search direction to establish whether it is a border point. This subroutine has been checked for stages 1 and 2, by printing out all points that were generated and selecting border points from this output. These border points could then be compared to values obtained by the subroutine.

Subroutine 4: This plots a graph of the attainable region for each stage. Interior points are included as well as border points. A number is given to each square indicating how many times a point has been located in that square (up to a maximum of 9).

Graphs have been prepared by hand for stages 1 and 2, from the output mentioned in subroutine 3. These graphs have been compared to the corresponding computer results and found to agree.

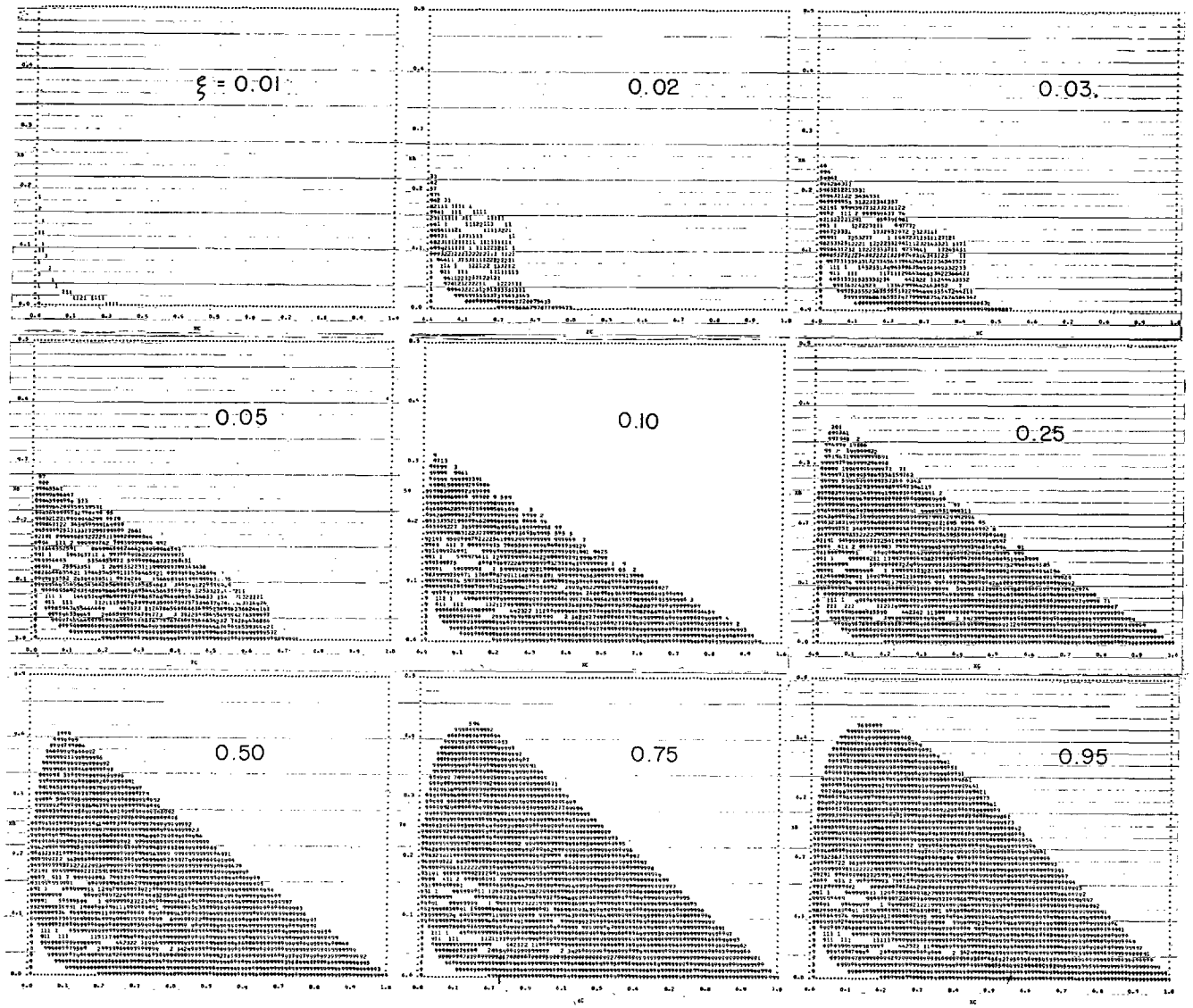
In one version of the computer programme, subroutine 4 has been omitted and input-output cards inserted in the programme, enabling values for the border points and their controls to be listed at each stage.

4.2.7 Results obtained with the procedure

The computer programme in binary form required 30 minutes on the IBM 7040 for solution. Results were obtained for a cascade of 27 stages, the first ten having $\Delta\xi = 0.01$ and the remainder with $\Delta\xi = 0.05$. The development of the attainable region with ξ is shown in figure (4.5), and the attainable region for stage 25 ($\xi = 0.85$) is shown enlarged in figure (4.6).

As would be expected, the results for the first few stages are much inferior to those obtained using Pontryagin in chapter three. However, the situation improves rapidly and by the time stage 7 is reached, there is little difference between the two methods. This is shown in figure (4.7). It is also interesting to note that the attainable region develops in an identical fashion to that already observed in chapter three. (See figures (3.8) and (3.11)). Thus for $\xi < 0.75$, the border to the left of the maximum turning point expands with ξ, whilst for $\xi > 0.75$ the only increase in the size of the attainable region takes place to the right of the maximum.

FIGURE 4.5- DEVELOPMENT OF THE ATTAINABLE REGION BY DIGITAL COMPUTER



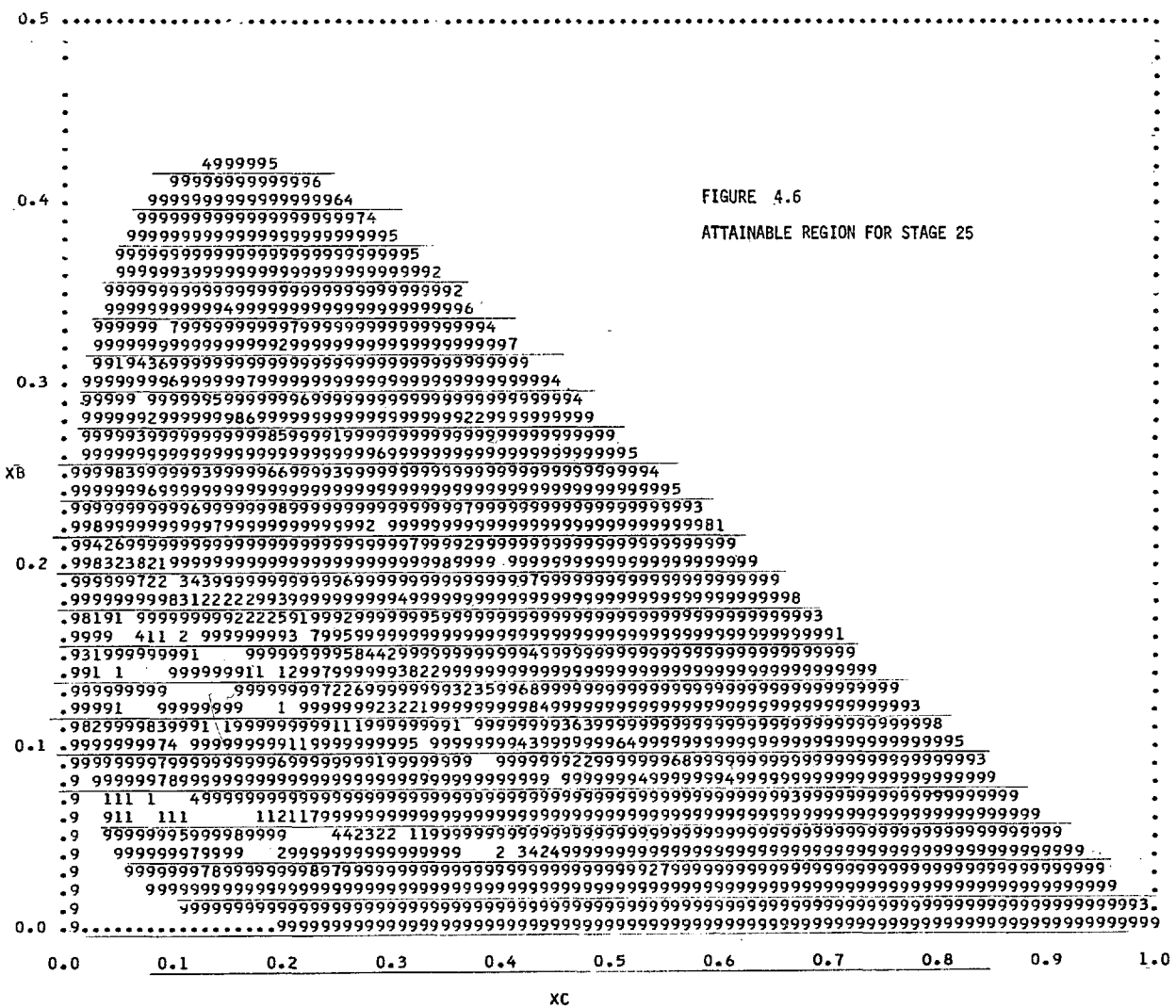


FIGURE 4.6

ATTAINABLE REGION FOR STAGE 25

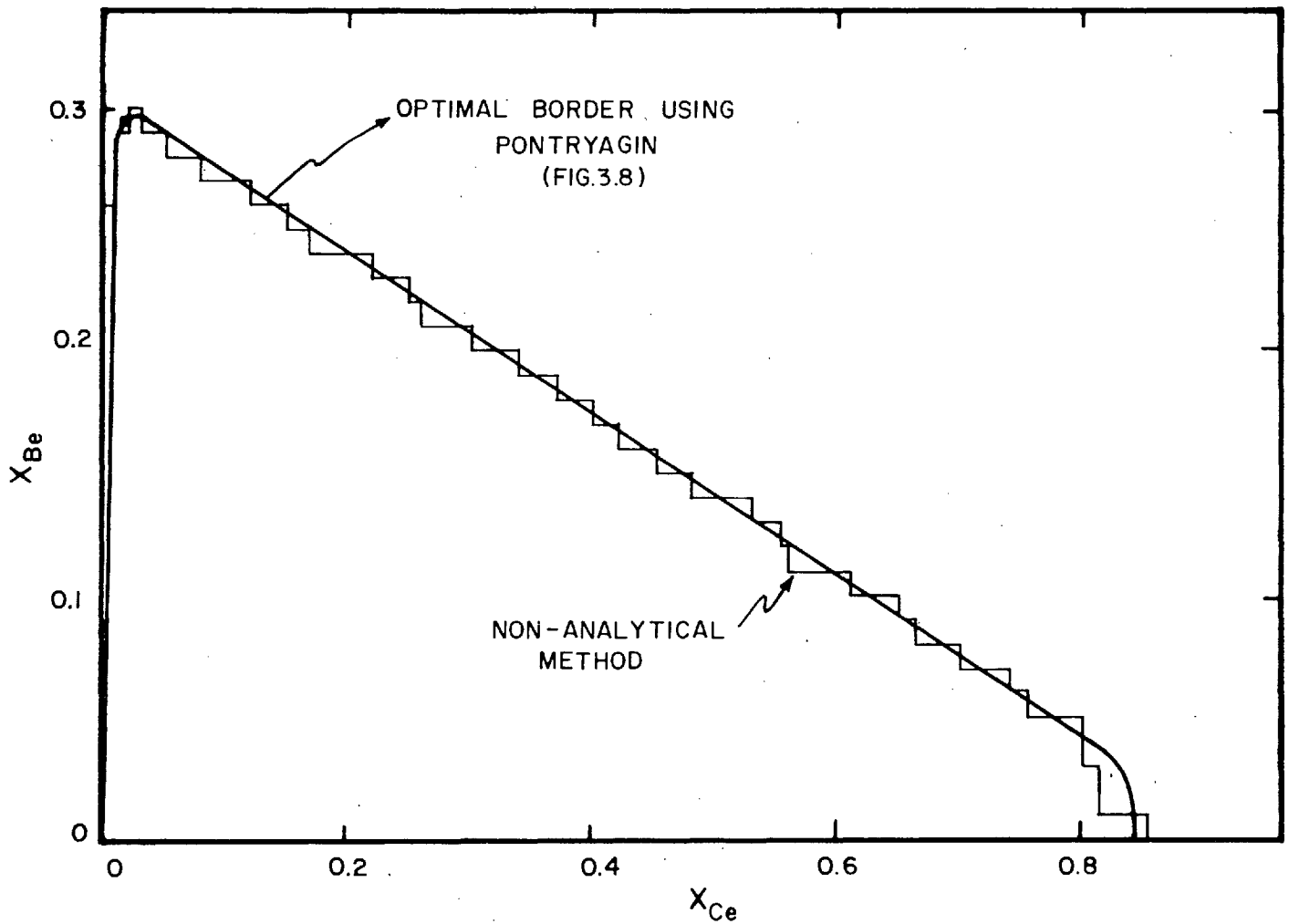


FIGURE 4.7 - COMPARISON BETWEEN PONTRYAGIN SOLUTION AND NON-ANALYTICAL METHOD FOR $\xi = 0.07$

Tabulated output was obtained from a binary programme in 36 minutes of IBM 7040 computing time. When the results are plotted against those of figure (3.8), excellent agreement is found. Figure (4.8) shows such a comparison, for ξ = 0.10, 0.75 and 0.95. Some typical control policies are indicated in table (4.2). Policy 1 corresponds to isothermal operation at the upper bound, to obtain maximum $x_C(\nu)$. (For ν = 17, all K $\geq$ 55 will give $x_C(17)$ = 0.99999999. The control K = 55 is accepted, since the programme has been devised to accept the lowest possible control). Policy 2 follows closely the maximum attainable $x_B(\nu)$, whilst policy 3 gives a typical trajectory. All three policies conform to falling temperature profiles as would be expected. Since the determination of border points at any stage ν does not depend on the previous history of individual profiles, but only on the points generated at stage ν, it is conceivable that some trajectories will not persist for all ν. This can be observed for policies 1 and 2.

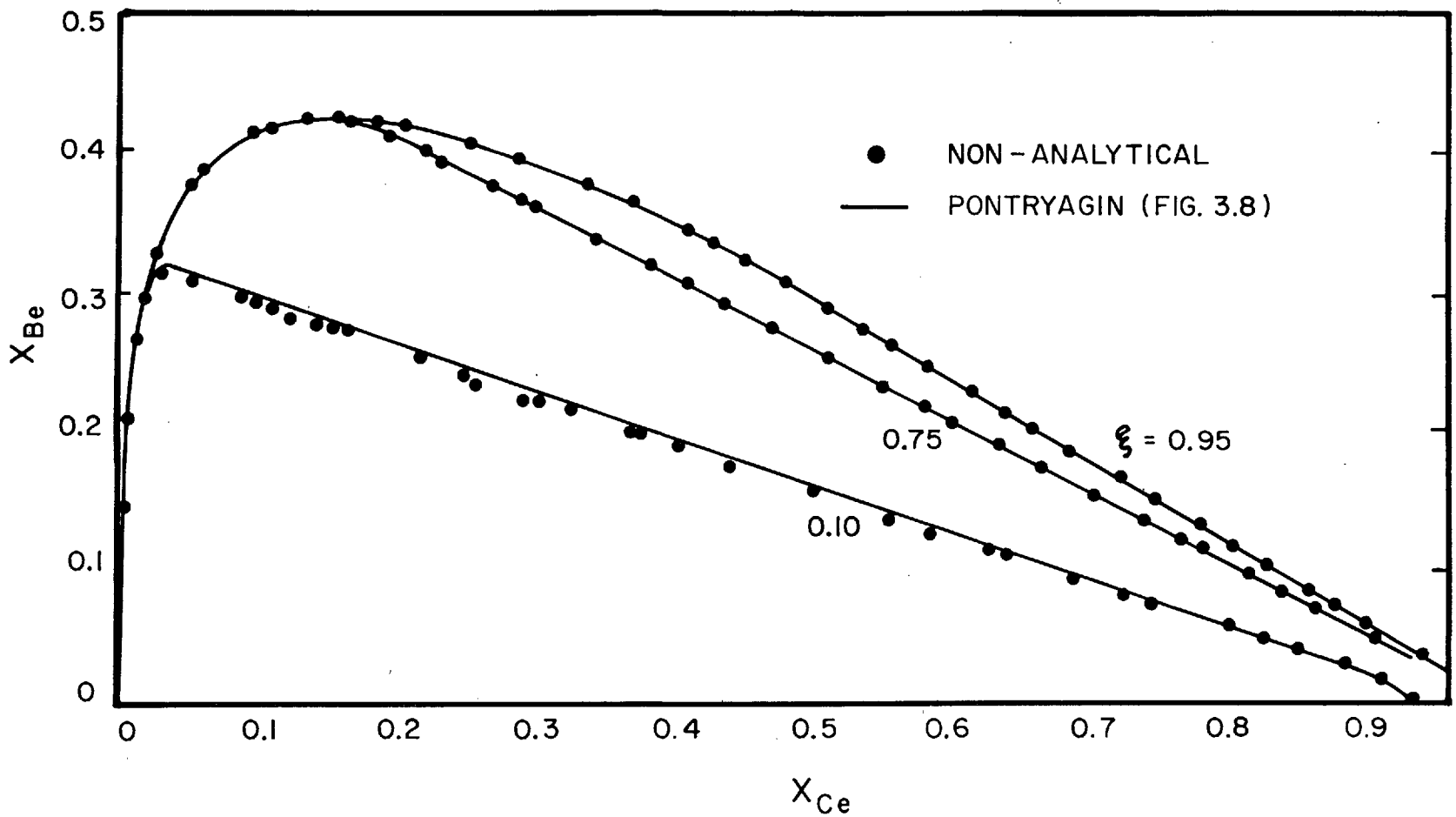


FIGURE 4.8 - COMPARISON BETWEEN PONTRYAGIN SOLUTION AND NON - ANALYTICAL METHOD

Table 4.2

Optimal control policies

ξ	ν	POLICY 1 $x_C(\nu)$	POLICY 1 $K(\nu+1)$	POLICY 2 $x_B(\nu)$	POLICY 2 $K(\nu+1)$	POLICY 3 $x_B(\nu)$	POLICY 3 $K(\nu+1)$
0	0	0	100	0	4	0	60
0.01	1	.22316322	100	.18933537	2.5	.01411438	4
0.02	2	.39962683	100	.22733984	2.25	.16388898	2.5
0.03	3	.53846421	100	.24955214	2	.19667810	2.25
0.04	4	.64713386	100	.26511248	1.75	.21577047	2
0.05	5	.73173751	100	.27683634	1.75	.22916172	2
0.06	6	.79724249	100	.28679056	1.5	.23933132	1.75
0.07	7	.84767217	100	.29466410	1.5	.24784633	1.75
0.08	8	.88626828	100	.30184202	1.5	.25499314	1.5
0.09	9	.91562865	100	.30836104	1.5	.26109987	1.5
0.10	10	.93782347	100	.31425691	1.25	.26663022	1.75
0.15	11	.98786625	100	.33596873	1.25	.27935855	1.5
0.20	12	.99806954	100	.35239493	1	.29240241	1.25
0.25	13	.99975963	100	.36435385	1	.30447537	1.25
0.30	14	.99997777	100	.37483759	0.9	.31189102	1
0.35	15	.99999857	100	.38345190	0.9	.32007059	0.9
0.40	16	.99999994	100	.39098878	0.8	.32685384	1
0.45	17	.99999999	55	.39731859	0.8	.33085808	0.9
0.50	18	.99999999	0	.40276363		.33474581	0.8
0.55	19	.99999999	0			.33829468	0.9
0.60	20	.99999999	0			.33658371	0.8
0.65	21	.99999999	0			.33601009	0.7
0.70	22	.99999999				.33555001	0.65
0.75	23					.33301485	0.65
0.80	24					.32427771	0.55
0.85	25					.31326414	0.5
0.90	26					.28990802	0.4
0.95	27					.24117585	

4.2.8 Discussion

The method is useful since a single computation will generate the complete attainable region in graphical form. We have considered a particular system. A general programme could be written for any system whose attainable region is unknown; only the relevant transformation equations need be inserted in a subroutine.

The method compares favourably with the Pontryagin Maximum Principle, in both computation time and simplicity. Although not as accurate as the analytical method, the precision is quite acceptable. No derivatives need be computed, which is an advantage. Transformation equations were obtained by integrating the state equations isothermally for the tubular reactor; the difference equation for a tank reactor could be employed instead, as long as sufficient stages are considered.

It is interesting to note that in our example, the piecewise continuous control policies for the tubular reactor are admissible controls in the Pontryagin formulation.

It is more convenient to store the border of the attainable region in digital form than to consider the systems equations as the representation of the reactor. Then for a particular objective function, the point on the border corresponding to the optimal reactor may easily be found. It is now a matter of selecting the appropriate control policy to realise this point. With the digital output in the current problem, this can easily be done. To each border point there belongs a control value and a number designating the previous border point from which the border point in question was generated.

CHAPTER FIVE

THE ISOTHERMAL ATTAINABLE REGION FOR THE SUCCESSIVE REVERSIBLE REACTIONS $A \underset{2}{\overset{1}{\rightleftharpoons}} B \underset{4}{\overset{3}{\rightleftharpoons}} C$ IN A YIELD PROBLEM

We discuss here some introductory work on the above system, which will indicate for which relationships between activation energies, the stoichiometrically attainable region is not essentially filled.

5.1 THE SYSTEMS EQUATIONS

There are four rate constants in this reaction scheme and a similar control transformation may be used as for the Denbigh reaction system [9, 39]. With the yield problem transformation

$$k = k_2/k_1 \tag{5.1}$$

we may then write

$$k_3/k_1 = ak^{-\alpha}; \quad k_4/k_1 = bk^{-\beta}; \tag{5.2}$$

with a, α as in equation (2.12) and b, β given by

$$b = \left[\frac{H_4}{H_1}\right]\left[\frac{H_2}{H_1}\right]^{\beta}; \qquad \beta = \frac{E_4 - E_1}{E_1 - E_2} \tag{5.3}$$

This reduces the number of parameters from eight to four.

There are two stoichiometrically independent reactions and the systems equations for the tubular reactor are

$$\frac{dx_B}{d\phi} = 1 - x_B(1 + k + ak^{-\alpha}) - x_C(1 - bk^{-\beta}) \tag{5.4a}$$

$$\frac{dx_C}{d\phi} = ak^{-\alpha}x_B - bk^{-\beta}x_C \tag{5.4b}$$

with $\phi = k_1 t$ and $x_B(0) = x_C(0) = 0$.

The solution to these equations is discussed by Lowry and John [40], who point out that the relative values of the rate constants will dictate whether the concentration of B goes through a maximum. Their solution is given in closed form by Frost and Pearson [4], in terms of the four rate constants. By setting the appropriate rate constants to zero, it may easily be verified that the expressions

reduce to those for $A \rightleftharpoons B \longrightarrow C$ or $A \longrightarrow B \longrightarrow C$ respectively. Levenspiel[11] presents isothermal trajectories from the work of Jungers et al[41], for various values of the four rate constants. These latter authors[41] have treated complex reactions very extensively.

The above solutions are complicated and we prefer to deal directly with the differential equations (5.4). These have been patched on an EAI TR-48 analogue computer, with separate potentiometers for $ak^{-\alpha}$ and $bk^{-\beta}$ to avoid using non-linear equipment. The circuit is not presented.

5.2 EQUILIBRIUM

Each isothermal attainable region contains an equilibrium curve, unlike the situation for $A \rightleftharpoons B \longrightarrow C$, where all trajectories end at $x_C = 1$. From (5.4b) at equilibrium

$$\frac{x_B}{x_C} = \left(\frac{b}{a}\right) k^{\alpha-\beta} \qquad (5.5)$$

When substituted into (5.4a), this gives

$$k = \frac{1 - x_B - x_C}{x_B} \qquad (5.6)$$

so that (5.5) becomes

$$\frac{x_B}{x_C} = \left(\frac{b}{a}\right)\left[\frac{1 - x_B - x_C}{x_B}\right]^{\alpha - \beta} \qquad (5.7)$$

Hence the equilibrium curve is dependent on only (b/a) and $(\alpha - \beta)$.

From (5.4), the same isothermal trajectory will be obtained for k = 1, whatever the values of α and β. All equilibrium curves will therefore pass through the equilibrium point for k = 1. This point is given by the intersection of the lines $2x_B = 1 - x_C$ and $x_B = \left(\frac{b}{a}\right)x_C$. When b = 0 (corresponding to $A \rightleftharpoons B \rightarrow C$) the equilibruim point is thus $x_B = 0$, $x_C = 1$; if a = 0 (corresponding to $A \rightleftharpoons B$), $x_B = 0.5$ at equilibrium.

5.3 THE CASE $(\alpha - \beta) < 0$

This is achieved with $(E_1 > E_2;\ E_3 < E_4)$ or $(E_1 < E_2;\ E_3 > E_4)$. For this case, we have found the border of the

isothermal attainable region to be given completely by the equilibrium curve. Since the curve depends on $(\alpha - \beta)$ and $(\frac{b}{a})$, we need only discuss the effect of these parameters.

We shall first consider $(\frac{b}{a}) = 1$. Variation of the isothermal attainable region with $(\alpha - \beta)$ is shown in figure (5.1). There is a marked change in shape for small deviations about $(\alpha - \beta) = -1$. In the range

$$-1 \leq \alpha - \beta < 0 \qquad (5.8)$$

not all x_C are attainable.

The shape of the attainable region is not dependent on $\alpha > 0$ or $\alpha \leq 0$. In the former case, however, isothermal trajectories cross one another; this is not so for the latter case as shown in figure (5.2).

Now changing $(\frac{b}{a})$ causes the equilibrium point for $k = 1$ to shift along the line $2x_B = 1 - x_C$ as indicated in #5.2. The effect is to move the attainable region in the same direction, which can be clearly seen in figure (5.3) for $(\alpha - \beta) = -1$.

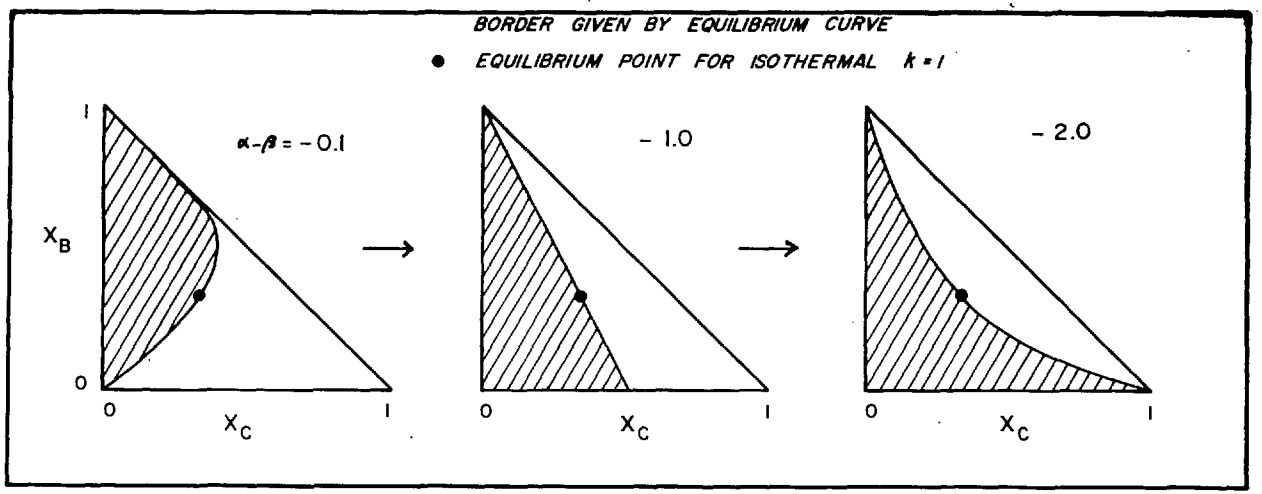


FIGURE 5.1 - ISOTHERMAL ATTAINABLE REGION FOR $A \rightleftharpoons B \rightleftharpoons C$ WITH $(\alpha-\beta)<0$ AND $(b/a) = 1$

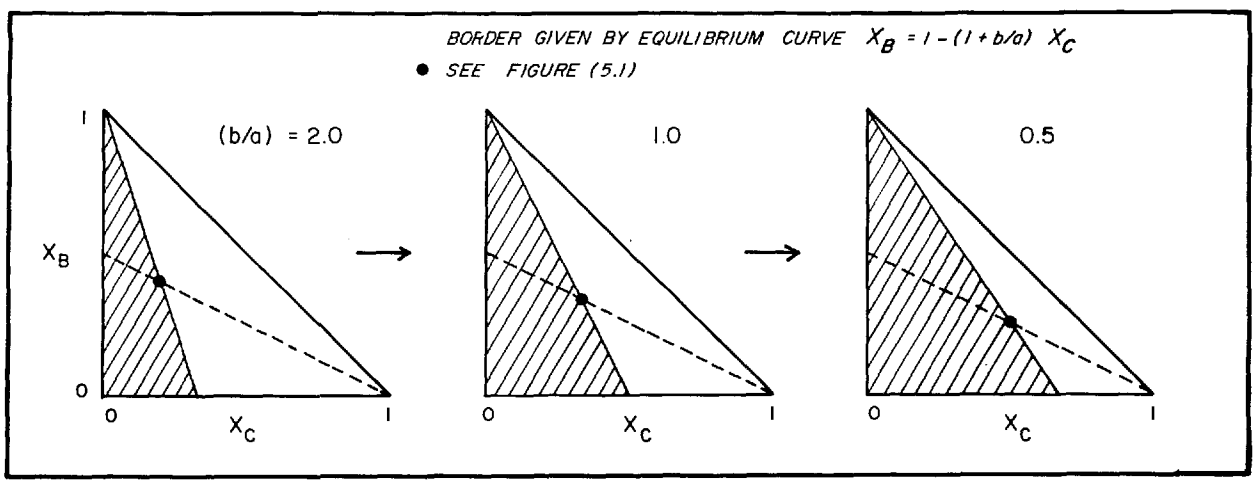


FIGURE 5.3 - EFFECT OF (b/a) ON THE ISOTHERMAL ATTAINABLE REGION FOR $(\alpha-\beta) = -1$

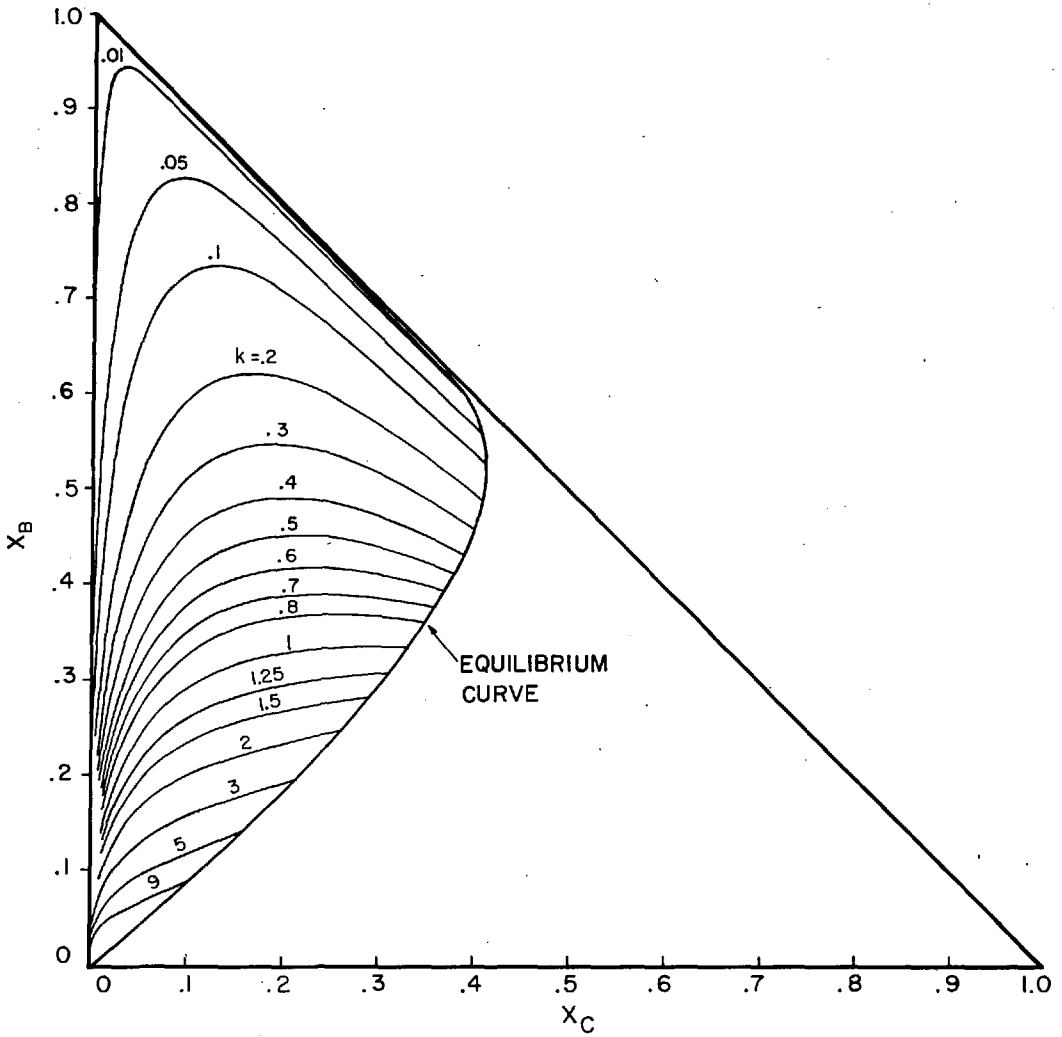


FIGURE 5.2 - ISOTHERMAL TRAJECTORIES FOR $\alpha = -1$, $\beta = -0.9$ AND $(b/a) = 1$

5.4 THE CASE $(\alpha - \beta) = 0$

This is the singular case $E_3 = E_4$. The equilibrium curve now forms only part of the border of the attainable region and is given by the line $x_B = (\frac{b}{a})x_C$. For $\alpha < 0$ the stoichiometrically attainable region above this line is filled, whilst for $\alpha > 0$ the envelope of isothermal trajectories completes the border. When $\alpha = 0$ (i.e. $E_1 = E_3 = E_4$) the isothermal $k = 0+$ is the upper border. These three cases are shown in figure (5.4). Their behaviour is essentially that of $A \rightleftharpoons B \rightarrow C$, except that the equilibrium line is now the lower border. Isothermal trajectories do not cross one another for $\alpha \leq 0$, whilst the converse is true for $\alpha > 0$. As $(\frac{b}{a})$ increases, the equilibrium curve approaches the x_B axis. When $(\frac{b}{a}) \rightarrow 0$, results approach those for $A \rightleftharpoons B \rightarrow C$.

5.5 THE CASE $(\alpha - \beta) > 0$

The attainable region border is no longer only the equilibrium curve. The cases $\alpha > 0$, $\alpha = 0$ and $\alpha < 0$ exhibit different behaviour from one another and will be discussed separately.

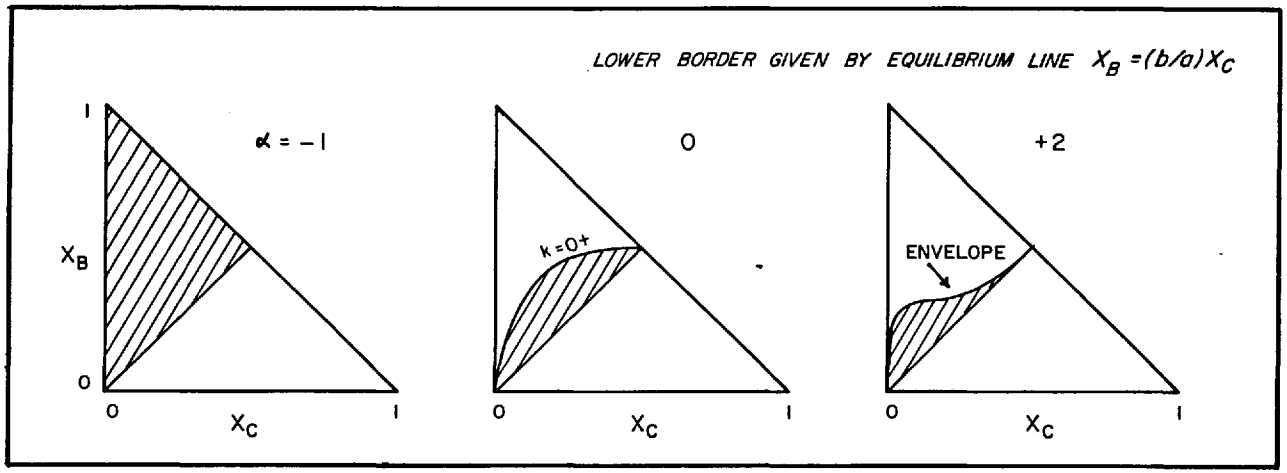


FIGURE 5.4 - ISOTHERMAL ATTAINABLE REGION FOR $A \rightleftharpoons B \rightleftharpoons C$ WITH $(\alpha - \beta) = 0$ AND $(b/a) = 1$

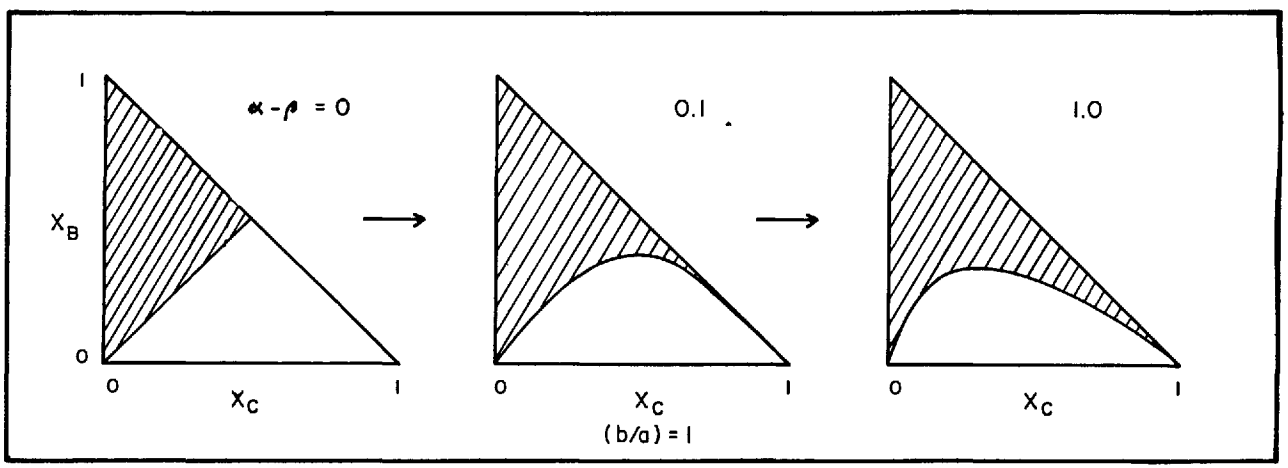


FIGURE 5.5 - ISOTHERMAL ATTAINABLE REGION FOR $A \rightleftharpoons B \rightleftharpoons C$ WITH $\alpha = -1$ AND $(\alpha - \beta) \geq 0$

With $\alpha < 0$, the border is composed of equilibrium curve and envelope of trajectories. The effect of $(\alpha - \beta)$ on the isothermal attainable region is shown in figure (5.5) for $(\frac{b}{a}) = 1$.

For $\alpha = 0$ the isothermal attainable region is a narrow strip bounded by the equilibrium curve, the isothermal k = 0+ and the envelope of isothermal trajectories.

For B the desired product, the situation is of interest when $\alpha > 0$ (c.f. $A \rightleftharpoons B \rightarrow C$). The effect of increasing $(\alpha - \beta)$ for $\alpha = 2$ may be found in figure (5.6).

When $(\frac{b}{a})$ increases, the attainable region is shifted to the left in the above three cases. The converse is also true.

5.6 PHYSICAL SIGNIFICANCE OF THE RESULTS

Consider conversion to desired product B.

$(\alpha - \beta) < 0$ complete conversion to B possible

$(\alpha - \beta) \geq 0$ complete conversion to B possible for $\alpha < 0$

not possible for $\alpha \geq 0$

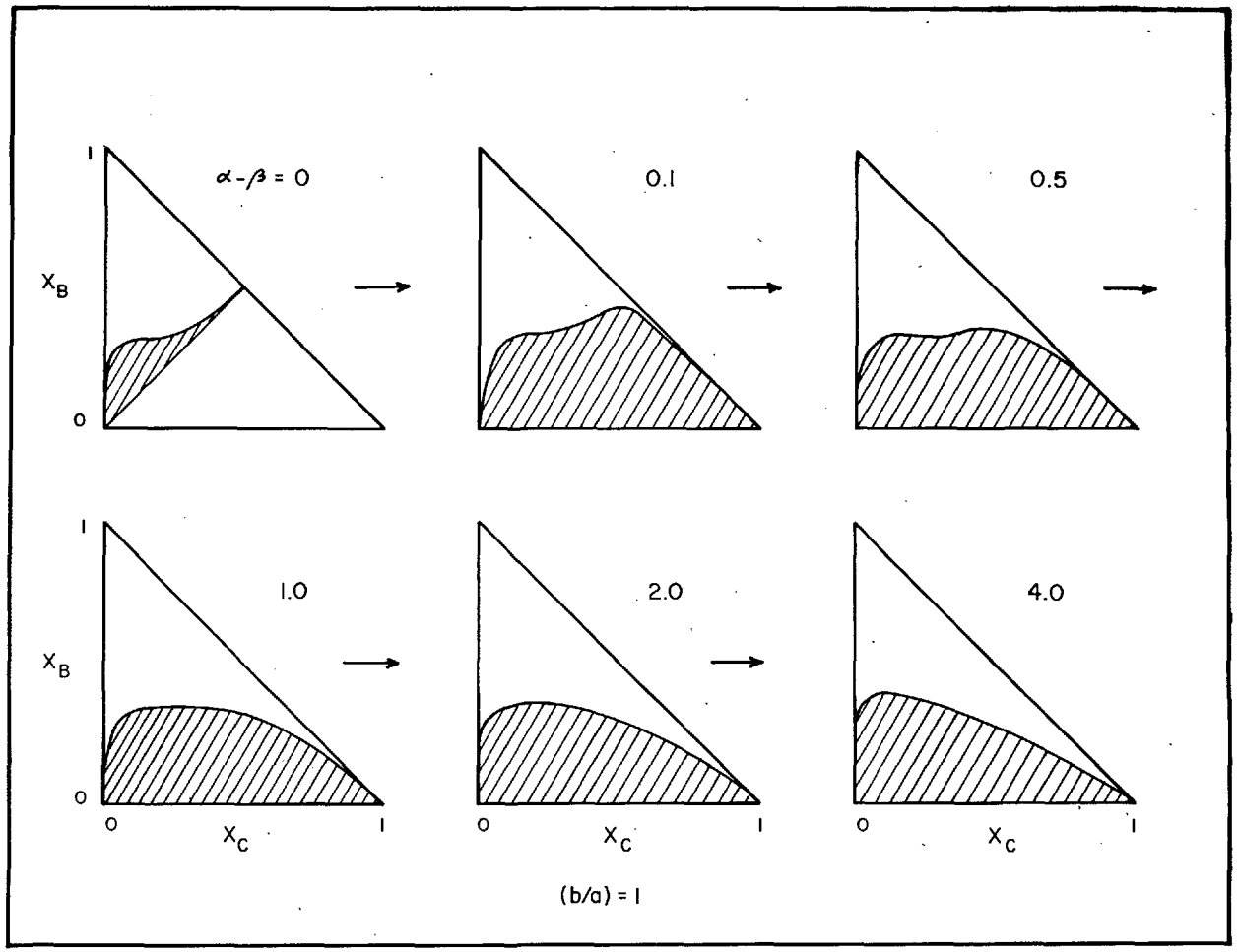


FIGURE 5.6 - ISOTHERMAL ATTAINABLE REGION FOR $A \rightleftharpoons B \rightleftharpoons C$ WITH $\alpha = 2$ AND $(\alpha - \beta) \geq 0$

This may be explained as follows. If we let $k_2 \longrightarrow 0$, then for $k_4 >> k_3$ we would expect to attain complete conversion to B.

i.e.

$$\frac{k_2}{k_1} << 1 \quad \text{and} \quad \frac{k_4}{k_3} >> 1$$

or

$$k << 1 \quad \text{and} \quad \left(\frac{b}{a}\right) k^{\alpha - \beta} >> 1$$

This means

$$(\alpha - \beta) < 0.$$

Now with $k_2 \longrightarrow 0$, $k_4 << k_3$, the system will approach $A \rightleftharpoons B \longrightarrow C$ and all x_B is attainable if $k_1 >> k_3$.

i.e.

$$k << 1; \quad ak^{-\alpha} << 1; \quad \left(\frac{b}{a}\right) k^{\alpha - \beta} << 1$$

Hence $\alpha < 0$ and $\alpha - \beta > 0$. The converse is true for $k_1 << k_3$, i.e. for $\alpha > 0$.

Note that when $E_4 \rightarrow \infty$, the system $A \rightleftharpoons B \rightleftharpoons C$ approaches $A \rightleftharpoons B \rightarrow C$ and we expect the stoichiometrically attainable region to be filled for $\alpha < 0$ and vice versa. Now $E_4 \rightarrow \infty$ implies $\beta \rightarrow \pm \infty$, depending on $E_1 > E_2$ or $E_1 < E_2$. Hence in the limit as $(\alpha - \beta) \rightarrow \pm \infty$ for $\alpha < 0$, the stoichiometrically attainable region will be filled out. This is not the case when $\alpha > 0$.

5.7 DISCUSSION

The conclusions reached in this isothermal study may be applied qualitatively to the case of perfect temperature control. When the border of the isothermal attainable region is the equilibrium curve, a more sophisticated control policy should be of no avail in the yield problem. An optimal study would also be unnecessary, when completing the convex hull of the isothermal attainable region causes the stoichiometrically attainable region to be filled out.

More sophisticated control should improve the yield of B for the case

$$(\alpha - \beta) \geq 0 \qquad \alpha \geq 0 \tag{5.9}$$

Similar optimisation methods may be employed to those for the Denbigh reaction system, such as discussed by Storey [42,43]. Instantaneous yield may be maximised as in #3.3.

Mah and Aris [44] have considered the yield problem for the consecutive reversible reactions carried out in a tank reactor and in a cascade of tanks. However they derive a method which enables optimal temperatures to be found for a range of initial conditions. This was not the purpose of the present study.

CHAPTER SIX

DISCUSSION

6.1 INITIAL CONDITIONS

We have considered in this study a reactor feed consisting of pure A, i.e.

$$x_A(0) = 1$$
$$x_B(0) = 0 \qquad (6.1)$$

The resulting attainable region is then valid for this feed condition and any objective function plotted in objective variable space.

Now consider an internal point of the attainable region as an initial condition. Since the state equations are autonomous, it is not possible to proceed from this point to a point outside the attainable region with an admissable control policy. Consequently the attainable region for which this point is an initial condition must be a subset of the attainable region with initial conditions (6.1). This provides useful qualitative information.

6.2 THE SOLUTION OF OPTIMAL PROBLEMS

More general optimisation problems than yield or output problems may be treated by an increase in dimensionality of the objective variable space. However yield and output problems provide valuable information. Even if temperature control costs (say) are important, it is wise to first solve the problem without including these costs in the calculation. Note that the output problem is a projection of the more general optimisation problem.

6.3 PERFECT TEMPERATURE CONTROL

The perfect optimal reactor cannot be realised in practice. Thus adiabatic operation with direct or indirect intercooling has for example been studied [45,46]. Nevertheless, the attainable region for perfect temperature control provides valuable information about the limits of attainability. It enables the design engineer to decide how sophisticated a control policy is necessary in a given problem.

In the present case for example, the isothermal attainable region is not much smaller than the attainable

region. Consequently little reduction in conversion will result from isothermal operation. It has been stated that isothermal operation may be expensive, especially for highly exothermic reactions, and that a more realistic approach would be to operate adiabatically. (See discussion on reference (18)). Whilst this is generally true, an isothermal study provides information very readily; indeed it is recommended that for a system of unknown parametric behaviour, the first step should be an isothermal investigation with an analogue computer. This will give very rapidly a qualitative idea of what can be attained.

6.4 COMPARISON BETWEEN ATTAINABLE REGIONS FOR TUBULAR REACTOR AND SINGLE TANK

The attainable region for the tube was found to contain that for the tank, for the cases considered in this study.

6.5 CONCLUSIONS

The attainable region has been obtained for a given system under specified initial conditions. The use of this region with a particular objective function has been

illustrated by means of examples. Once the border of the attainable region has been found, the optimal problem is easily solved for all objective functions plotted in objective variable space.

Although our results apply quantitatively only to the parameter values used, the attainable region is a qualitative representation of an exothermic reversible reaction with irreversible product decay. The methods described are general and may also be applied to other reaction systems.

REFERENCES

1. Horn F., Third European Symposium on Chemical Reaction Engineering, Pergamon (1964)

2. Bellman R., "Dynamic Programming", Princeton University Press, Princeton N.J. (1957)

3. Zwietering T.N., Chem.Eng.Sci. 11 (1959) 1

4. Frost A.A. and Pearson R.G., "Kinetics and Mechanism", 2nd Edn., Wiley and Sons, New York (1961)

5. Roxin E., Bol. Soc. Mat. Mex. 5 (1960) 125

6. Roxin E., "Nonlinear Differential Equations and Nonlinear Mechanics", eds. J.P. LaSalle and S. Lefschetz, Academic Press, New York (1963) pp. 303

7. Halkin H., ibid., pp. 284

8. Halkin H., "Advances in Control Systems, Volume I", Academic Press, New York (1964) pp. 173

9. Denbigh K.G., Chem.Eng.Sci. 8 (1958) 125

10. Pontryagin L.S. et al, "Mathematical Theory of Optimal Processes", Wiley and Sons, New York (1962)

11. Levenspiel O., "Chemical Reaction Engineering", Wiley and Sons, New York (1962)

12. Denbigh K.G., "Chemical Reactor Theory", Cambridge University Press (1965)

13. Douglas J.M., Chem.Eng.Prog. Symp.Ser. 60 (1964) 1

14. Horn F. and Kuchler L., Chem.Ing.Tech. 31 (1959) 1

15. Kramers H. and Westerterp K.R., "Elements of Chemical Reactor Design and Operation", Netherlands University Press, Amsterdam (1963)

16. Horn F. and Troltenier U., Chem.Ing. Tech. 33 (1961) 413

17. Horn F., "Optimalprobleme bei kontinuierlichen chemischen Prozessen", Dissertation Techn. Hochschule, Wien (1958)

18. Horn F., Z.Elektrochem. 65 (1961) 209

19. Chermin H.A.G. and van Krevelen D.W., Chem.Eng.Sci. 14 (1961) 58

20. Bilous O. and Piret E.L., A.I.Ch.E.J. 1 (1955) 480

21. Trambouze P.J. and Piret E.L., A.I.Ch.E.J. 5 (1959) 384

22. Franckaerts J. and Froment G.F., Chem.Eng.Sci. 19 (1964) 807

23. Bilous O. and Amundson N.R., Chem.Eng.Sci. 5 (1956) 81, 115

24. Aris R., Chem.Eng.Sci. 13 (1960) 18

25. Coward I. and Jackson R., Chem.Eng.Sci. 20 (1965) 911

26. Denbigh K.G. Chem.Eng.Sci. 14 (1961) 25

27. Rozonoer L.I., Automation and Remote Control 20 (1959) 1288, 1405, 1517

28. Horn F., Chem.Eng.Sci. 14 (1961) 77

29. Horn F., Alta Tecnologia Chimica, Academia Nationale dei Lincei, Roma (1962) pp. 45

30. MIDAS Programming Guide, IBM Technical Documentary Report No. SEG-TDR-64-1 (1964)

31. Lance G.N., "Numerical Methods for High Speed Computers", Iliffe and Sons, London (1960) pp. 56

32. Fox L., "Numerical Solution of Ordinary and Partial Differential Equations", Pergamon, Oxford (1962) pp. 24

33. Kolbel H. et al, Third European Symposium on Chemical Reaction Engineering, Pergamon (1964)

34. Kuchler L. and Langbein D., Ibid

35. Lee E.S., A.I.Ch.E.J. 10 (1964) 309

36. Horn F. and Jackson R., Ind.Eng.Chem.Fund. 4 (1965) 110

37. Katz S., J.Elect.Cont. 13 (1962) 179

38. Fan L.T. and Wang C.S., "The Discrete Maximum Principle", Wiley and Sons, New York (1964)

39. Horn F. and Troltenier U., Chem.Ing.Tech. 32 (1960) 382

40. Lowry T.M. and John W.T., J.Chem.Soc. 97 (1910) 2634

41. Jungers J.C. et al, "Cinétique chimique appliquée", Technip, Paris (1958)

42. Storey C., Chem.Eng.Sci. 17 (1962) 45

43. Storey C., Trans.I.Ch.E. 42 (1964) 345

44. Mah R.S.H. and Aris R., Chem.Eng.Sci. 19 (1964) 541

45. Horn F., Z.Elektrochem. 65 (1961) 295

46. Dyson D.C., Ph.D. Thesis, University of London (1965)

NOMENCLATURE

C_i	concentration of component i
E_i	activation energy for reaction i
H_i	frequency factor for reaction i
H	Hamiltonian function
k_i	reaction velocity constant for reaction i
k	control variable
K	transformed control variable
M	objective function
r	ratio of activation energies
s	ratio of activation energies
t	measure of reaction time
T	temperature
v	reaction rate
x	state variable
X	ratio of state variables

Subscripts

A	component A
B	component B
C	component C

e exit condition

o initial condition

u upper bound

Greek symbols

ϵ truncation error

λ adjoint variable

ϕ dimensionless time

τ mean residence time in tank

ξ $\phi/(1+\phi)$

$\Gamma(v)$ attainable region for stage v

μ eigenvalue

Ψ integration variable

APPENDIX I

1. For A⟶B⟶C, the isothermal trajectory for the tubular reactor lies above that for the tank

Refer to figure (2.3). If x_{Ae} be equal in tube and tank, then from equations (2.8) and (2.9)

$$\exp(\phi_e) = 1 + \phi \tag{A1.1}$$

We must prove

$$\frac{\exp(-\phi_e) - \exp(-k\phi_e)}{k - 1} \geq \frac{\phi}{(1 + \phi)(1 + k\phi)} \qquad k \neq 1$$

$$\phi_e \exp(-\phi_e) \geq \phi/(1 + \phi)^2 \qquad k = 1 \tag{A1.2}$$

(a) $k \neq 1$ Substitute (A1.1) into (A1.2). Then we must prove

$$\frac{(1 + \phi)^{-1} - (1 + \phi)^{-k}}{k - 1} \geq \frac{\phi}{(1 + \phi)(1 + k\phi)}$$

i.e.

$$\frac{1}{k - 1}\left[\frac{1}{1 + \phi} - \frac{1}{(1 + \phi)^k}\right] \geq \frac{1}{k - 1}\left[\frac{1}{1 + \phi} - \frac{1}{1 + k\phi}\right]$$

(i) $k > 1$ $\quad (1 + x)^n \geq (1 + nx)$ $\quad x \geq 0$

$n > 1$, and the result follows.

(ii) $0 \leq k < 1$ $\quad (1 + x)^n \leq (1 + nx)$ $\quad x \geq 0$

$0 \leq n < 1$, and the result again follows.

(b) $\underline{k = 1}$ We must now prove

$$\phi_e \geq \phi/(1 + \phi)$$

i.e.

$$\ln (1 + \phi) \geq \phi/(1 + \phi)$$

Since $\ln(1 + x) \geq x/(1 + x)$ $\quad x \geq 0$, the result follows.

2. <u>For A→B→C isothermally, then for the same feed and conversion of A, a tube will produce larger conversion to B than a tank, and in a shorter time</u>

For x_{Ae}(tube) = x_{Ae}(tank), we have already proved x_{Be}(tube) $\geq$ x_{Be}(tank) in #1. Now since $\exp x \geq 1 + x$ for all x, the result $\phi \geq \phi_e$ follows directly from equation (A1.1).

3. <u>For A→B→C, a tank reactor can always be represented by a tubular reactor system in such a way that the holding time for the tubular reactor system is less than that for the tank</u>

Refer again to figure (2.3). We must prove $\phi_u \leq \phi$, where $\phi_u = (V_u/v)$ and $\phi = (V_a/v)$ from figure (2.2).

Now

$$v_1 + v_2 = v$$

$$v_1 x_{Bu} = v x_{Ba}$$

$$\frac{x_{Bu}}{x_{Ba}} = \frac{1 - x_{Au}}{1 - x_{Aa}} = \frac{V_u}{v_1}\frac{v}{V_u} = \frac{\phi_e}{\phi_u} \qquad \text{(A1.3)}$$

We must thus prove

$$\phi \geq \left[\frac{1 - x_{Aa}}{1 - x_{Au}}\right] \phi_e$$

i.e.

$$1 + \phi \geq \frac{\phi_e}{1 - \exp(-\phi_e)}$$

Eliminate ϕ from (A1.3)

$$\frac{\left[1 + k\phi\right]\left[\exp(-\phi_e) - \exp(-k\phi_e)\right]}{k - 1} = 1 - \exp(-\phi_e)$$

$$1 + \phi = \frac{(k - 1)\left[1 - \exp(-k\phi_e)\right]}{k\left[\exp(-\phi_e) - \exp(-k\phi_e)\right]}$$

Hence we must prove

$$\left[\frac{k - 1}{k}\right]\left[\frac{1 - \exp(-k\phi_e)}{\exp(-\phi_e) - \exp(-k\phi_e)}\right] \geq \frac{\phi_e}{1 - \exp(-\phi_e)}$$

The proof of this follows from #4.

4. $\left[\frac{k - 1}{k}\right]\left[\frac{1 - x^k}{1 - x^{k-1}}\right] \geq \frac{x \ln x}{x - 1}$ $\quad 0 \leq k \leq k_u \quad 0 \leq x \leq 1$

(i) True for $x = 1$ (by L'Hopital)

(ii) $0 \leq x < 1$ Put $f(k) = (1 - x^k)/k$

(a) $\underline{k = 0}$

$$\lim_{k \to 0} f(k)/f(k - 1)$$

$$= \lim_{k \to 0} f'(k)/f'(k - 1) = \frac{x \ln x}{x - 1}$$

(b) $\underline{k \geq 0}$ Show $f(k)/f(k-1)$ increases with k

From #5,

$$\frac{x^k (\ln x^k)^2}{(x^k - 1)^2} \leq 1 \qquad \text{since } \frac{\ln x^k}{x^k - 1} > 0$$

This is for $x^k \geq 0$, i.e. for any k.

Hence

$$\frac{d^2[\ln f(k)]}{dk^2} \geq 0$$

$$\frac{d \ln f(k)}{dk} \qquad \text{increases with } k$$

$$\left.\frac{d \ln f(k)}{dk}\right|_k \geq \left.\frac{d \ln f(k)}{dk}\right|_{k-1}$$

$$\ln f(k) - \ln f(k-1) \qquad \text{increases with } k$$

$$f(k)/f(k-1) \qquad \text{increases with } k$$

5. $\underline{\dfrac{\ln x}{x - 1} \leq x^{-\frac{1}{2}}} \qquad x \geq 0$

(a) $\underline{x = 1} \qquad \lim_{x \to 1} \dfrac{\ln x}{x - 1} = \lim_{x \to 1} x^{-1} = 1$

(b) $\underline{x > 1}$ $\quad (1 - y^{-1})^2 \geq 0$ $\quad$ all y

$$\int_1^y (1 + y^{-2})\, dy \geq 2 \int_1^y y^{-1}\, dy \qquad y \geq 1$$

$$(y - y^{-1}) \geq \ln y^2$$

$$y^{-1} > \frac{\ln y^2}{y^2 - 1} \qquad y > 1$$

Hence

$$x^{-\frac{1}{2}} > \frac{\ln x}{x - 1} \qquad x > 1$$

(c) $\underline{0 < x < 1}$ Put $y = x^{-1}$; then $y > 1$ and the result follows from (b).

(d) $\underline{x = 0}$ Result true. The inequality #5 is important in the proof of (2.10).

APPENDIX II

1. The output problem for $A \underset{2}{\overset{1}{\rightleftharpoons}} B \xrightarrow{3} C$

If $k_R = k_1(T_R) = k_2(T_R)$, then $(k_1/k_R) = k$ implies $(k_2/k_R) = k^r$, $r = E_2/E_1$.

Now

$$(k_3/k_R) = \frac{H_3 \exp(-E_3/RT)}{k_R}$$

$$= \left[\frac{H_3}{k_R}\right] \left[\frac{H_1 \exp(-E_1/RT)}{k_R}\right]^{E_3/E_1} \left[\frac{H_1}{k_R}\right]^{-E_3/E_1}$$

$$= a' k^s, \text{ where } s = E_3/E_1$$

$$a' = (H_3/k_R)\ (H_1/k_R)^{-s} = (H_3/H_1)\ H_1^{1-s}\ k_R^{s-1}$$

$$k_R = H_1 \exp(-E_1/RT_R) = H_2 \exp(-E_2/RT_R)$$

$$\exp(-1/RT_R) = (H_2/H_1)^{1/(E_1-E_2)}$$

so

$$k_R = H_1 (H_2/H_1)^{1/1-r}$$

Hence $a' = (H_3/H_1)\ (H_2/H_1)^{s-1/1-r}$

$\equiv$ a in equation (2.20), (2.12)

2. <u>The roots of $\mu^2 - (1+k+ak^{-\alpha})\mu + ak^{-\alpha} = 0$</u> $\quad k \geq 0$

$$\mu_1,\ \mu_2 = \Theta\left[1 \pm (1 - ak^{-\alpha}/\Theta^2)^{\frac{1}{2}}\right]$$

where

$$\Theta = (1 + k + ak^{-\alpha})/2$$

Now

$$(1 + k - ak^{-\alpha})^2 + 4ak^{-\alpha} > 0$$

$$\Theta^2 > ak^{-\alpha} \qquad *$$

Hence

μ_1, μ_2 real and positive.

*(Note that $\Theta^2 \neq ak^{-\alpha}$, so $\mu_1 \neq \mu_2$)

APPENDIX III

1. The Hamiltonian as function of control

Many of the inequalities which follow are obvious and their proof has consequently been omitted. Those marked with an asterisk are less simple to verify and may be proved with the aid of the inequalities at the end of this section.

Now from equation (3.34)

$$H = \lambda_1 \left[K^3(1 - x_B - x_C) - (K^4 + \tfrac{1}{4}K^2)x_B\right] + \lambda_2 K^2 x_B/4$$

$$= \lambda_1 \left[-K^4 x_B + K^3(1 - x_B - x_C) - K^2(1 - \lambda \overbrace{x_B}^{x_B})/4\right]$$

where

$\lambda = \lambda_2/\lambda_1$ and $0 \leq K \leq K_u$. Consider $\lambda_1 > 0$.

(a) $H = -\lambda_1 x_B K^2 (K - \alpha_1)(K - \alpha_2) = 0$ at

$K = 0$ (twice), α_1, α_2; where $\alpha_1, \alpha_2 = \dfrac{1 \pm a}{2X}$ and

$X = \dfrac{x_B}{1 - x_B - x_C}$; $a = (1 + A)^{\frac{1}{2}}$ with $A = (\lambda - 1)X^2$.

(i) $\lambda \geq 1$ $\quad a \geq 1$

$\alpha_1 \geq 1/X$

$\alpha_2 \leq 0$

(ii) $\lambda \leq 1$ $\quad 0 \leq a \leq 1$

$1/2X \leq \alpha_1 \leq 1/X$

$0 \leq \alpha_2 \leq 1/2X$

(b) $\frac{dH}{dk} = -4\lambda_1 x_B K(K - \beta_1)(K - \beta_2) = 0$ at

$K = 0, \beta_1, \beta_2$; where $\beta_1, \beta_2 = \frac{3(1 \pm b)}{8X}$ and $b = (1 + 8A/9)^{\frac{1}{2}}$

(i) $\lambda \geq 1$ $\quad a \geq b \geq 1$

$\alpha_1 \geq \beta_1 \geq 3/4X$

$\alpha_2 \leq \beta_2 \leq 0$

(ii) $\lambda \leq 1$ $\quad 0 \leq a \leq b \leq 1$

$3/8X \leq \beta_1 \leq 3/4X$

$\alpha_2 \leq \beta_1 \leq \alpha_1$ *

$$0 \leq \beta_2 \leq 3/8X$$

$$0 \leq \beta_2 \leq \alpha_2$$

(c) $\frac{d^2H}{dK^2} = -12\,\lambda_1 x_B (K - \gamma_1)(K - \gamma_2)$; where

$\gamma_1, \gamma_2 = \frac{1 \pm c}{4X}$ and $c = (1 + 2A/3)^{\frac{1}{2}}$

(i) $\underline{\lambda \geq 1}$ $\qquad 1 \leq c \leq b \leq a$

$$\beta_1 \geq \gamma_1 \geq \gamma_2$$

$$\beta_2 \leq \gamma_2 \leq \gamma_1$$

(ii) $\underline{\lambda \leq 1}$ $\qquad 1 \geq c \geq b \geq a \geq 0$

$$\beta_1 \geq \gamma_1 \geq \gamma_2 \quad *$$

$$\gamma_2 \leq \beta_2 \leq \gamma_1 \quad *$$

$K = 0$: $\frac{d^2H}{dK^2} > 0$ when $\lambda > 1$ (minimum)

< 0 $\lambda < 1$ (maximum)

$= 0$ $\lambda = 1$ (inflection)

$K = \beta_1 : \frac{d^2H}{dK^2} < 0$ $\qquad \lambda > 1,\ \lambda < 1,\ \lambda = 1$ (maximum)

$K = \beta_2 : \frac{d^2H}{dK^2} < 0$ $\qquad \lambda > 1$ (maximum)

> 0 $\qquad \lambda < 1$ (minimum)

$= 0$ $\qquad \lambda = 1$ (inflection)

(d) $H \longrightarrow -\infty$ as $K \longrightarrow \pm\infty$[see (a)]. The graphs are given in figure (3.2). When $\lambda_1 < 0$, the graph of Hamiltonian vs. control will be the mirror image of the curves shown in figure (3.2).

Inequalities

$\lambda < 1 \qquad -1 \leq A \leq 0 \qquad 0 \leq a \leq b \leq c \leq 1$

(i) $4a - 3b + 1 > 0$

Put

$$f(A) = 4(1 + A)^{\frac{1}{2}} - 3(1 + 8A/9)^{\frac{1}{2}} + 1$$

Now $\qquad f(-1) = 0$

$$\frac{df(A)}{dA} = 2/a - 4/3b > 0$$

(ii) $\underline{3b - 2c + 1 > 0}$

$$f(A) = 3(1 + 8A/9)^{\frac{1}{2}} - 2(1 + 2A/3)^{\frac{1}{2}} + 1$$

Here $f(-1) > 0$

$$\frac{df(A)}{dA} = 2(2/b - 1/c)/3 > 0$$

(iii) $\underline{3b + 2c - 1 > 0}$

$$f(A) = 3(1 + 8A/9)^{\frac{1}{2}} + 2(1 + 2A/3)^{\frac{1}{2}} - 1$$

Hence $f(-1) > 0$ and

$$\frac{df(A)}{dA} = 2(2/b + 1/c)/3 > 0$$

2. To show that λ_1 will not change sign along a trajectory.

The adjoint ratio $\lambda = \lambda_2/\lambda_1$ is given by (3.42)

$$\frac{d\lambda}{d\phi} = \frac{K^2}{4}\left[\lambda^2 - (2K + 1)^2\lambda + 4K\right] \qquad \text{(A3.1)}$$

Also equation (3.39a) for λ_1 may be rewritten

$$\frac{d\lambda_1}{d\phi} = \frac{K^2}{4}\,\lambda_1\left[(2K+1)^2 - \lambda\right] \qquad \text{(A3.2)}$$

From (A3.2), as long as $\lambda(0)$ is chosen $< (2K+1)^2$, $\frac{d\lambda_1}{d\phi}$ and λ_1 will have the same sign. Hence if $\lambda_1(0) > 0$, $\lambda_1(\phi)$ will increase with ϕ, and vice versa. However this will only be true if $\lambda(\phi)$ remains $< (2K+1)^2$ for $\phi \geq 0$.

Let us examine the behaviour of $\lambda(\phi)$ with ϕ.

$$\frac{d\lambda}{d\phi} = \frac{K^2}{4}\,f(\lambda) \quad ,$$

where

$$f(\lambda) = \lambda^2 - (2K+1)^2\lambda + 4K$$

Then $\frac{d\lambda}{d\phi}$ and $f(\lambda)$ will have the same sign for all λ. The behaviour of $f(\lambda)$ with λ is shown in figure (A3.1). In this figure the roots are given by

$$\rho_1, \rho_2 = \Theta\left[1 \pm (1 - 4K/\Theta^2)^{\frac{1}{2}}\right]$$

where

$$\Theta = (2K+1)^2/2$$

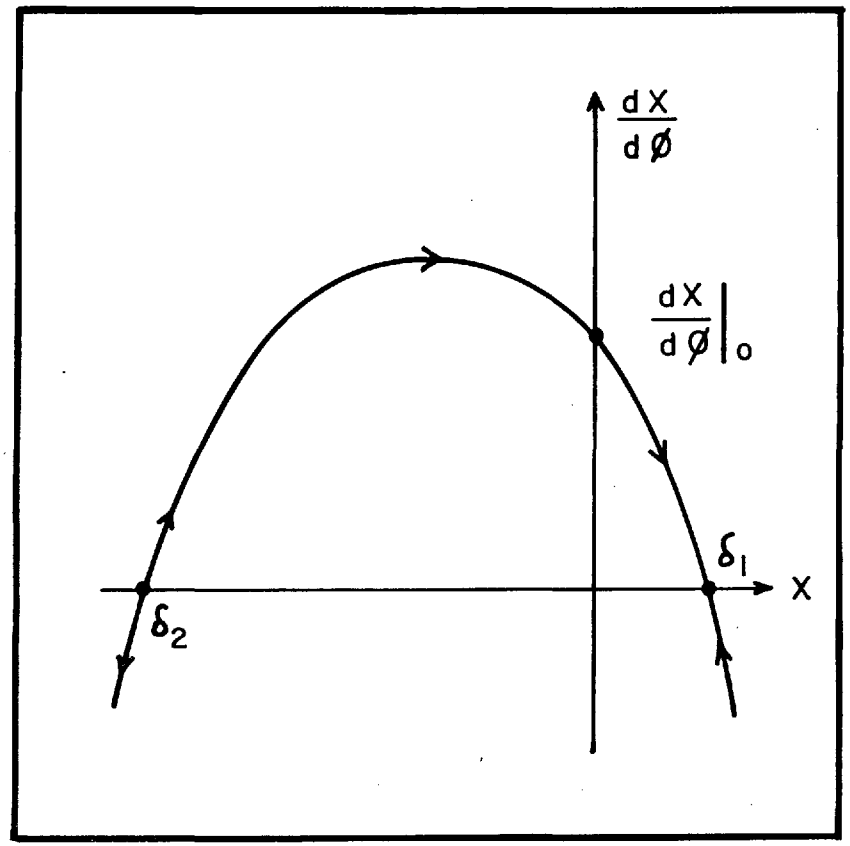


FIGURE A3.2 - BEHAVIOUR OF THE RATIO OF STATE VARIABLES X

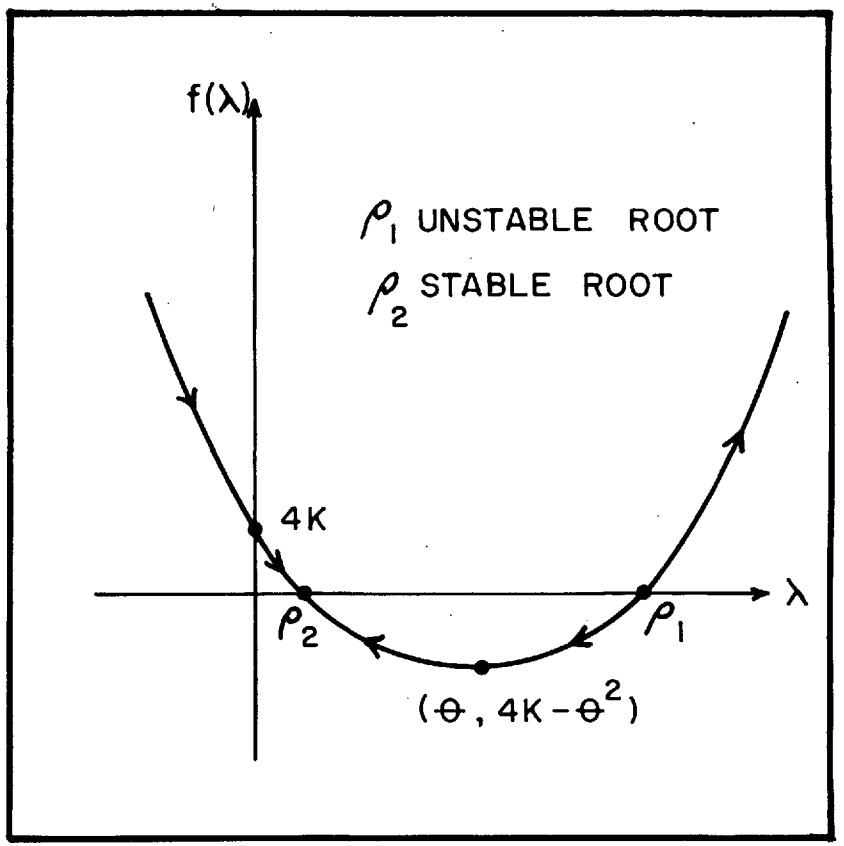


FIGURE A3.1 - SIGN OF THE ADJOINT RATIO λ

Now

$$\Theta^2 - 4K = 2K^2(2K^2 + 4K + 1) + (2K - \tfrac{1}{2})^2 > 0$$

Hence the roots are real and positive. The coordinates of the minimum turning point are $(\Theta,\ 4K - \Theta^2)$.

It is clear from figure (A3.1) that if $\lambda(0) < \rho_1$, $\lambda(\phi) \longrightarrow \rho_2$ for $\phi > 0$. Since $\rho_1 < 2\Theta$, this means $\lambda(\phi) < 2\Theta$ for $\phi \geq 0$ and $\lambda_1(\phi)$ will not change sign for $\phi \geq 0$.

$$K_u = 100,\ \rho_1 \text{ just } > 40,400.99$$

$$K_u = 2,\quad \rho_1 \text{ just } > 24.675795$$

3. Behaviour of $X = x_B/x_A$ on the isothermal K_u

From equation (3.51),

$$\frac{dX}{d\phi} = -\frac{K^2}{4}\left[4K^2X^2 + (2K - 1)^2X - 4K\right]$$

The behaviour of $\frac{dX}{d\phi}$ with X can be seen in figure (A3.2). Here the roots are

$$\delta_1, \delta_2 = \Delta\left[1 \pm (1 + 1/K\Delta^2)^{\frac{1}{2}}\right]$$

where

$$\Delta = -(1 - 1/2K)^2/2$$

Now $X(0) = 0$, which gives $\left.\frac{dX}{d\phi}\right|_o = K_u^3 > 0$. Hence $X(\phi)$ will increase with ϕ on the isothermal K_u, up to the stable root δ_1 at steady state.

$K_u = 100$, $\delta_1 \doteq 0.01$ and $X \longrightarrow 0.01$ rapidly

$K_u = 2$, $\delta_1 \doteq 0.47973724$

APPENDIX IV #1

```
NON-TRIVIAL ATTAINABLE REGION, 3-D OUTPUT PROBLEM
INDEPENDENT VARIABLE CHANGED TO DIMENSIONLESS TIME
UPPER BOUND ON CONTROL KU = 2
CONSTANTS
      CON      8OVER9,ONE,3OVER8,HALF,QUARTR,ZERO
      CON      10EXP8,TR,KU
PARAMETERS
      PAR      FINALT
INITIAL CONDITIONS
      IC       I2
PROGRAMME
      M1       I1,I1
      M2       I1,M11
      M3       S1,M13
      M4       I2,I2
      M5       I2,S7
      M6       S2,M14
      M7       8OVER9,M1
      M8       S3,M7
      M9       3OVER8,S5
      M10      HALF,NEG4
      M11      S6,S6
      M12      L1,L1
      M13      M12,M12
      M14      QUARTR,M12
      M15      S8,M18
      M16      E1,I1
      M17      L1,I1
      M18      L1,M12
      M19      S13,S13
      I1       D6
      I2       D5
      I3       D4
      D1       M9,I1
      D2       ONE,L1
      D3       IT,S13
      D4       M15,M19
      D5       M6,M19
      D6       NEG2,M19
      S1       M2,NEG4,M1
      S2       M4,NEG1,S12
      S3       I2,NEG3
      S4       M8,ONE
      S5       ONE,OR1C
      S6       ONE,M10
      S7       S11,ONE,S12
      S8       NEG3,M17
      S9       M16,E1
      S10      ONE,NEG5
      S11      M12,M12,M12,M12
      S12      L1,L1,L1,L1
      S13      ONE,NEG6
      SQR1     ABS1
      ABS1     S4
      OR1      SQR1,S4
      L1       FSW1,KU,ZERO
      E1       I3
      NEG1     M5
      NEG2     M3
      NEG3     ONE
      NEG4     FSW2
      NEG5     S9
      NEG6     IT
      FSW1     D1,10EXP8,D1,I1
      FSW2     D2,10EXP8,D2,L1
FINISH STATEMENT
      FIN      IT,FINALT
HEADER
      HDR      DTIME,TIME,XA,XB,XC,X
      HDR
      HDR       , ,LAMDA,K,8,NDGO
      HDR
READOUT
      RD       IT,D3,E1,M16,S10,I1
      RD        , ,I2,L1,OR1C,OR1D
      RD
END STATEMENT
      END
```

APPENDIX IV #2

```
C     KUTTA-MERSON INTEGRATION OF SYSTEMS EQUATIONS AND ADJOINTS
C     FOR 3-D OUTPUT PROBLEM ATTAINABLE REGION
      DIMENSION X(3),XO(3),ACC(3),XPRIME(3),Y(3,5)
      REAL KU,K
      INTEGER TWICEH,HFAILS,REPEAT
C     READ IN INITIAL CONDITIONS FOR STATES AND CONTROL
   18 READ (5,1)KU,(X(I),I=1,3)
C     READ IN INTEGRATION INTERVAL AND FINAL TIME

      READ (5,2)H,FINALT
C     READ IN PREDETERMINED INTEGRATION ACCURACY
      READ (5,3)(ACC(I),I=1,3)
C     READ IN INITIAL TIME AND TLPRNT
      READ (5,30)TIME,TLPRNT
    1 FORMAT (F6.1,3E15.8)
    2 FORMAT (2E11.4)
    3 FORMAT (3E8.1)
   30 FORMAT (2F7.4)
      WRITE (6,4)
      WRITE (6,5)
    4 FORMAT(7H1 DTIME,15X,4HTIME,16X,2HXB,18X,2HXC,18X,5HLAMDA,15X,1HK)
    5 FORMAT(3HO H,19X,1HB,19X,7HXBPRIME,13X,7HXCPRIME,13X,10HLAMDAPRIME
     1,10X,1HN)
      PRINTT=.01
      NUMBER=1
      REPEAT=0
      N=0
    7 CALL AUX(X,KU,H,TIME,NUMBER,XPRIME,B,K,Y,XO,TIMEO)
      IF (NUMBER-1)6,8,8
    8 SMALLT=TIME/(1.-TIME)
      WRITE (6,10)TIME,SMALLT,(X(I),I=1,3),K

      WRITE (6,11)H,B,(XPRIME(I),I=1,3),N

   10 FORMAT (1HO,6(E14.7,6X))
   11 FORMAT(1H ,5(E14.7,6X),I3)
      IF(TIME-FINALT)20,21,21
   20 NUMBER=0
      TLPRNT=TLPRNT+PRINTT
      GO TO 7
    6 CALL ERROR(Y,ACC,H,TWICEH,HFAILS,XO)
      IF (HFAILS-1)12,9,9
    9 TIME=TIMEO
      DO 13 I=1,3
   13 X(I)=XO(I)
      GO TO 7
   12 TIME=TIMEO+H
      N=N+1
      DO 14 I=1,3
   14 X(I)=XO(I)+.5*(Y(I,1)+4.*Y(I,4)+Y(I,5))
      IF (TWICEH-3)15,19,19
   19 H=2.*H
      IF (H-.005)15,22,22
   22 H=.005
   15 IF (REPEAT-1)16,23,23
   23 H=HO
      REPEAT=0
   24 NUMBER=1
      GO TO 7
   16 THETA=ABS(TIME-TLPRNT-PRINTT)
      CLOSE=1.0E-08
      IF (THETA-CLOSE)24,24,25
   25 IF (TIME-TLPRNT-PRINTT)7,17,17
   17 HO=H
      H=TLPRNT+PRINTT-TIMEO
      N=N-1
      REPEAT=1
      GO TO 9
   21 GO TO 18
      END
```

```
C       SUBROUTINE TO EVALUATE KUTTA AUXILIARIES
        SUBROUTINE AUX(X,KU,H,TIME,NUMBER,XPRIME,B,K,Y,XO,TIMEO)
        DIMENSION X(3),XO(3),Y(3,5),XPRIME(3)
        REAL KU,K
        J=0
        DO 200 I=1,3
  200   XO(I)=X(I)
        TIMEO=TIME
  203   CALL DERIVS(X,KU,TIME,B,XPRIME,K)
        IF (NUMBER-1)212,208,208
  212   J=J+1
        DO 201 I=1,3
  201   Y(I,J)=(H/3.)*XPRIME(I)
        GO TO (204,205,206,207,208),J
  204   TIME=TIMEO+H/3.
        DO 202 I=1,3
  202   X(I)=XO(I)+Y(I,1)
        GO TO 203
  205   DO 209 I=1,3
  209   X(I)=XO(I)+.5*Y(I,1)+.5*Y(I,2)
        GO TO 203
  206   TIME=TIMEO+H/2.
        DO 210 I=1,3
  210   X(I)=XO(I)+(3./8.)*Y(I,1)+(9./8.)*Y(I,3)
        GO TO 203
  207   TIME=TIMEO+H
        DO 211 I=1,3
  211   X(I)=XO(I)+(3./2.)*Y(I,1)-(9./2.)*Y(I,3)+6.*Y(I,4)
        GO TO 203
  208   RETURN
        END



C       SUBROUTINE FOR COMPUTING DERIVATIVES
        SUBROUTINE DERIVS(X,KU,TIME,B,XPRIME,K)
        DIMENSION X(3),XPRIME(3)
        REAL KU,K
        Z=X(1)/(1.-X(1)-X(2))
        IF (Z-1.0E-20) 106,106,150
  150   BSQD=1.+(8./9.)*(X(3)-1.)*(Z*Z)
        IF (BSQD-0.)101,102,102
  101   WRITE (6,103)
  103   FORMAT (14HOBSQD NEGATIVE)
        STOP
  102   B=SQRT(BSQD)
        K=(3./(8.*Z))*(1.+B)
        IF (K-KU)105,106,106
  106   K=KU
  105   TAU=1./((1.-TIME)*(1.-TIME))
        XPRIME(1)=TAU*K*K*(K*(1.-X(2))-(K+.5)*(K+.5)*X(1))
        XPRIME(2)=TAU*(K*K/4.)*X(1)
        XPRIME(3)=TAU*(K*K/4.)*(4.*K-X(3)*((2.*K+1.)*(2.*K+1.)-X(3)))
        RETURN
        END


C       SUBROUTINE FOR TESTING ERROR CRITERION
        SUBROUTINE ERROR(Y,ACC,H,TWICEH,HFAILS,XO)
        DIMENSION ERROR5(3),Y(3,5),ACC(3),ABSACC(3),XO(3)
        INTEGER TWICEH,HFAILS
        HFAILS=0
        TWICEH=0
        DO 301 I=1,3
        IF (HFAILS-1)302,301,301
  302   ERROR5(I)=Y(I,1)-(9./2.)*Y(I,3)+4.*Y(I,4)-.5*Y(I,5)
        ERROR5(I)=ABS(ERROR5(I))
        ABSACC(I)=ACC(I)*XO(I)
        IF (5.*ABSACC(I)-ERROR5(I))303,301,304
  303   H=.5*H
        HFAILS=1
        GO TO 301
  304   IF (ERROR5(I)-(5./32.)*ABSACC(I))305,305,301
  305   TWICEH=TWICEH+1
  301   CONTINUE
        RETURN
        END
```

APPENDIX IV #3

```
C     DETERMINATION OF THE ATTAINABLE REGION BY NON-ANALYTICAL PROCEDURES
C     PROPAGATION OF THE ATTAINABLE REGION BOROER
C     BY TRANSFORMATION OF BORDER POINTS
C     OUTPUT IN GRAPHICAL FORM
      COMMON QUAY(50),F(50),G(50),H(50),W(50),TAU,MARKER
      COMMON /SHARE1/XB,XC,XBDASH,XCDASH,N,J,K,L
      COMMON/SHARE2/XAYES,XBYES,XA,JA,VACANT
      COMMON/SHARE3/M
      DIMENSION JA(472),XAYES(472),XBYES(472),XAZERO(472),XBZERO(472),
     1NODOT(472),M(43,100),VACANT(472)
      INTEGER VACANT
      XA0 =1.
      XB0=0.
      AID=2.
      HELP=.5*SQRT(AID)
      MARKER = 1
      TAU=0.
C     PROPAGATION STEP - START OF EACH TIME-SLICE CALCULATION
   11 IF(MARKER.GT.10)TAU=TAU+.04
      TAU=TAU+.01
      CALL MATRIX
      DO 5 NODE=1,472
      IF(NODOT(NODE).EQ.1)GO TO 15
C     GENERATION STEP - LINEAR TRANSFORMATIONS
      DO 2 I=1,50
      XA=F(I)*XA0+G(I)*XB0
      XB=H(I)*XA0+W(I)*XB0
      XC=1.-(XA+XB)
C      TRANSFORMATION OF AXES
      XBDASH=HELP*(XB-XC)+1.
      XCDASH=HELP*(XB+XC)
      CALL COLUMN
      M(J,N)=M(J,N)+1
      IF(M(J,N).GT.9)M(J,N)=9
      CALL BORDER
    2 CONTINUE
      IF(MARKER.EQ.1)GO TO 14
   15 IF(NODE.EQ.472) GO TO 14
      NOG1=NODE+1
      XA0=XAZERO(NOG1)
      XB0=XBZERO(NOG1)
    5 CONTINUE
   14 CALL GRAPH
      DO 501 I=1,472
  510 IF(VACANT(I).EQ.0)GO TO 502
      NODOT(I)=0
      XAZERO(I)=XAYES(I)
      XBZERO(I)=XBYES(I)
      GO TO 500
  502 NODOT(I)=1
  500 JA(I)=0
      VACANT(I)=0
  501 CONTINUE
      IF(MARKER.EQ.27)STOP

      XA0=XAZERO(1)
      XB0=XBZERO(1)
      MARKER=MARKER+1
      GO TO 11
      END
```

```
C       SUBROUTINE TO EVALUATE MATRIX OF COEFFICIENTS
        SUBROUTINE MATRIX
        COMMON QUAY(50),F(50),G(50),H(50),W(50),TAU,MARKER
        DIMENSION EIGEN1(50),EIGEN2(50),C(50),D(50),E(50)
        EQUIVALENCE (A,T1),(B,T2),(LAMDA,RLAMDA)
        REAL LAMDA
        IF(MARKER.GT.10)GO TO 603
        DELTAT=.01/((1.-TAU)*(1.01-TAU))
        IF(MARKER.GT.1) GO TO 600
        READ (5,102) QUAY
  102   FORMAT(8F10.1)
        GO TO 600
  603   DELTAT=.05/((1.-TAU)*(1.05-TAU))
  600   CONTINUE
        DO 100 I=1,50
        IF (MARKER.GT.1)GO TO 101
C       FIRST ENTRY ONLY-EVALUATION OF PARAMETERS WHICH ARE F(K)
        Z=QUAY(I)
        A=Z*(Z+.5)*(Z*(Z+.5))
        B=Z/(Z+.5)**4
        LAMDA=A*SQRT(1.-B)
        EIGEN1(I)=.5*(A+LAMDA)
        EIGEN2(I)=.5*(A-LAMDA)
        RLAMDA=1./LAMDA
        C(I)=Z**3*RLAMDA
        D(I)=C(I)-EIGEN2(I)*RLAMDA
        E(I)=C(I)-EIGEN1(I)*RLAMDA
C       ALL ENTRIES - CALCULATION OF COEFFICIENT MATRIX
  101   T1=EXP(-EIGEN1(I)*DELTAT)
        T2=EXP(-E(GEN2(I)*DELTAT)
        IF(I.EQ.1)GO TO 602
        F(I)=D(I)*T1-E(I)*T2
        H(I)=C(I)*(T2-T1)
        G(I)=H(I)*QUAY(I)
        W(I)=D(I)*T2-E(I)*T1
        GO TO 100
  602   F(I)=1.
        G(I)=0.
        H(I)=0.
        W(I)=1.
  100   CONTINUE
        RETURN
        END


C       SUBROUTINE TO MAP FROM ATTAINABLE POINT TO COLUMN CONTAINING IT
        SUBROUTINE COLUMN
        COMMON /SHARE1/XB,XC,XBDASH,XCDASH,N,J,K,L
        EQUIVALENCE(YY,NLESS1,N),(XX,JLESS1,J),(ZZ,KLESS1,K),(WW,LLESS1,L)
C       NORTH-SOUTH COLUMN=N
        YY=100.*XC
        NLESS1=YY
        N=NLESS1+1
C       EAST-WEST COLUMN=J
        XX=100.*XB
        JLESS1=XX
        J=JLESS1+1
C       NORTHWEST-SOUTHEAST COLUMN=K
        ZZ=100.*XCDASH
        KLESS1=ZZ
        K=KLESS1+1
C       NORTHEAST-SOUTHWEST COLUMN=L
        WW=100.*XBDASH
        LLESS1=WW
        L=LLESS1+1
        RETURN
        END
```

```
C     SUBROUTINE TO CHECK IF THERE IS A POINT ALREADY IN THE COLUMN
C     IF THERE IS, IS THE ATTAINABLE POINT THE BEST IN THE COLUMN
      SUBROUTINE BORDER
      COMMONQUAY(50)/SHARE1/XB,XC,XBOASH,XCOASH,N,J,K,L
      COMMON/SHARE2/XAYES,XBYES,XA,JA,VACANT
      DIMENSION JA(472),XAYES(472),XBYES(472),XBMAX(100),XCMIN(43),
     1XCMAX(43),DISTNW(100),DISTNE(143),DISTSW(43),KOUNT(472),LOUIS(472)
      INTEGER OUI,VACANT(472)
      LL=L-100
      LOPERA=0
      DO 711 NU=1,6
      GO TO (712,713,701,715,716,704),NU
  712 M=N
  705 IF(JA(M).EQ.1)GO TO(13,60,730,61,62,731),NU
      JA(M)=1
      GO TO(750,751,752,714,721,722),NU
  713 M=100+J
      GO TO 705
  701 M=143+J
      GO TO 705
  715 M=186+K
      GO TO 705
  716 IF(L.LE.100)GO TO 711
      M=186+L
      GO TO 705
  704 M=329+L
      GO TO 705
   13 IF(XBMAX(N).GE.XB)GO TO 711
  750 XBMAX(N)=XB
      GO TO 31
   60 IF(XCMIN(J).LE.XC)GO TO 711
  751 XCMIN(J)=XC
      GO TO 31
  730 IF(XCMAX(J).GE.XC)GO TO 711
  752 XCMAX(J)=XC
      GO TO 31
   61 IF(DISTNW(K).GE.XBOASH)GO TO 711
  714 DISTNW(K)=XBOASH
      GO TO 31
   62 IF(DISTSW(LL).LE.XCOASH)GO TO 711
  721 DISTSW(LL)=XCOASH
      GO TO 31
  731 IF(DISTNE(L).GE.XCOASH)GO TO 710
  722 DISTNE(L)=XCOASH
C     ACCEPTANCE OF A NEW BORDER POINT, PERHAPS AT THE EXPENSE OF AN OLD
   31 LOPERA=LOPERA+1
C     IS THE NEW POINT OVERWRITING ANOTHER POINT
      KLEF=LOUIS(M)
      IF(KLEF.EQ.0)GO TO 2000
C     COMES HERE IF IT IS OVERWRITING AN OLDER POINT
C     IS THE POINT BEING OVERWRITTEN STILL RETAINED ELSEWHERE
      IF(KOUNT(KLEF).GT.1)GO TO 2001
C     POINT NOT BEING RETAINED ELSEWHERE, SO VACATE IT
      VACANT(KLEF)=0
      GO TO 2000
C     THE POINT IS RETAINED ELSEWHERE
 2001 KOUNT(KLEF)=KOUNT(KLEF)-1
C     GET A OUI VALUE FOR THE NEW POINT
 2000 IF(LOPERA.GT.1)GO TO 2003
      DO 2002 OUI=1,472
 2002 IF(VACANT(OUI).EQ.0)GO TO 2003
 2003 LOUIS(M)=OUI
  711 CONTINUE
  710 IF(LOPERA.EQ.0)GO TO 2005
      XAYES(OUI)=XA
      XBYES(OUI)=XB
      KOUNT(OUI)=LOPERA
      VACANT(OUI)=1
 2005 RETURN
      END
```

```
C     SUBROUTINE TO DRAW GRAPH OF ATTAINABLE REGION
      SUBROUTINE GRAPH
      COMMON QUAY(50),F(50),G(50),H(50),W(50),TAU,MARKER
      COMMON/SHARE3/M
      DIMENSION M(43,100),LINE(116),NUMBER(9)
      INTEGER BLANK,DOT,X,B
      DATA BLANK,DOT,X,8/1H ,1H.,1HX,1H8/
      DATA NUMBER/1H1,1H2,1H3,1H4,1H5,1H6,1H7,1H8,1H9/
C     PRINT HEADING AT TOP OF PAGE
      WRITE(6,559)
  559 FORMAT(1HI,46X,27HATTAINABLE REGION SLICE FOR)
C     PRINT TAU AND MARKER VALUES
      WRITE(6,572)MARKER,TAU
  572 FORMAT(1HO,48X,7HMARKER=,I3,9H      TAU=,F5.2)
C     BLANK THE FIRST 15 SPACES
      DO 589 N=1,15
  589 LINE(N)=BLANK
C     PRINT 0.5 TO LEFT OF AXIS
      LINE(12)=0
      LINE(13)=DOT
      LINE(14)=NUMBER(5)
C     PRINT A LINE OF DOTS AS TOP OF GRAPH
      DO 588 N=16,116
  588 LINE(N)=DOT
      WRITE(6,587)LINE
  587 FORMAT(1HD,116A1)
C     PLOT THE GRAPH
      DO 597 JBACK=1,50
C     BLANK THE LINE
      DO 598 N=11,116
  598 LINE(N)=BLANK
C     PUT A DOT IN LINES (16) AND (116) TO PRODUCE VERTICAL BORDERS
      LINE(16)=DOT
      LINE(116)=DOT
C     PRINT AXIS ONLY FOR FIRST 7 SPACES
      IF(JBACK.LE.7) GO TO 586
      J=51-JBACK
C     PUT XB TO LEFT OF AXIS IF JBACK=25
      IF(JBACK.NE.25)GO TO 596
      LINE(11)=X
      LINE(12)=B
C     PUT SCALE TO LEFT OF AXIS
  596 IF(JBACK.EQ.10.OR.JBACK.EQ.20)GO TO 595
      IF(JBACK.EQ.30.OR.JBACK.EQ.40)GO TO 595
      IF(JBACK.NE.50)GO TO 560
  595 LINE(12)=0
      LINE(13)=DOT
      IF(JBACK.EQ.50)GO TO 520
      MJBACK=5-JBACK/10
      LINE(14)=NUMBER(MJBACK)
      GO TO 560
  520 LINE(14)=0
C     PRINT A LINE OF DOTS TO PRODUCE HORIZONTAL AXIS
      DO 579 N=16,116

  579 LINE(N)=DOT
C     PUT M(J,N) VALUE IN SELECTED LOCATION
  560 DO 591 N=1,100
      NN=N+16
      IDUMMY =M(J,N)
  591 IF(IDUMMY.GT.0) LINE(NN)=NUMBER(IDUMMY)
C     PRINT THE LINE
  586 WRITE(6 580)LINE
  580 FORMAT(1H ,116A1)
  597 CONTINUE
C     PUT IN SCALE ON XC AXIS
      WRITE(6,594)
  594 FORMAT(1HO,14X,3HO.O,7X,3HO.1,7X,3HO.2,7X,3HO.3,7X,3HO.4,7X,3HO.5,
     17X,3HO.6,7X,3HO.7,7X,3HO.8,7X,3HO.9,7X,3H1.0)
C     PRINT XC BELOW AXIS
      WRITE(6,573)
  573 FORMAT(1HO,60X,2HXC)
      RETURN
      END
```

TABLE A.1

Isothermal results for $K_u = 2$ *

$x_B(0) = x_C(0) = 0$ $\lambda(\xi)$ from $X(\xi)$ and equation (3.54)

ξ	$x_B(\xi)$	$x_C(\xi)$	$\lambda(\xi)$
0.46	0.24924	0.23122	7.98 **
0.48	0.24355	0.24877	
0.50	0.23755	0.26727	
0.52	0.23122	0.28680	
0.54	0.22453	0.30744	
0.56	0.21745	0.32928	
0.58	0.20995	0.35240	
0.60	0.20201	0.37692	
0.62	0.19357	0.40294	
0.64	0.18461	0.43058	
0.66	0.17508	0.45996	
0.68	0.16495	0.49120	
0.70	0.15418	0.52443	
0.72	0.14272	0.55976	
0.74	0.13056	0.59728	
0.76	0.11768	0.63702	
0.78	0.10408	0.67897	
0.80	0.08982	0.72296	
0.82	0.075009	0.76862	
0.84	0.059891	0.81527	
0.86	0.044838	0.86170	
0.88	0.030482	0.90598	
0.90	0.017758	0.94523	
0.92	0.0078952	0.97565	
0.94	0.0020451	0.99369	

* Obtained from MIDAS isothermal integration; 2.8 minutes on IBM 7090

** $\lambda(\xi)$ stays at 7.98 for all ξ, since X approaches within less than 10^{-8} of its steady state value, at $\xi = 0.446$

TABLE A.2

Isothermal results for $K_u = 100$ *

$x_B(0) = x_C(0) = 0$ $\quad \lambda(\xi)$ from $X(\xi)$ and equation (3.54)

ξ	$x_B(\xi)$	$x_C(\xi)$	$\lambda(\xi)$
.001	.9658456-02	.2447199-01	19,999.51**
.002	.9421625-02	.4839258-01	
.003	.9190142-02	.7177285-01	
.004	.8963900-02	.9462391-01	
.005	.8742789-02	.1169567	
.006	.8526704-02	.1387818	
.007	.8315540-02	.1601099	
.008	.8109195-02	.1809512	
.009	.7907570-02	.2013158	
.010	.7710566-02	.2212137	
.015	.6791545-02	.3140371	
.020	.5974320-02	.3965789	
.025	.5248526-02	.4698859	
.030	.4604752-02	.5349086	
.035	.4034468-02	.5925088	
.040	.3529946-02	.6434667	
.045	.3084199-02	.6884882	
.050	.2690913-02	.7282111	
.060	.2039499-02	.7940056	
.070	.1536591-02	.8448004	
.080	.1150589-02	.8837876	
.100	.6328024-03	.9360854	
.150	.1255105-03	.9873231	
.200	.2033612-04	.9979460	
.250	.2585045-05	.9997389	

* Obtained from Fortran IV programme; 4 minutes on IBM 7090

** $\lambda(\xi)$ stays constant for all ξ, since X approaches very close to its steady state value in a $\xi << .001$